THE APPLICATION OF SEMI-SYNTHETIC BIOPOLYMER NANO-CARRIER COMPLEXES FOR DRUGS WITH LOW ORAL BIOAVAILABILITY

MDUDUZI NKOSINATHI SITHOLE

A dissertation submitted to the Faculty of Health Science, University of the Witwatersrand, in fulfilment of the requirements for the degree of Masters of Science in Medicine

Supervisor:

Professor Viness Pillay

University of the Witwatersrand, Department of Pharmacy and Pharmacology,

Johannesburg, South Africa

Co-Supervisors:

Professor Yahya Essop Choonara

University of the Witwatersrand, Department of Pharmacy and Pharmacology,

Johannesburg, South Africa

Professor Lisa Claire du Toit

University of the Witwatersrand, Department of Pharmacy and Pharmacology,

Johannesburg, South Africa

And

Mr. Pradeep Kumar

University of the Witwatersrand, Department of Pharmacy and Pharmacology,

Johannesburg, South Africa

2016

DECLARATION

I, Mduduzi Nkosinathi Sithole, declare that this dissertation is my own work. It has been submitted for the degree of Masters of Science in Medicine in the Faculty of Health Science at the University of the Witwatersrand, Johannesburg, South Africa. It has not been submitted before for any degree or examination at this or any other University.

.....

Signed at Wits. day of 16 May 2016

RESEARCH OUTPUTS

1. Research Publications

Semi-Synthetic Biopolymer Complexes: Modified Polysaccharides as Oral Drug Nano-Carriers for Enhancement of Oral Bioavailability. Mduduzi N. Sithole[1], Yahya E. Choonara[1], Lisa C. du Toit[1], Pradeep Kumar[1], Pierre P. D. Kondiah[1] and Viness Pillay[1*]. Submitted to Pharmaceutical Development and Technology, (Abstract in the Appendix A).

Development of Novel Polymeric Nano-Composite Complex for Low Bioavailability Drugs. Mduduzi N. Sithole[1], Yahya E. Choonara[1], Lisa C. du Toit[1], Pradeep Kumar[1], Pierre P. D. Kondiah[1] and Viness Pillay[1*]. Submitted to AAPS Pharm SciTech, (Abstact in the Appendix B).

ANIMAL ETHICS DECLARATION

I, Mduduzi Nkosinathi Sithole, hereby confirm the study entitled "*In vivo* assessment of innovative polymeric oral drug delivery systems in Large White Pigs" was approved by the Animal Ethics Screening Committee (AESC) of the University of the Witwatersrand with Ethics Clearance Number 2014/38/C (Appendix C). The approval for the use of animal tissue samples letter from the University of the Witwatersrand is attached in Appendix D.

ABSTRACT

The major challenge in pharmaceutical research is the improvement of drug efficacy, including enhancement of solubility and permeability, leading to an improved oral bioavailability of drugs. Semi-Synthetic Biopolymer Complexes (SSBC) as drug nano-enabled delivery systems have gained significant interest in recent years. Their significance originated from the fact that they show great potential as drug nano-carriers used for oral drug delivery. This resulted from their exceptional properties obtained by merging the properties of synthetic (e.g. good thermal and mechanical properties) with natural polymers (e.g. biocompatibility); thus forming a new class of biopolymeric materials combining the best of both aspects.

This research employed a class of polymers called SSBC as oral drug nano-carriers. This investigation attempted to improve the permeability and solubility of acyclovir (ACV). It also sought to develop guiding principles in examining and solving key issues of ACV nano-encapsulation as means to enhance its oral bioavailability. The use synthetic or natural polymers independently pose limitations in their properties as drug carriers. In this research, a delivery system was designed for ACV with desirable physicochemical and physicomechanical properties, engineered by modifying hyaluronic acid (HA) with poly (acrylic acid) (PAA), conjugated with (2-hydroxypropyl)-β-cyclodextrin (HP-β-CD), yielding an "intelligent" nano-enabled drug delivery system to regulate ACV permeability and solubility. The synthetic method employed was based on the covalent coupling of the polymeric chains at their respective reactive functional groups, followed by conjugation with the HP-β-CD.

A Face-Centred Central Composite Design (FCCCD) was utilized for the generation of an optimized formulation. The formulation was analysed using the following dependent parameters: the size, drug entrapment, solubility and permeation. The comparative *In vitro* studies for ACV-loaded polymeric nanoparticle compared with ACV from the comparator product revealed that both formulations had significant different profiles, since f_1 (the difference factor 1) was calculated to be 104.02 and f_2 (the similarity factor 2) was 31.83. The current investigation also provided evidence that the SSBC nano-system improved the solubility of ACV by 30%. Hence the *ex vivo* permeation studies was performed using pig intestinal mucosa. Therefore, *ex vivo* studies revealed that the prepared ACV-loaded polymeric nanoparticle ($p < 0.05$) significantly enhanced the cumulative value of ACV compared to the ACV from conventional formulation (comparator product). *In vivo* studies were performed using Large White Pig model to assess the pharmacokinetics of ACV from the SSBC nano-system, compared to the comparator product. The study revealed that the conventional dosage (comparator product) maximum drug release occurred at 3 hours after dosing (T_{max} = 3 hours), with a peak plasma concentration of ~400ng/mL (C_{max}= ~400ng/mL). Ultra-Performance Liquid Chromatography (UPLC) was employed for drug sample analysis. In relation to these results, the optimized synthesised ACV-loaded polymeric nanoparticles possessed a T_{max} of 8 hours with peak concentration, C_{max} of ~850ng/mL. The area under the plasma profile curve (AUC) for the optimized ACV-loaded polymeric nanoparticles was calculated to be ~10301ng.h/mL, while the comparator product displayed an AUC of ~2468ng.h/mL. It can thus be concluded that relative bioavailability of the synthesised optimized ACV-loaded polymeric nanoparticles relative to the comparator product formulation was enhanced by a factor of ~4.17.

ACKNOWLEDGEMENTS

My heartfelt thanks to my parents, Cate Elizabeth and Zibuse Sithole, for their support in my academic journey, especially to my mother and her friends for all their guidance and prayers throughout my life. I thank God for blessing me with such wonderful amazing parents and I pray that I continue to make you'll proud. My humblest appreciation and thanks to the Lord of the universe for constantly guiding me and showering His love always.

A special thanks to my brother Kenny who always supported me emotionally and financially and my little brother Sibongiseni who always supported and believed in me.

This project would have not been possible without the mentoring and inspiration of my supervisor Professor Viness Pillay and my co-supervisors, Professor Yahya Choonara, Professor Lisa du Toit, and Mr Pradeep Kumar. I am most grateful for the knowledge and skills I have gained under your mentorship and look forward to another prosperous journey in the field of research which I intend on undertaking in the near future.

A special thanks to Dr. Pierre P. D. Kondiah for all his mentoring and guidance, assisting with all areas of the project and publications, constantly supporting and encouraging success.

I would like to acknowledge Dr. Divya Bijukumar and all my dear colleagues at Wits Advance Drug Delivery Platform (WADDP) research unit, for all your help, laughs and motivation which carried me forward throughout my duration of research.

Thank you to Mr. Sello Ramarumo, Mr. Bafana Temba and Ms. Phumzile Madondo for their indispensable assistance with the running of the laboratories.

My sincere thanks to the staff of Wits Department of Pharmacy and Pharmacology and the staff of Central Animal Services (CAS) at the University of the Witwatersrand for their assistance and expertise during *in vivo* studies.

A special thanks to the National Research Foundation (NRF) for all their financial assistance throughout the duration of this research.

And we know that all things work together for good to them that love God, to them whom are the called according to His purpose
Romans 8:28

DEDICATION

This dissertation is dedicated to the pillar of my existence, my motivator, my mother, Cate Elizabeth Dube. Thank you for being there for me during my entire academic journey.

TABLE OF CONTENTS

CHAPTER ONE
INTRODUCTION AND BACKGROUND

CHAPTER TWO
SEMI-SYNTHETIC BIOPOLYMER COMPLEXES: MODIFIED POLYSACCHARIDES AS ORAL DRUG NANO-CARRIERS FOR ENHANCEMENT OF ORAL BIOAVAILABILITY

CHAPTER THREE

SYNTHESIS, DEVELOPMENT AND CHARACTERIZATION OF A NOVEL SEMI-SYNTHETIC BIOPOLYMER COMPLEX AS AN ORAL NANO-CARRIER SYSTEM

CHAPTER FIVE

***IN VIVO* ASSESSMENT OF THE DRUG-LOADED SEMI-SYNTHETIC BIOPOLYMER COMPLEX IN THE LARGE WHITE PIG MODEL**

CHAPTER SIX

CONCLUSIONS AND RECOMMENDATIONS

APPENDICES

LIST OF FIGURES

LIST OF TABLES

LIST OF EQUATIONS

CHAPTER ONE
INTRODUCTION AND BACKGROUND

1.1. BACKGROUND OF THIS STUDY

Oral administration of therapeutic agents is the most favoured and convenient route due to patient compliance. Currently, the major focus in drug delivery is the design of non-conventional oral drug delivery systems, with improved pharmacokinetic profiles (Vashista *et al.,* 2012). Conventional capsules or tablets move through the gastrointestinal tract (GIT) and release drugs in non-specific regions within the GIT (Park, 1990). Therefore, the design of site-targeted drug release systems is an essential factor for improved oral bioavailability of various drug molecules.

There are various drug molecules with poor aqueous solubility, resulting in low bioavailability when administered orally, due to the limitations of their carrier system (Lipinski *et al.,* 2000). It has been reported that approximately 70% of new drug candidates have a problem of low water solubility (Kakran *et al.,* 2012). There are a number of negative clinical effects shown by poorly soluble drugs such as inefficient treatment, increase risk of toxicity or even death. Hence, poor solubility of drugs is amongst one of the major obstacles in the development of high efficacy pharmaceuticals (Kakran *et al.,* 2012), for example, anti-viral drugs (e.g. acyclovir) are mostly regarded as poorly permeable across the GIT membrane and have low solubility mainly in the small intestinal region (Tomar *et al.,* 2010). Additional groups of drugs such as anti-fungal, hormonal agents, chemotherapeutic and anti-parasitic are also regarded as poorly water soluble. This brings about limitations in their use. Hence the implementation of specially designed carriers/nanostructures for the improvement of their delivery is required (Yuri *et al.,* 2002). Researching alternative drug delivery systems during the early stages of drug development is therefore significant to avoid pitfalls in drug delivery to the body.

Manipulation of polymer features through nanotechnology provides advanced drug carriers for enhanced disease management and treatment. The polymers used during synthesis as a carrier system, determines the type of nanostructure and the kind of drug that can be incorporated as well as the release characteristics of the system (Husseini and Pitt, 2008). Polymeric nanoparticles are colloidal solid particles (Yih and Al-Fandi, 2006) that exist as shells or spherical structures (Kingsley *et al.,* 2006). Drugs can be integrated into polymeric nanoparticles by one of the following methods: encapsulation, attachment, dissolution, entrapment, or by adsorption (Arnal *et al.,* 2008). Nanoparticles also have the capability to penetrate the body tissues due to their small size. However, adequate knowledge on how

these nanoparticles interact with organisms and living cells is essential for effective treatment (Wang *et al.,* 2012).

This research focuses on improving the permeation and solubility of oral drugs, consequentially enhancing their oral bioavailability, as well as seeking to develop guiding principles to examine and solve key issues of their nano-encapsulation as a means to enhance their oral bioavailability. The physicochemical and physicomechanical properties of the drug delivery system was engineered by modifying specialised biopolymers to specifically regulate the solubility, permeability and bioavailability of the drug molecules and to produce an "intelligent" polymeric nano-enabled drug delivery system. Therefore, this study proposed a new integration of natural with synthetic polymers to develop a novel Semi-Synthetic Biopolymer Complex (SSBC) as a polymeric nanoparticle drug delivery system. This polymeric nanoparticle drug delivery system is anticipated to enhance the permeation and solubility of poorly permeable and soluble oral drugs, while ensuring low toxicity after oral administration.

1.2. RATIONALE AND MOTIVATION FOR THIS STUDY

This research study proposed to develop a novel Semi-Synthetic Biopolymer Complex (SSBC) loaded with acyclovir (ACV) as an orally administered enteric coated capsule. Acyclovir was selected as the drug of choice in this investigation in order to examine the functionality of the synthesized drug carrier (SSBC). Acyclovir was reported to be slightly soluble in water (pH 7.4) (2.558µg/mL) at room temperature (22–25^{o}C), possessing pH-dependent solubility (Susantakumar *et al.,* 2011). A study conducted on the pH dependence of ACV found that it had higher solubility in pH 9.8 (61.842µg/mL) in comparison to pH 6.8 (2.250µg/mL). **Table 1.1** shows the solubility profiles of ACV at different pH conditions (Chaudhary and Verma, 2014).

Table 1.1: The solubility profiles of acyclovir tested in different pH buffer solutions. (Chaudhary and Verma, 2014)

Sample number	Buffer solution	Solubility (µg/mL)
1	HCl buffer of pH1.2	18.315
2	Acetate buffer of pH4.5	10.064
3	Phosphate buffer of pH5.5	2.515
4	Phosphate buffer of pH6.8	2.250
5	Phosphate buffer of pH7.4	2.558
6	Borate buffer of pH9.8	61.842

The SSBC was developed to enhance the oral solubility and permeation of low permeable and soluble drugs such as ACV. As indicated, ACV is mostly poorly soluble in the small intestine (pH 5.5-6.8) compared to the stomach (pH 1.2) as observed in **Table 1.1**. Hence,

the final formulation was enteric coated to avoid degradation of ACV in the acidic conditions of the stomach (Khokale and Patil, 2004; Sinha *et al.,* 2007) and only release the nano-formulation in the small intestine. Therefore, the solubility and permeability of ACV is believed to be enhanced by the SSBC so as to achieve the maximum absorption through the small intestinal duodenal epithelium. Novel synthetic methods employing natural and synthetic polymers were used to fabricate the ACV-loaded SSBC and to additionally modify the physicomechanical and physicochemical properties of the polymer nano-structure in order to achieve a superior solubility and permeation of ACV.

Following preliminary investigations for identification of the appropriate polymers that could be integrated into the SSBC, it was found that the complex would comprise of a natural polysaccharide (e.g. hyaluronic acid) (HA) and a synthetic polymer (e.g. poly (acrylic acid)) (PAA) with an addition of a synthetic permeation enhancer (e.g. **(**2-hydroxypropyl)-β-cyclodextrin (HP-β-CD)). This newly developed SSBC would not just enhance intestinal oral drug permeation and solubility, but would also protect the encapsulated drug against harsh GIT conditions, allowing more ACV to be available at the membrane barrier for entry into the blood.

The SSBC comprised of three components as described above. The nano-size and spherical shape of the final formulation would be facilitated by emulsion techniques and the solution subsequently subjected to spray-drying (Nano Spray Dryer B-90, Buchi, Switzerland) in order to obtain a free-flowing powder of spherical nanoparticles. This formulation of ACV-loaded SSBC may be an alternative formulation for the already existing ACV formulation on the market. The selected polymers and the chosen size were proposed so as to enhance the dissolution of low soluble oral drug in aqueous medium by enhancing the surface area for hydration. The SSBC formulation was proposed to give an enhanced bioavailability compared to the existing formulation in the market, due to the improved solubility and reduced size as mentioned. The targeted area for the drug absorption is the small intestinal region as shown in **Figure 1.1**. For the protection of the capsule against ACV degradation in the acidic gastric conditions (Khokale and Patil, 2004; Sinha *et al.,* 2007), the capsule was enteric-coated as highlighted, thus targeting release of the ACV-loaded SSBC in the small intestine.

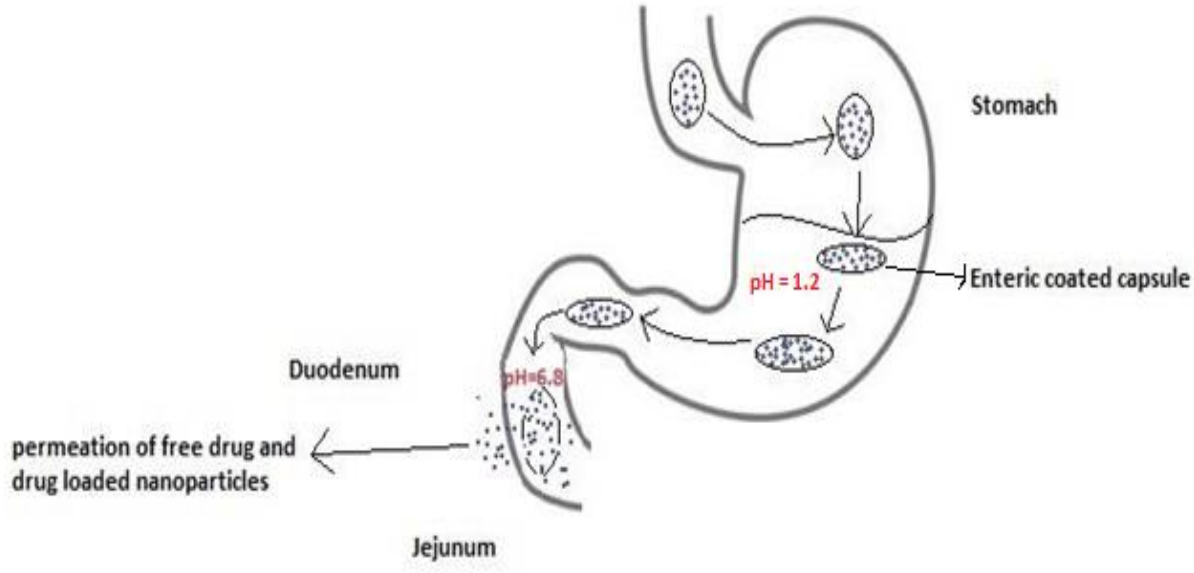

Figure 1.1: Representation of the site of permeation\absorption of the drug loaded nanoparticles and free-drug.

Many strategies have being developed to overcome the challenge of low permeation and solubility of drugs using polymeric and lipid systems. Even so, many of these drugs still present multiple side-effects and high toxicity not only associated with their low solubility, but also with the method of drug delivery. Designing SSBC polymeric system will be beneficial because the drug can be entrapped in the core of the system (as shown **Figure 1.2**) and this nano-structure has the potential to enhance the solubility and permeation of the encapsulated drug. **Figure 1.2** highlights the general process of drug encapsulation within the polymeric complex matrix.

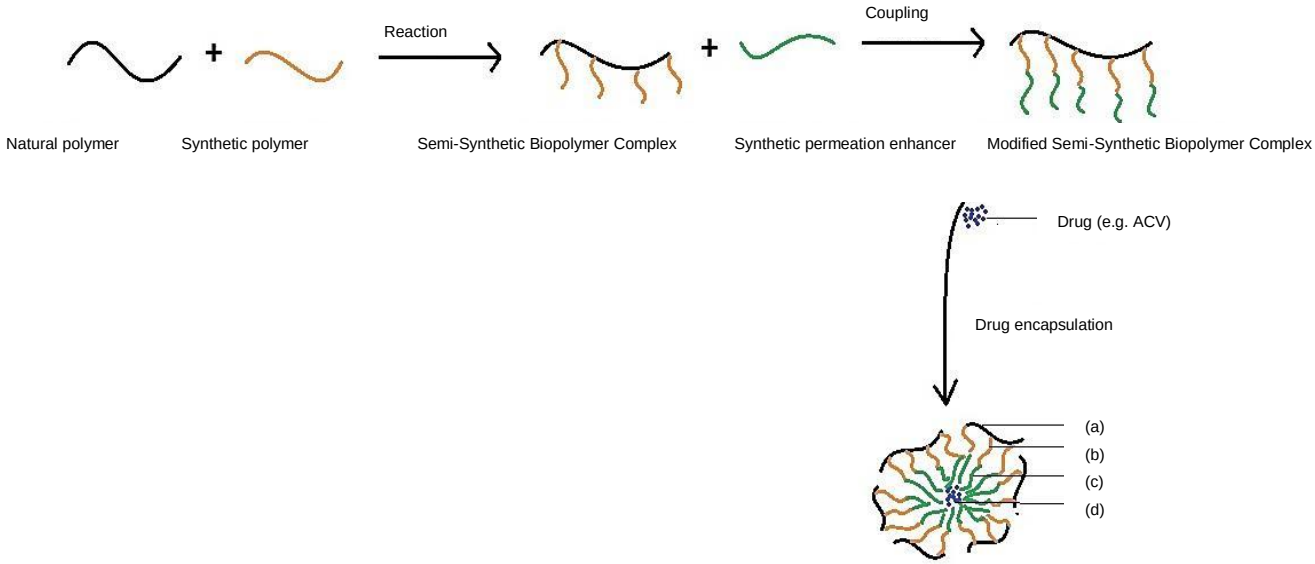

Figure 1.2: Schematic representation of the encapsulation of drug, where (a) natural polymer, (b) synthetic polymer, (c) additional synthetic chemical and (d) encapsulated drug.

1.3. AIM AND OBJECTIVES OF THIS STUDY

The aim of this study was to synthesize a novel Semi-Synthetic Biopolymer Complex (SSBC) oral drug delivery system, which led to the enhancement of oral bioavailability of low permeable and soluble drugs. This aim was achieved with the following objectives:

1. Selection and modification of suitable polymers (natural and synthetic polymers) that may be employed for the development of the Semi-Synthetic Biopolymer Complex (SSBC).
2. Critical literature evaluation in the field of SSBC as oral nano-enable drug delivery systems, in order to acquire knowledge on the research accomplished in this field of study.
3. Development of novel SSBC loaded with an appropriate prototype drug molecule and characterized to obtain fundamental physicochemical and physicomechanical properties.
4. To optimize the developed nanopolymeric formulation using a face-centred central composite design.
5. To perform *in vitro* drug release analysis for determination of drug release characteristics of the SSBC system.
6. To perform e*x vivo* tissue permeation studies of the nanostructure, using pig intestinal tissue, as well as undertaking cytocompatibility analysis using caco-2 cells.
7. To conduct *In vivo* drug release evaluation to assess the nano-delivery system in a suitable animal model.

1.4. NOVELTY OF THIS STUDY

1. An integrated novel system known as SSBC has been synthesised in the effort to overcome the limitations associated with previous polymeric drug delivery systems. The SSBC will comprise of at least two new chemical integrated components: i.e. natural and synthetic polymers. The drug delivery system/complex is completely novel, and has not been formulated in previous studies published.
2. The novel drug-loaded polymeric nano-system powder was prepared by an innovative combination of two processes: The first being the emulsification process, followed by the unique nano-spray drying technique.
3. Different bioactive molecules such as drugs, genes and proteins can be entrapped, adsorbed, or covalently attached in the hybrid system of the SSBC. The polysaccharide (natural polymer) component of the system core is biocompatible and the composite structure of the SSBC exhibits similar attributes to that of the cell membrane.

4. The selection of polymers was directed toward enhancement of permeation and solubility of oral drugs and the potential to be reduced to nanoparticles.

1.5. OVERVIEW OF DISSERTATION

CHAPTER 1: This chapter provides a background of current research in the field, providing challenges faced with oral drug delivery systems, particularly for drugs with low permeation and solubility in the GIT. The rationale for this research is stressed, with the aims and objectives of undertaking this research outlined in detail.

CHAPTER 2: A literature review, substantiating the science behind the formulation of Semi-Synthetic Biopolymer Complex (SSBC) systems, as drug delivery carriers. This chapter focuses on various ways of fabricating SSBC systems and the critical factors to be considered when synthesising these complexes. The limitations of using natural or synthetic polymers alone and the benefits of using a hybrid of natural and synthetic polymers as drug delivery systems are also discussed in detail.

CHAPTER 3: This chapter provides the preliminary experimental laboratory formulation synthesis, as well as physicochemical and physicomechanical characterization, in conjunction with *in vitro* release analysis and permeation studies. The preformulation parameters of this complex are also discussed, with various techniques used to characterize the interaction of the precursors and the newly-formed complex. Some of the studies undertaken include attenuated total reflection transform infrared spectroscopy (ATR-FTIR), Differential scanning calorimetry (DSC), thermogravimetric analysis (TGA), and proton nuclear magnetic resonance imaging (^{1}H NMR).

CHAPTER 4: This chapter describes in detail the analysis and optimization of the drug-loaded SSBC, prepared according to variables using a face-centred central composite design program. The formulation was analysed using four main parameters, namely: particle size, drug entrapment, solubility, permeation efficiency. Following responses from the central composite design, an optimised formulation was determined.

CHAPTER 5: *In vivo* studies are the main focus in this chapter, employing a Large White Pig model for clinical pharmacokinetic observation. At predetermined time intervals, blood samples were collected and analysed, after dosing the synthesised SSBC ACV-loaded nanoparticles and comparative formulations. The amount of the drug present in blood plasma was quantified and detected using Ultra Performance Liquid Chromatography (UPLC), thereby determining the percentage bioavailability of drug.

CHAPTER 6: This chapter completes the dissertation, providing a conclusion and a perspective recommendation in the field of SSBC technologies for drug delivery.

CHAPTER TWO

SEMI-SYNTHETIC BIOPOLYMER COMPLEXES: MODIFIED POLYSACCHARIDES AS ORAL DRUG NANO-CARRIERS FOR ENHANCEMENT OF ORAL BIOAVAILABILITY

2.1. INTRODUCTION

Oral drug delivery remains the most convenient and preferred route of pharmaceutical administration. Historically, progress has been made in oral drug delivery technology, including controlled release of various active pharmaceutical ingredients (APIs). Currently, the major focus in drug delivery systems is designing cheap and non-conventional oral drug delivery systems with improved pharmacokinetics (Vashista *et al.,* 2012). Conventional capsules or tablets move through the gastrointestinal tract (GIT) and release drug in non-specific regions within the GIT (Helliwell, 1993). Therefore, the design of specifically targeted drug carrier systems is a pre-requisite to advance the oral bioavailability of various drug molecules. Nano-engineered drug carrier systems are believed to have the ability to enhance delivery of variety of APIs orally, by improving their bioavailability and they gained substantial recognition in this pharmaceutical research.

Polymeric nanoparticles have thus achieved greater significance in pharmaceutical research because of their capability to distribute APIs in various parts of the body for prolonged periods of time. Polymeric nano-carriers can be fabricated from synthetic or natural polymers (Bala *et al.,* 2004) or semi-synthetic polymeric (Adikwu, 2009). The usage of different polymeric resources and their handling permits conjoining of their physical and chemical properties (e.g. surface charges, hydrophobicity/hydrophilicity). Polymeric nanoparticles flexibility permits them to be used in delivery of extensive variety of APIs intended for oral delivery (Chan *et al.,* 2010). The mechanism of enhanced oral drug absorption from polymeric nanoparticles involves the extension of the drug residence time in the GIT, shielding of the APIs from the harsh environment of the gut, endocytosis of the particles and/ or an enhanced permeability effect of the polymer.

Each prepared oral polymeric nanoparticulate system (Bala *et al.,* 2004; Adikwu, 2009) is designed to possess enhanced properties. However, both natural polymers and synthetic polymers individually have limitations in performance as nano-based delivery systems. **Table 2.1** describes the limitations of synthetic and natural polymers over semi-synthetic polymers in drug delivery. Interest has increased greatly in material science and pharmaceutical research for combining synthetic and natural polymers into hybrid polymer structures known as SSBC. The functionality of biopolymers or natural polymers can be

combined with the synthetic polymers versatility and adaptability, thus generating a new type (class) of polymer constituents harnessing the best of both worlds (Deming, 1997; Hawker *et al.,* 2001; Matyjaszewski and Xia, 2001; Cunliffe*, et al.,* 2004; Vandermeulen and Klok, 2004; Alarcon *et al.,* 2005; Moad *et al.,* 2005; van Hest, 2007).

These SSBC are currently exploited in drug delivery systems as carriers/nano-carriers for a variety of drugs in an attempt to overcome limitations associated with both synthetic and natural polymers as well as poor solubility of many of the drug molecules. This chapter primarily focuses on the application of SSBC as nano-carriers for oral delivery of drugs. Insight into the factors influencing their solubility and permeability leading to high oral bioavailability, such as physicochemical properties, is provided; and their methods of preparation are also discussed in detail.

Table 2.1: Limitations and benefits of natural polymers, synthetic polymers and semi-synthetic biopolymer complexes

Polymers	Limitations	Benefits
Natural polymers	Natural polymers have poor thermal and mechanical properties (Sionkowska, 2011), hence their native structures are easily destroyed during high temperature processing thereby limiting their use in the biomedical field.	Have good biodegradability and biocompatibility (Giusti *et al.,* 1993).
Synthetic polymers	Synthetic polymers contain impurities or other compounds that affects biocompatibility (Sionkowska, 2011). Environmental pollution by synthetic polymers from developing countries has also been identified in dangerous proportion (Joshi and Patel, 2012).	Synthetic polymers are flexible in structural make up and also flexible with the manner in which molecules are related (Deming, 1997; Hawker *et al*., 2001; Matyjaszewski and Xia, 2001; Moad *et al*., 2005). They have a very good thermal stability and mechanical properties compared to most natural occurring polymers (Giusti *et al.,* 1993).
Semi-synthetic biopolymers	The limitation of semi-synthetic polymers depends on the particular mixture or combination of synthetic and natural polymers.	Natural polymers modified by blending/grafting/crosslinking amongst others with synthetic polymers or synthetic chemicals result in new materials that contains properties of both polymers, thus possessing good mechanical and thermal properties, while at the same time being biocompatible (Sionkowska, 2011).

2.2. ORAL NANO-POLYMERIC ADMINISTRATION OF DRUGS EMPLOYING SEMI-SYNTHETIC POLYMER COMPLEXES

A noteworthy study was conducted for the preferred route of administration for patients with breast cancer. The investigation on the study of delivery of anticancer drugs revealed that the oral route of administration is preferred by patients over intravenous therapy (Banna *et al.,* 2010). Liu and co-workers (1997) stated that oral administration is preferred by ~89% of patients over intravenous administration, primarily because of home-based therapy. It was also reported from a study on patient's preference about the route of administration that ~2.7% patients prefer to be treated using parental route, whereas almost ~78.7% prefers oral route and ~18.6% had with no preference (Wojtacki *et al.,* 2006). Oral delivery of drugs has huge challenges originating from their unusual physicochemical properties, and physiological barriers such as gastrointestinal instability leading to low bioavailability of APIs. For example, in the case of drugs such as docetaxel, paclitaxel amongst others, the available drug content detected in systemic circulation (oral bioavailability) is only in the range of 5-20% after oral administration.

Oral administration of drugs such as insulin also poses a huge challenge. Insulin is mainly parentally administered and this form of administration suffers from stress generated from the various regimens, such as pain, skin bulges, allergic reactions, common infections amongst others. The invasive parenteral (injected) route of administration of insulin is also associated with poor pharmacodynamics, weight gain and delivery of drugs to the wrong tissues. An alternative transport path is essential so as to reach the circulation by non-invasive ways. Currently, in the case of insulin, advanced nanotechnology has been applied to various modified natural polymers (SSBC) (Abbad *et al.,* 2015) and natural/biological polymers as delivery systems for problems associated with its oral administration (Mukhopadhyay *et al.,* 2012).

2.2.1. Semi-Synthetic Complexes as Oral Drug Permeation/Absorption Enhancer

Most of the polysaccharides used in design of drug delivery systems are bioadhesive polymers (e.g. chitosan, hyaluronic acid, oxidised dextran, starch) (Hoffmann *et al.,* 2009; Yerushalmi and Margalit, 1998). Nanoparticles formulated from these modified polysaccharides (bioadhesive) systems (complexes) adhere to the mucosa surface of the cell membrane resulting in the modification of the properties of the mucosa surface through polymer bioadhesion; this will increase the residence time and contact of the drug with the epithelium. Consequentially, the drug amount (concentration) will increase at the absorption/permeation site; this will minimize drug degradation and dilution by the luminal contents, leading to the enhancement of the drug absorption into the circulation system.

Semi-Synthetic Biopolymer Complexes are mainly composed of two or more polymeric components as mention before, one of the components can be either bioadhesive (e.g. polysaccharides) or a permeation enhancer (e.g. (2-Hydroxypropyl)-β-cyclodextrin). Briefly, the intestinal mucous permeation enabled by absorption enhancers involves membrane agitation which increases the permeability of drugs (Moideen and Kuppuswamy, 2014).

2.2.2. Factors Influencing Drug Release after Oral Administration

Oral drug release is influenced by solubility of the drug in relation to the ratio of dispersed and continuous phase, the concentration of polymer to drug (Niwa *et al.,* 1993; Niwa *et al.,* 1994), polymer concentration and type of polymer (Dhakar *et al.,* 2010). Hence, the amount of drug loaded has a profound influence on the drug release kinetics (Makadia and Siegel, 2011). Certain drugs have the capability to degrade the polymer matrix either through bulk erosion or by surface degradation, thereby controlling the rate of polymer degradation. Even though there is no significant correlation between the drug chemistry and hydrophilicity to the release kinetics, in order to explain the drug release mechanism of certain drug delivery systems, one must consider the effect of chemical properties of drugs on biodegradability of the polymers (Makadia and Siegel, 2011).

2.3. POLYMERIC PHYSICOCHEMICAL AND MECHANICAL ATTRIBUTES THAT INFLUENCE ORAL BIOAVAILABILITY

The physical and chemical characteristics of polymeric micro/nano-particulate delivery systems affect the absorption and possess an essential role in the internalization of particles through the GIT membrane. Some of these attributes are the shape and size of particles, particle surface properties, as well as excipients, amongst others (Thanki *et al.,* 2013). The excipients (e.g. polymers or chemicals) exist in many forms and were considered inert due to the fact that they do not produce any therapeutic action, but modify the drug's pharmacokinetics. It is known that excipients do in fact influence the rate and the extent of drug absorption, hence drug bioavailability (Vilar *et al*., 2012).

2.3.1. The Influence of Size on the Internalization of Particles

Particle size of the drug loaded biopolymeric or SSBC carriers do influence the amount of drug that reaches the circulatory system; consequently it influences bioavailability (Makadia and Siegel, 2011). It is well established that a small change in size, atomic arrangement or molecular structure of particles can have an intense impact on their behaviour and chemical properties (Guihen, 2013). The internalization of particles within the intestine and the degree of absorption depend mostly on the particle size, hence, the extent of drug absorption increases with a decrease in the size of particles and surface area specificity. It has been

shown that the ratio of surface area to volume has significant effects on degradation. The increase in surface area increases the degradation rate of the matrix (Makadia and Siegel, 2011). Jani and co-workers (1990) examined the size-dependent internalization of nanoparticles through rat intestine by analyzing their presence in the blood system and their delivery to different organs. After administration of the same dose of nanoparticles, (34% of nanoparticles) were detected in the intestinal mucosa and gut-associated lymphoid tissue having a size of 50nm; whereas this decreased to 26% detection for nanoparticles of a size of 100nm; and for 500nm particles, only 10% were found in the intestinal tissues (Francis *et al.,* 2004). However, the internalization of large particles (~1µm in diameter) was found to be marginal. These micro-particles were mostly found in the lymph nodes of the small intestine. Desai and co-workers (1996) observed similar findings for internalization of nanoparticles fabricated from poly (lactide-co-glycolic acid) (PLGA). It was observed that 100nm nanoparticle internalization was improved compared to micro-particles of 1 and 10µm diameter (Desai *et al.,* 1996*).* Consequently, size is a significant parameter in controlling the internalization of nanoparticles into the GI membrane, and as a result, the required size for the internalization of particles must be smaller than 500nm (Francis et *al*., 2004). The preferred nano-carrier range for internalization in the GI tract are particles in the size range of 50-300nm, with a hydrophobic surface and positive zeta potential (Thanki *et al.,* 2013). In one study, it has been reported that the solvent choice and the aqueous solution ratio to organic solvent can also control the size of the nanoparticles (Nordstrom, 2011).

2.3.2. The Composition Effect or Chemical Effect

There is extensive literature available signifying that the hydrophobicity of the particles has a major role in drug absorption. Francis and co-workers (2004) reported that particles that are hydrophobic e.g. poly (styrene) (Murayama *et al.,* 1993) absorbs drug more readily than poly (lactide-co-glycolic acid), a less hydrophobic polymer compared to poly (styrene) (Francis *et al.,* 2004). This affects the bioavailability as well, since very polar molecules have difficulties crossing biological membranes whilst hydrophobic molecules more readily partition across biological membranes (Mansy, 2015).

2.3.3. The Carrier Geometry Effect

In drug delivery field there is a great interest in the role played by the carrier geometry in its functions such as drug loading and release, stability, toxicity and ultimately delivery performance. A spherical geometry is the most common geometry in nano drug delivery systems. Theoretically non-spherical drug carriers can provide great benefit for drug targeting. Firstly, the larger surface area to volume ratio of a non-spherical nano-carrier leads to a large surface area available for conjugation of targeting moieties, hence avoiding

limitations such as retention. Correspondingly, the smaller nano dimension of non-spherical nano-carriers allows effective perfusion through capillaries, potentially enhancing access to varied targets that are inaccessible by larger spheres. This results in the enhancement of bioavailability (Simone *et al.,* 2008).

2.4. PREPARATION OF SEMI-SYNTHETIC BIOPOLYMER COMPLEXES

Semi-Synthetic Biopolymer Complexes can be prepared by modification of natural polymers through blending/crosslinking/grafting amongst others with synthetic polymers or synthetic chemicals.

2.4.1. Blending

Blending is a convenient route to develop new copolymers or new polymeric materials with improved mechanical properties as well as biocompatibility of the individual polymer components. The new material or copolymer is called a biosynthetic, bio-artificial, or SSBC material (Sionkowska, 2011). Blending of biopolymers or natural polymers with synthetic chemicals or synthetic polymers has been reviewed and carried out in various investigations (Giusti et *al.,* 1993; Cascone. 1997; Werkmeister *et al.,* 1998; Sionkowska, 2003).

Blending is also an alternative way of tailoring hydrophilicity/hydrophobicity of the matrix without incurring any major changes in the mechanical reliability. For the blending of polymers, the two polymers are mixed to form one versatile material. The same solvent can be used to dissolve the polymers and/or the polymers can be mixed in the molten state. Solid-phase modification of polymers is one of the more promising methods because of the combined action of shear deformation and high pressure on the mixture of solid components (Sionkowska, 2011). The conditions allow the precursor polymers to be subjected to plastic flow with unlimited strain. The high temperature and pressure employed can damage proteins. Protein denaturation can be avoided by preparing biopolymer blends that are solubilized in the same solvent.

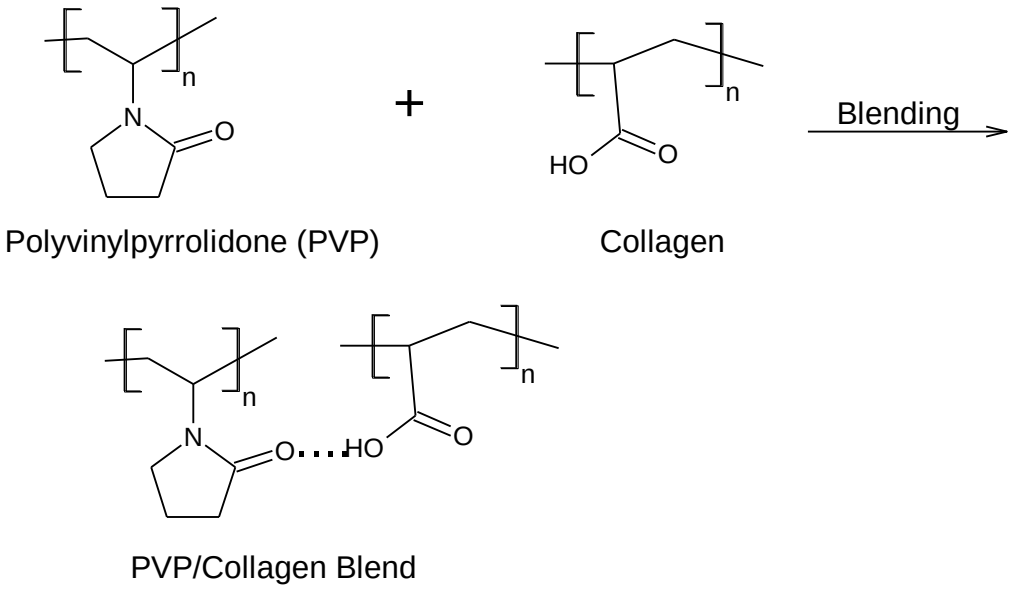

Figure 2.1: Collagen/PVP polymeric blend formed through hydrogen bonding.

For the synthesis of SSBC, the basic properties of the synthetic and natural/biological polymers need detailed understanding. Miscibility of different polymers will determine the blending characteristics of the complex (Sionkowska, 2003). Blending methods are advantageous because they are cheaper and it takes less time for the development of new materials that have improved properties. A supplementary benefit of polymer blends is the fact that it is easy to change the blend composition to improve their properties (He and Inoue, 2004). The process of blending of collagen (natural polymer) (Sell *et al.,* 2010) with polyvinylpyrrolidone (PVP) (synthetic polymers) (Kowalonek and Kaczmarek, 2010) is shown in **Figure 2.1**.

2.4.2. Crosslinking

Crosslinking of natural polymers with synthetic polymers or synthetic chemicals is another method of preparing SSBC. For example, modification of hyaluronic acid (HA) with functionalized hydrazides (via crosslinking), as visualized in **Figure 2.2,** furnishes an adaptable and mild method for generating new biomaterials for drug delivery. For example, crosslinking has demonstrated the ability to develop novel biomaterials by chemical modification of hyaluronic acid (Prestwich *et al.,* 1998).

Starch is another natural carbohydrate polymer that is used in many aspects of life, as a foodstuff, in chemical sectors, as well in pharmaceutical research. Starch is mostly used as a tablet excipient, but not in its unmodified form (Adikwu, 2009). In the past years, structural modification of starch has been reported for the improvement of its utility in various

applications. A number of techniques have been employed in starch modification; this involves the addition of chemicals which provide a novel chemical functionality and/or shape, size change, or alterations to the structure of molecules of starch. In current pharmaceutical research, starch plays a huge role in the development of novel drug carriers (Adikwu, 2009). Starches are mainly hydrophilic with long chains which increase the viscosity, independent of temperature. Amylose chains have an inner hydrophobic section and have a tendency of coiling up into helices (spirals). Hence, within the helix it allows the entrapment of fats, oils, aromatics and hydrophobic drugs. A few examples of crosslinked starch are rice starch crosslinked with epichlorohydrin for altering the properties of rice starch (Xiao *et al.,* 2012), waxy maize starch crosslinked with phosphorous oxychloride ($POCl_3$), and citric acid crosslinked starch to improve tensile strength, thermal stability and decrease dissolution of the starch films in water (Reddy and Yang, 2010).

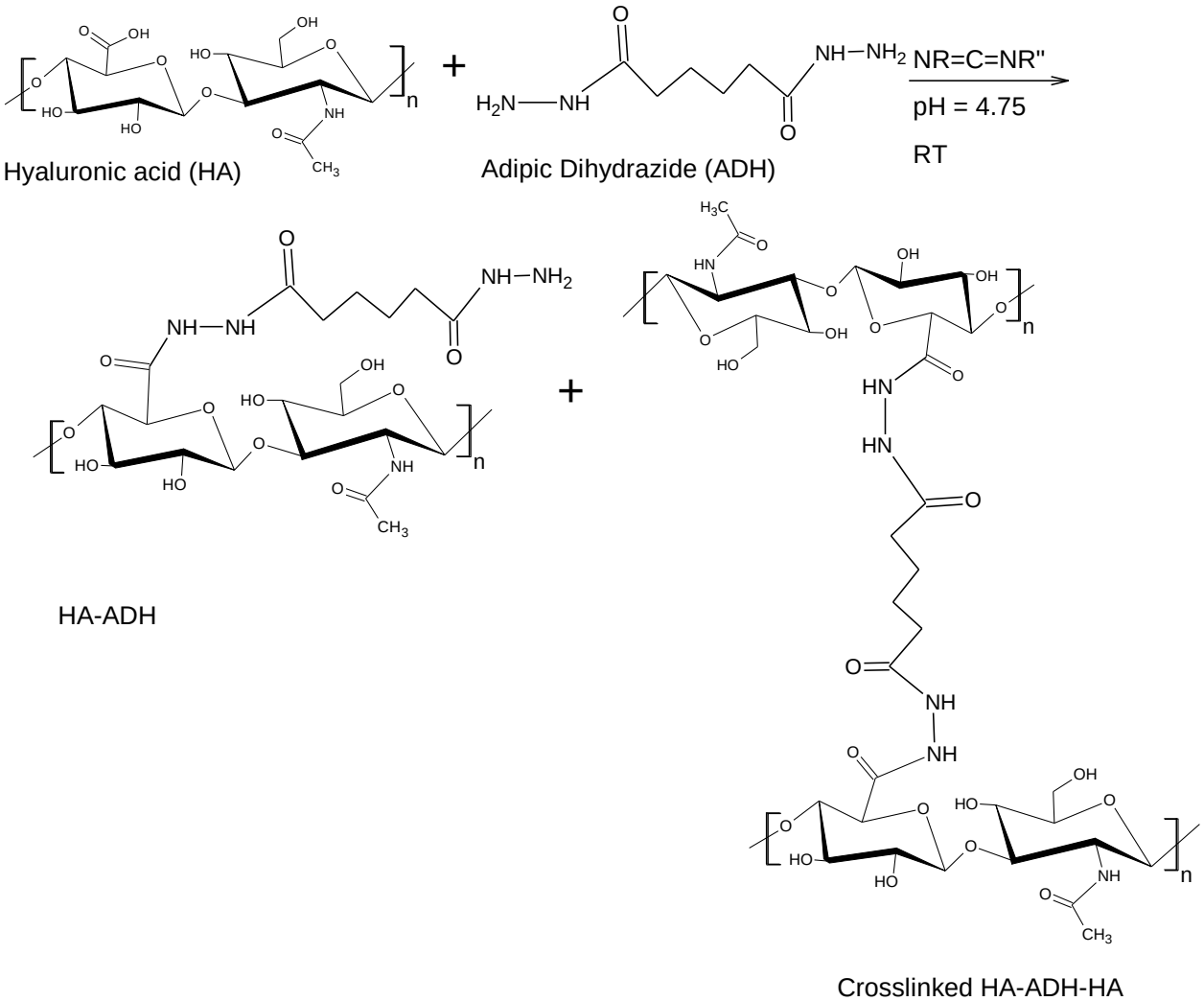

Figure 2.2: Modified and Crosslinked HA with Adipic Dihydrazide (ADH).

2.4.3. Grafting

Grafting is an additional method of preparing SSBC, where one or more blocks of macromolecule side chains are connected to the main polymer chain (Athawale and Rathi, 1999). Grafted copolymers consist of "a polymer backbone with adjacent covalently connected chains". The side-chain and the backbone polymers both can be copolymers or homopolymers (O'Connell *et al.,* 2008). The principle of polymer grafting is based on generation of the active sites, such as functional groups or free radicals on the backbone. **Figure 2.3** shows an example of alginic acid grafted with poly (acrylamide) for the modification of alginic acid physicomechenical properties.

They are several methods suggested for the preparation of graft copolymers by conventional chemical techniques (Battaed and Tregear, 1967; Burlant and Hoffmann, 1960). Formation of an active site in the precursor polymeric backbone is a favoured path in most methods of polymeric grafting. This active site (functional/chemical group or free radical) may be involved via condensation or an ionic polymerization process. Ionic polymerization takes place either in a substantial amount of alkali metal hydroxide and/or in hydrous medium. The chemical graft copolymerization method uses chemicals that act as initiators to produce active sites on the polymeric backbone. The use of different redox initiators such as string bases, Lewis acids and metal carboxyls has been reported for chemical grafting (Misra and Dgra, 1980; Chiang Wy, 1996; Cho and Lee, 2002; Hsu and Pan, 2007).

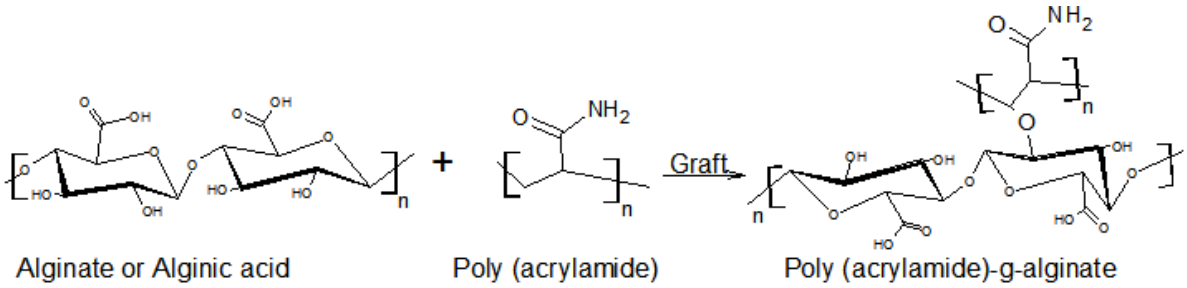

Figure 2.3: The chemical structure of an alginate graft copolymer.

Other methods that are adopted to prepare graft copolymers are electron beam or gamma ray irradiation, microwave irradiation and conventional redox grafting (Wong, 2011). Microwave irradiation was preferred amongst these methods for grafting and falls under the concept of green chemistry, where additional free radical initiators can be avoided, with no significant steric hindrance. Nonetheless, microwave grafting for alginate copolymerization is employed less often than the redox approach (Wong, 2011).

2.5. SYNTHESIS OF SEMI-SYNTHETIC BIOPOLYMERIC NANO-COMPLEXES AND DRUG LOADING

Nano-complexes or nanoparticles of SSBC for oral administration of drugs are synthesized using different methods, such as micro-emulsion, self-assembly (reverse micelle formation), emulsified solvent diffusion, emulsion-droplet coalescence, complex coacervetion/solvent evaporation, ionic gelation, and polyelectrolyte complexation (PEC). Most of these methods are mild and simple hence maintaining the drug integrity (Mukhopadhyay *et al.,* 2012). Drug loading into the nano-polymeric copolymers or polymers can be achieved via two methods. In the first method, the drug is incorporated at the same time or during the synthesis of the nano-polymeric formation; and in the second method, the drug is adsorbed after the preparation of the nano-polymeric system, by incubating the nano-polymeric system in the solution of the drug. However, it was noted that a greater amount of a drug was entrapped when using the incorporation approach (first method) compared with adsorption (second method) (Alenso *et al.,* 1991; Ueda *et al.,* 1998). Though, choice of a suitable method also depends on the solubility properties of the drug and polymeric materials used. **Figure 2.4** shows an overview of polymeric nanoparticles' preparation.

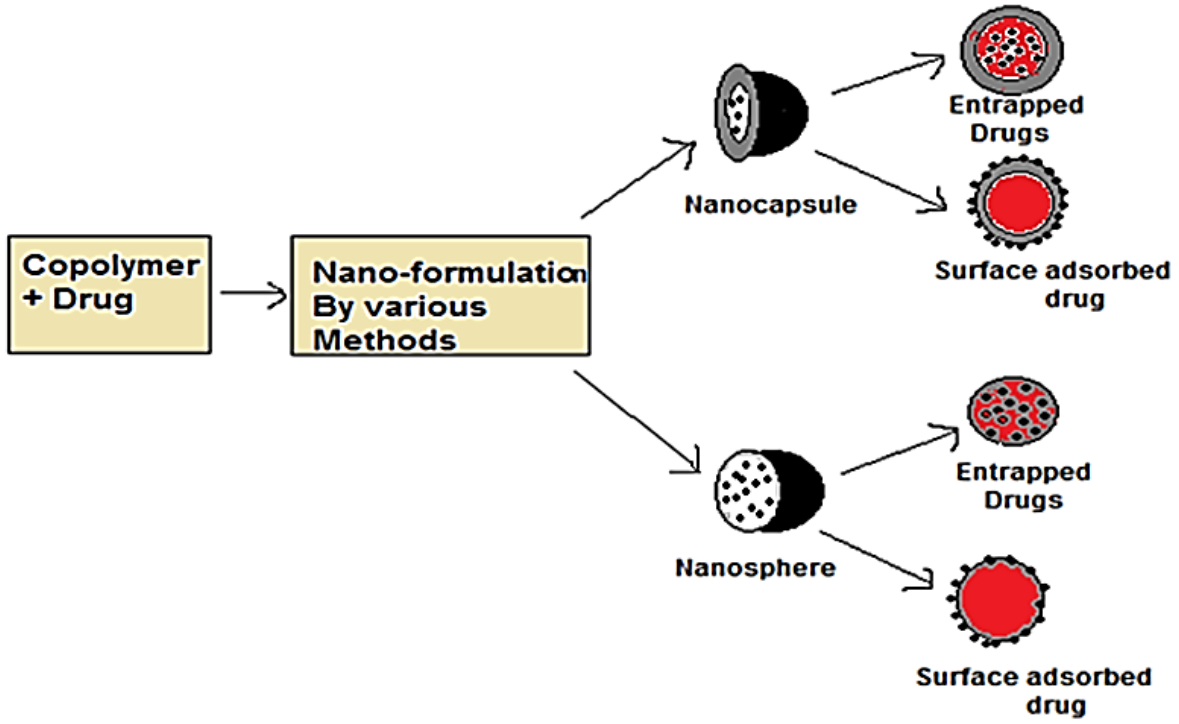

Figure 2.4: Schematic overview of preparation and drug incorporation into semi-synthetic polymeric nanoparticles (Kumari *et al.,* 2010).

2.6. BENEFITS OF THE SEMI-SYNTHETIC BIOPOLYMER NANO-COMPLEXES FOR DRUG DELIVERY

A group of chemotherapeutic, antifungic, antiparasitic and hormonal drugs are poorly soluble in water. This is a limiting factor in their use and requires the implementation of specially designed nanostructures for improving their delivery. Nano-encapsulation of such poorly soluble drugs is significant, since this may decrease toxicity and side-effects related with these drugs (Christian and Schwendeman, 2008). Novel nano-enabled drug distribution carriers need to be advanced and improved for them to effectively deliver these drugs (Yuri, 2002). Most new drug molecules have low molecular weights. It has being predicted that up to 70% of New Chemical Entities (NCEs) show poor solubility. Researching alternative delivery systems during the early development phase of the drug is therefore significant to avoid pitfalls of the drug delivery to the body.

Many approaches have been established to overcome the hydrophobicity of drugs using polymeric and lipid systems. Even so, many hydrophobic drugs still present multiple side-effects and high toxicity not only associated with their low solubility, but also with the method of drug loading in the delivery system. Designing amphiphilic or SSBC as a hydrophobic drug loading system is beneficial, due to the fact that the hydrophobic drug can be entrapped in the core (**Figure 2.5**) and this nano-system will be able to reduce the insolubility of these hydrophobic drugs (Trimaille *et al.,* 2006). Lipid-polymer complexes are also used since they are compatible with the biological system and pose minimal risk of toxicity, or rejection by the body's immune system (Cheow and Hadinoto, 2011).

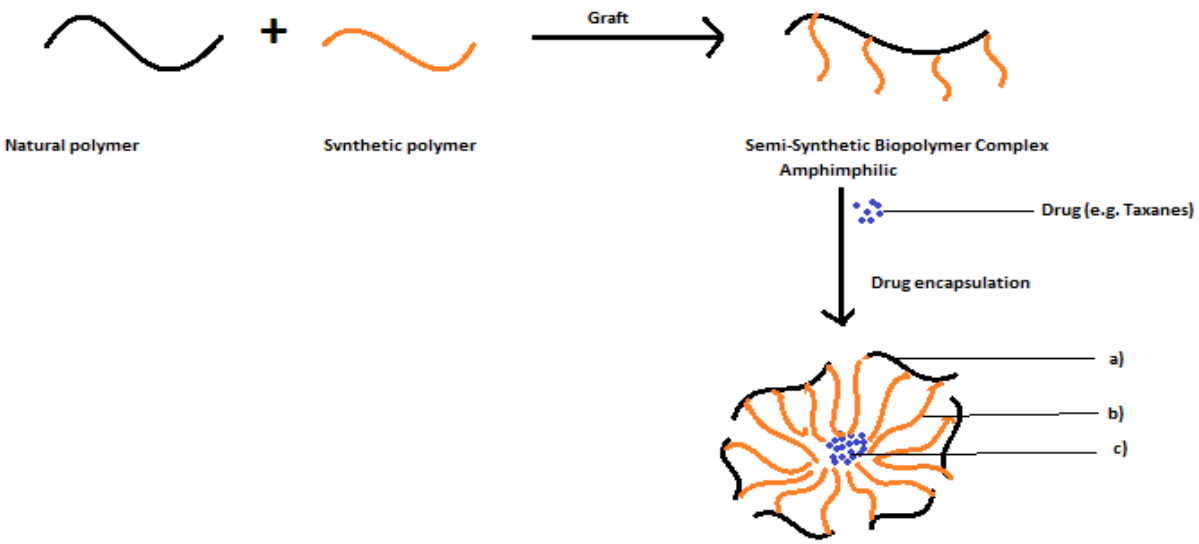

Figure 2.5: Schematic representation of the encapsulation of hydrophobic drugs: (a) hydrophilic polymer (b) hydrophobic polymer (c) encapsulated hydrophobic drug.

The development of different biopolymer drug delivery systems such as those based on polysaccharides (Oh *et al.,* 2009), proteins such as albumin, and aminopolysaccharides such as chitosan have attracted great attention in drug delivery research. The majority of these designed SSBC are amphiphilic (Pandey *et al.,* 2011). Therefore, amphiphilic nano-systems reduce the insolubility of poorly water soluble drugs, leading to an increase in bioavailability (Trimaille *et al.,* 2006). Most of these amphiphilic systems are micelles; hence their thermodynamic stability depends on their critical micelle concentration (CMC). A stable thermodynamic system has a concentration above the CMC. The hydrophilic-lipophilic balance (HLB) of the complex is largely affected by the CMC; it has being stated in many studies that: if the hydrophilic component is kept unhanged (constant), enlargement (increase) of the hydrophobic component will result in a low CMC compared to the complex concentration. This low CMC allows the complex to retain it micelle structure even after a series of dilutions. These micelle complexes retain their drug content and integrity before reaching the site target because of their slow dissociation, this is beneficial in the enhancement of oral bioavailability (Xu *et al.,* 2013).

2.7. EXAMPLES OF SEMI-SYNTHETIC BIOPOLYMER COMPLEXES AS DRUG NANO-CARRIERS

Polysaccharides contain various functional or reactive groups such as hydroxyl, carbonyl and amino groups (Lee *et al.,* 2000), which makes them easy to modify to enhance their properties. To date, nanopolymeric drug delivery systems have been developed using natural, synthetic or SSBC (Sarmento *et al.,* 2007). Polysaccharides possess favourable qualities as drug carriers (Sinha and Kumria, 2001), as most polysaccharides are hydrophilic, non-toxic, biodegradable, and highly stable. There are various reports about polysaccharides and their modified versions as drug nano-carriers (Rubinstein, 2000; Vandamme, *et al.,* 2002; Lemarchand *et al.,* 2004; Soumya *et al.,* 2013). In this review, three currently used modified polysaccharides, alginate, hyaluronic acid, and chitosan, having application in the formulation of SSBC for nano-systems formulation are discussed in detail below. **Table 2.2** highlights additional SSBC, their methods of preparation and route of administration. Routes of administration in addition to the oral route are provided as a point of comparison.

Table 2.2: Overview of the semi-synthetic biopolymer nano-complex-based bioactive delivery systems

Semi-Synthetic Biopolymer	Bioactive	Modification Method	Non-System	Rout of administration	References
Poly(oligo)saccharide grafted poly(D, l-lactide)	DNA	Reductive amination reaction	Nanoparticles	Intravenous	(Maruyama *et al.,* 1997)
Pullulan-grafted-Poly(l-lactide)	Doxorubicin	Free radical polymerization. Self-assembled amphiphilic copolymer system	Nanoparticle Micelles	Intravenous	(Zhang *et al.,* 2013)
Dextran-g-Poly(e-caprolactone)(PCL)	BSA and Lectins	Coupling agent	Nanoparticles	Oral	(Rodrigues *et al*., 2003)
Chitosan-g-Methoxy Poly(ethylene glycol)	Anionic drug	Oxidation method	Nanocarrier micelles	intravenous	(Yang *et al.,* 2009) and (Lin *et al*.,2008)
Chitosan-tripolyphosphate	Hydrophobic/hydrophilic drugs	Cross-linking	Gel/ nanoparticles	Intravenous	(Liu *et al*., 2008)
Poly(DL-lactide-co-glycolide)-graft pullulan(PuLG)	Doxorubicin/Adriamycin	Free radial polymerization	Micelles.	Intravenous	(Zhang *et al*., 2013)

2.7.1. Hyaluronic Acid Derivatives as Semi-Synthetic Biopolymer Complexes for Nanocarrier Formulation

Hyaluronic acid (HA) is a natural polysaccharide comprising of interchanging 1, 4-linked units of 1, 3-linked N-acetylglucosamine and glucuronic acid. Hyaluronic acid is immune-neural, mainly hydrophilic and has biodegradable short half-life; hence it is an ideal drug carrier for delivery of a wide range of bioactive materials. Hyaluronic acid biodegradable half-life is short. Hyaluronic acid can easily undergo chemical modification or chemical reactivity, due to its numerous functional groups (─CO_2H and ─OH) to form a new class of polymeric materials (Oh *et al.,* 2010; Xu *et al.,* 2012). Different chemical crosslinkers can be attached to HA allowing a wide range of potential methods for the fabrication of novel copolymeric systems for tissue engineering (Prestwich *et al.,* 1998). New drug bio-carriers can also be developed from the modification of HA and their preparation conditions methods are mild and versatile. As discussed in **Section 2.4.2**, HA crosslinked with polyhydrazides and further incorporation of therapeutic drugs leads to the formation of novel biomaterials for drug delivery.

A number of macromolecular prodrugs are already developed as HA-drug conjugates (Lapcik *et al.,* 1998; Toole, 2004). Deng and co-workers (2012) investigated HA modified with tetraethylene glycol for the attachment of cholesterol, thus forming an amphiphilic SSBC (Deng *et al.,* 2012). The formed amphiphilic SSBC, as shown in **Figure 2.6,** was used to form micelles loaded with doxorubicin hydrochloride drug, a poorly water soluble anticancer

drug. It was observed that this drug delivery system enhanced the permeation and retention effect in the tumour tissue and also enhanced the solubility of the hydrophobic drug, since many anti-cancer drugs are poorly soluble in water. This carrier led to the enhancement of the drug bioavailability by increasing the drug release with 20% compared to hyaluronidase free micelles during the *in vitro* drug release study.

Even though there is substantial literature reporting on modified HA as a drug carrier specifying the benefits such as enhancement of permeability at the tumour site and the solubility enhancement of hydrophobic drugs, only a few mentioned the chosen route of administration (Deng *et al.,* 2012).

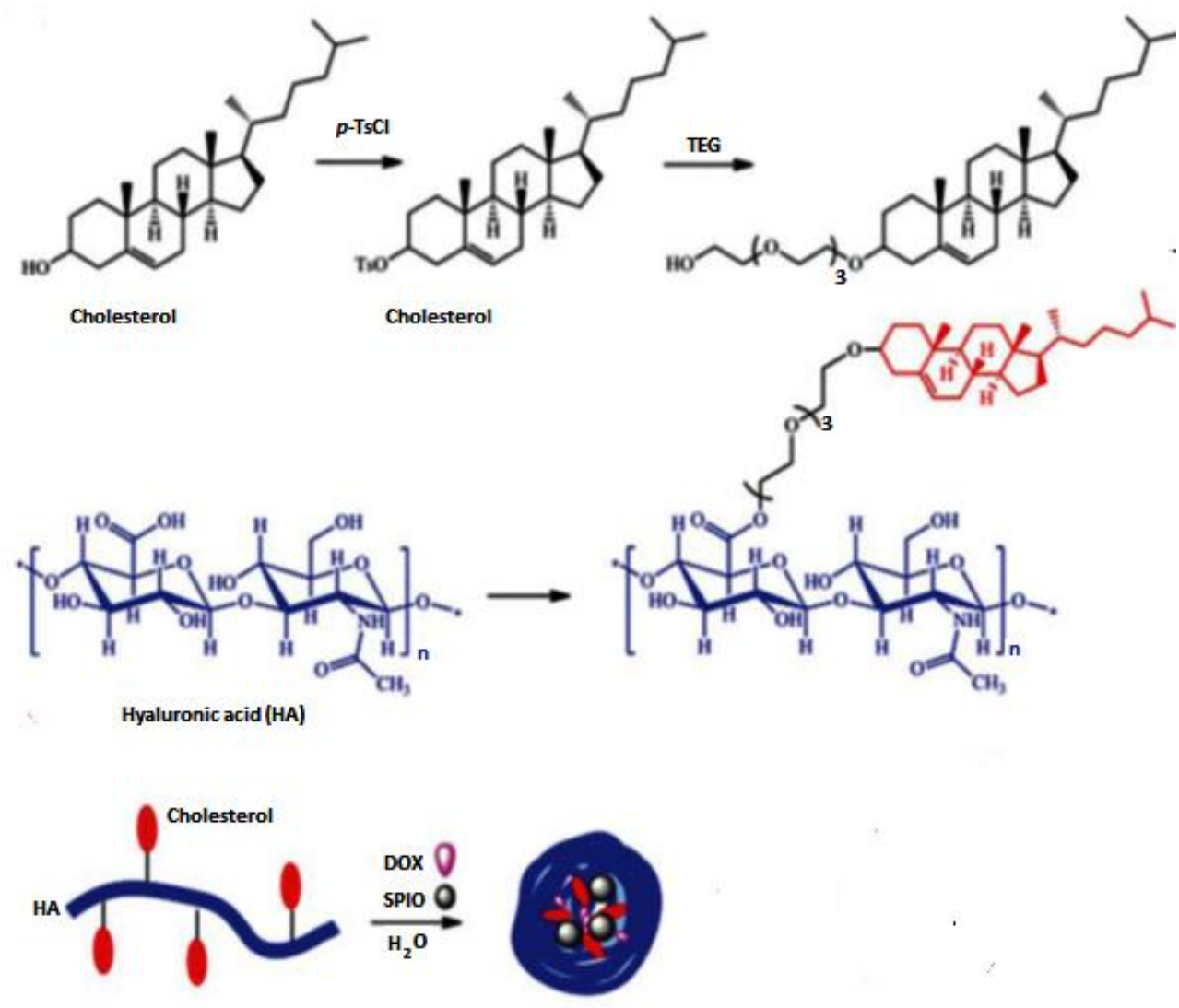

Figure 2.6: Schematic representation of DOX loaded Cholesterol-HA micelles (Deng *et al.,* 2012).

2.7.2. Chitosan Derivatives as Semi-synthetic Biopolymer Complexes for Nanocarrier Formulations

The available hydroxyl and amino groups of chitosan enable it to be modified easily to form derivatives of chitosan for oral drug delivery with desired properties (Werle *et al.,* 2009). Chitosan has been used in gene and protein delivery, especially as oral absorption enhancers (Khan and Khiang, 2002). Unmodified chitosan has limitations since at low pH, chitosan is highly soluble (Adikwu, 2009).

Lee and co-workers (1998) developed a hydrophobically modified chitosan possessing 5.1 deoxycholic acids per 100 anhydroglucose, showing self-assembling properties upon sonication. Hence, these self-assembling hydrophobic properties, modified chitosan, having an average diameter of 160nm, complexing with DNA, leading to a larger complex with the mean diameter of 300nm. Therefore, they are categorized under nanoparticles and considered to be the best delivery system in transferring genes in mammalian cells. They solve the problem associated with most gene delivery systems (e.g. viral vector) (Lee *et al.,* 1998).

Chitosan has been mostly used as a biopolymer for nanoparticle preparation among the various natural polymers (Allemann *et al.,* 1998), and it is highly exploited for oral insulin delivery leading to valuable outcomes for both *in vitro* and *in vivo* systems. For the design of protein/peptide oral nanoparticulate delivery systems (such as insulin), chemically-modified chitosan derivatives are more commonly employed than natural chitosan. Fernandez-Urrusuno and co-workers (1999) supported the concept that nanoparticles of chitosan maybe more efficient at enhancing protein uptake than chitosan solution (Fernandez-Urruuno *et al.,* 1999). Hence, greater cell uptake and binding was observed from chitosan-insulin nanoparticles after incubation with Caco-2 cells compared with chitosan-insulin solution. Therefore, oral administration of cyclosporine A encapsulated in chitosan hydrochloride nanoparticles to dogs, led to relative bioavailability of >73% compared with the commercial microemulsion (Neoral®) (Bowman and Leong, 2006). Chitosan's fundamental skeleton is not changed by the chemical modification, but its modification brings about improved properties, such as enhanced permeation and sustained release of drugs (Chaudhury and Das, 2011). Chitosan nanoparticles have been reported great carriers for oral insulin delivery systems. Notable results have been observed in SSBC nanoparticle grafts of poly (ethylene glycol) (PEG) with trimethyl chitosan (TMC) (PEG-g-TMC), enhancing oral biological activities after administration. Lin and co-workers (2007) also produced nanoparticles prepared from chitosan with poly (γ-glutamic acid) (γ-PGA) for oral insulin administration. It was found that this novel nanoparticle delivery system may permanently open the tight junctions between

the intestinal epithelial cells, overcoming the obstacle associated with the delivery of oral insulin solution without excipients. As observed from the oral administration of insulin from the diabetic rat model, rats that were orally administered with insulin-loaded nanoparticles significantly reduced the level of glucose by approximately 40% compared to rats that orally received insulin solution. A number of chitosan blends or grafts have been highlighted as attempts at enhancing permeability, leading to increased oral bioavailability (Mukhopadhyay *et al.,* 2012).

Advantages in the development of chitosan nanoparticulate systems includes the absence of hazardous organic solvents during their preparation, since chitosan is soluble in aqueous acid solutions, and they contain the amine functionality that can be used for crosslinking, as well as possessing low toxicity. It has been reported to be non-toxic *in vivo* in rats up to 10% of the diet (Arai *et al.,* 1968). For the development of new gene and GI delivery systems, chitosan is the best choice of polymer. Chitosan polymer can be used as an absorption enhancer as mentioned and has bioadhesive/mucoadhesive properties for oral administration. Illum and co-workers (1994*)*, demonstrated that chitosan has permeation-enhancing potential. *In vivo* studies in rats confirmed the intestinal permeation enhancement of peptide drugs due to the co-administration of chitosan hydrochloride (Luessen *et al.,* 1996).

Lactic acid-grafted chitosan nanoparticles were developed for prolonging drug release, achieving high drug loading. Modification of chitosan by grafting with lactic acid can be undertaken at neutral pH, providing an extra advantage for the uniform incorporation of drugs and proteins with minimal or no denaturization in the matrix structure (Kosta *et al.,* 2012).

For diseases such as colon cancer, it is important to achieve high concentrations of the active ingredient in the large intestine. Chitosan has been assessed as a potential drug carrier for colon–specific delivery. Modification of chitosan by crosslinking with succinic anhydride results in a SSBC delivery system.

2.7.3. Alginate Derivatives as Semi-Synthetic Biopolymer Complexes for Nanocarrier Formulation

Alginate (ALG) is a non-branched binary polysaccharide, which in its alginic acid form, has highly reactive carboxylic groups available for modification for various applications with chemical flexibility, making it possible for further modification to tailor its properties (Pawar and Edgar, 2012). Alginate is also extensively investigated for drug delivery system design (Sonia and Sharma, 2011). Alginate has very good cytocompatibility and biocompatibility,

biodegradation and a number of chemical and physical properties, making them suitable for many applications (George and Abraham, 2006; Khotimchenko, 2004). Alginate is one among the most explored biomaterials. The main disadvantage of ALG in drug delivery development is their poor cell adhesion. Alginate is pH-sensitive; hence encapsulated drugs are not released at low pH (gastric environment) and shrink under this condition (Sonia and Sharma, 2011).

Grafting is also used to modify native chains of ALG to bring about new properties, such as targeting, hydrophobic/hydrophilic bioactive encapsulation and sustained drug release. There are some drawbacks associated with oral drug formulations prepared from ALG graft copolymers. Few clinical studies have been reported concerning the risk or potential of ALG as a carrier for the commercial sector. Furthermore, there is little information on comparison of the oral formulations comprised of ALG graft copolymer with a non-grafted ALG formulation. Regardless of these uncertainties, one can regard the grafting of ALG as a means of adding unique properties to a drug delivery system formulated, therefore which are not possible by systems obtained from the mere physical mixing of polymers. For example, a synthetic polymer poly (acrylamide) was grafted with sodium alginate (Poly (acrylamide)-g-sodium alginate) to produce hydrogels with higher swelling properties (Wong, 2011).

Though ALG has been used in preparation of oral drug delivery systems, such as tablets, it has also been employed in microsphere, microcapsule and nanoparticle formulations (Wong, 2011; Khotimchenko, 2004; Braga *et al.,* 2005; Sen *et al.,* 2012). Based on the successful experience of ALG microparticles, the study of ALG nanoparticles was expected to gain impetus due to the benefit of particle size reduction to reach cellular and subcellular structures in the gastrointestinal epithelium and subepithelial dome regions that are relevant for mucosal vaccination (Borges *et al.,* 2006) and drug transport to the blood stream (Yi *et al.,* 1999). However, as opposed to chitosan, literature on ALG nanoparticles is relatively scarce. One of the challenges was the modification of production methods to achieve such small sizes (Rajaonarivony *et al.,* 1993; Ahmad *et al.,* 2006).

2.8. CONCLUDING REMARKS

The combination of polysaccharides with synthetic polymers or synthetic chemicals provides many possibilities in development and preparation of drug delivery vehicles with specific properties and functions. Pharmaceutical industries prefer the development of drugs that can be orally administered to patients. Progress in SSBC as nano-carrier systems has been made, in terms of understanding molecular interactions implicated in their formation.

As reviewed in this chapter, it is observed that a number of semi-synthetic nanoparticulate systems are under investigation. The most widely investigated oral polysaccharide nano-carrier systems are chitosan bio-complexes. Further investigation into the design of SSBC and nano-complexes especially as oral drug nano-carriers are necessary. The design of new and effective oral nano-enabled drug delivery systems for enhanced drug bioavailability will improve effectiveness of already available therapies for the treatment of various diseases. It is anticipated that in the next decade, some of these new approaches will reach clinical evaluation.

CHAPTER THREE

SYNTHESIS, DEVELOPMENT AND CHARACTERIZATION OF A NOVEL SEMI-SYNTHETIC BIOPOLYMER COMPLEX AS AN ORAL NANO-CARRIER SYSTEM

3.1. INTRODUCTION

Permeation and solubility enhancement of orally administered drugs in order to improve their solubility are amongst the major challenges experienced in pharmaceutical research. The use of both synthetic and natural polymeric materials have shown improvements in permeation and solubility of poorly permeable and soluble oral drugs as discussed in **Chapter 2**. However, using synthetic or natural polymers independently as carriers poses certain limitations (Sionkowska, 2011; Joshi and Patel, 2012), such as the poor mechanical and thermal properties of natural polymers (Sionkowska, 2011), therefore at higher processing temperature their structures can be easily destroyed, limiting them from being used in the biomedical field. On the other hand, synthetic polymers contain compounds or impurities that can affect their biocompatibility (Sionkowska, 2011). Interests in merging synthetic polymers with natural polymers into hybrid polymeric structures have increased greatly in scientific and pharmaceutical research. Hence, the functionality of natural polymers can be integrated with adaptability and versatility of synthetic polymers, resulting in a new class of polymeric material (van Hest, 2007) called Semi-Synthetic Biopolymer Complexes (SSBC), which harnesses the properties of both polymeric types. As a result of the growth in synthetic methodologies, the ability to combine natural and synthetic polymers to create well-defined hybrid materials has improved greatly (van Hest, 2007; Sionkowska, 2011).

A natural biopolymer, hyaluronic acid (HA), a synthetic polymer, poly (acrylic acid) (PAA), and a synthetic chemical (2-hydroxypropyl)-β-cyclodextrin (HP-β-CD) (Chouhan and Saini, 2014), were employed in this research for the design of a novel SSBC (HA─PAA─HP-β-CD) for the improvement of oral solubility and small intestinal permeation of our model drug acyclovir (ACV). Acyclovir belongs to the BCS class III according to the Biopharmaceutic Classification System, however in other regulatory authorities; it falls within BCS class IV (Amal *et al.,* 2008). Acyclovir is an anti-viral drug which is used as an anti-herpes agent for the treatment of orofacial, cutaneous, and genetic herpes, and Herpes simplex (type 1) keratitis among others (Tomar *et al.,* 2010). Acyclovir is the drug of choice to treat the aforementioned diseases, but has a problem of low oral bioavailability (ranging from 10-20%). Low solubility in the GIT and permeation of ACV across the human GIT epithelium are the major factors affecting ACV absorption, leading to its poor bioavailability. Consequentially, ACV has to be administered in high doses with frequent dosing, ultimately

resulting in various side effects (Tomar *et al.,* 2010). The SSBC has the potential to entrap poorly permeable and soluble drugs within its core, while the hydrophilic component of the polymeric complex stabilizes the surface when immersed in water and ensuring a prolonged circulation-life of the drug within the systemic circulation (Pandey *et al.,* 2011). The SSBC was subsequently formulated as a nano-system carrier to potentially increase the permeation and solubility of drugs (such as ACV) with low permeation and solubility; consequently increasing their bioavailability (Trimaille *et al.,* 2006).

Literature has described numerous chemical modifications of HA designed to improve the therapeutic action of drugs and for the development of new chemical products (Schante *et al.,* 2011). Hyaluronic acid has been the subject of many previous reviews, focusing on its biological functions and medical applications (Laurent and Fraser, 1992; Laurent, 1998; Kogan *et al.,* 2007). Hyaluronic acid, among biodegradable polymers (Leach *et al.,* 2003), has been represented as an attractive drug delivery polymeric material because of its biocompatibility, high responsiveness for specific degradation, and feasibility for incorporating drugs into its matrices (Ferguson *et al.,* 2010; Li *et al.,* 2010). Hyaluronic acid has also been used in signalling molecules in cell motility, cell differentiation, wound healing, and cancer metastasis. Its immunoneutrality makes it an excellent biomaterial building block to be employed for drug delivery (Prestwich *et al.,* 1998). Due to its biodegradability, it has also been used in the production of hydrogels through cross-linking and chemical modification for tissue regeneration and drug delivery systems. Hyaluronic acid often exhibits weak mechanical strength with rapid erosion/degradation behaviour *in vivo* due to its extremely high water absorbing properties and enzymatic degradation (Leach *et al.,* 2003). Hyaluronic acid is able to influence cell adhesion, migration, aggregation and proliferation (Cascone *et al.,* 1995). On the other hand, PAA is a synthetic polymer that becomes ionized and dissolves rapidly at high pH, which also contains pendant acidic or basic groups that either release or accept protons in response to changes in pH (Qiu and Park, 2012). The combination of these two polymers furnishes an enhanced material containing benefit of both polymers. Previously, Cascone and co-workers (1995) blended HA with PAA in different ratios for the release of growth hormones. Hyaluronic acid was also blended with poly (vinyl alcohol) (PVA) to form hydrogels as drug carriers (Cascone *et al.,* 1995).

Polymeric nano-materials (Hans and Lowman, 2002; Bussière *et al.,* 2013) have received huge attention as modifiers of pharmacokinetics of pharmaceutical molecules (Lehner *et al.,* 2013; Mahouche-Cherguia *et al.,* 2013). In medicine, nanotechnology has a constantly increasing impact on the preclinical development of drugs (Lehner *et al.,* 2013). There is an increase in the number of publications concerning nanoparticles which meet a huge range of

market needs and applications (Rao and Geckeler, 2011). Polymeric nanoparticles could improve pharmacokinetics for the delivery of drugs, but there is still a huge need to rationally design smart nano-carriers capable of effective therapeutically outcomes (Han *et al.,* 2013).

The aim of this research was to improve permeation and solubility of ACV, by encapsulating it into the prepared HA─PAA─HP-β-CD polymeric complex composition. A Semi-Synthetic Biopolymer Complex was successfully fabricated and loaded with ACV. The prepared ACV-loaded nanopolymeric complex and its native components were characterised using different characterization techniques to confirm the formation of a novel composite. Nuclear Magnetic Resonance (NMR) and Fourier Transform Infrared (FT-IR) spectroscopy were employed for highlighting chemical transitions, whilst differential scanning calorimetry (DSC) and X-ray Diffraction (XRD) spectroscopy were applied to understand the structural modifications that occurred with HA modification. Scanning electron microscopy (SEM) and Transmission electron microscope (TEM) were used to examine the morphology of the composite.

3.2. MATERIALS AND METHODS

3.2.1. Materials

Poly (acrylic acid) (PAA) (Mw=1,800g/mol), hyaluronic acid (HA), (2-hydroxypropyl)-β-cyclodextrin (HP-β-CD) (Mw=1,460g/mol), acyclovir (ACV), *N*-Hydroxysuccinimide (NHS), and 1-Ethyl-3-(3-dimethylaminopropyl) carbodiimide (EDC) were purchased from Sigma-Aldrich (St. Louis, MO, USA). Acetone, methanol (MeOH), dichloromethane (DCM), sodium hydroxide (NaOH), hydrochloric acid (HCL), orthophosphoric acid and monobasic potassium phosphate (KH_2PO_4) were supplied by Merck (Pty Ltd., South Africa) and were of analytical reagent grade.

3.2.2. Synthesis of Hyaluronic Acid Modification with Poly Acrylic Acid (HA─PAA)

HA─PAA polymeric complex was synthesized by dissolving HA (8.50mg.mL^{-1}) in a sodium hydroxide (0.5M NaOH) solution for 8 hours at room temperature (25^{o}C) to activate the hydroxyl (OH) group of the hyaluronic. Poly (acrylic acid) (17mg.mL^{-1}) was completely dissolved in double deionized water. The two solutions were combined with moderate stirring overnight and the pH was adjusted to 8.5 with NaOH. Precipitation in acetone afforded HA─PAA, then centrifuged or filtered, if necessary. The product was washed with methanol to remove non-reacted PAA.

3.2.3. Conjugation of HP-β-CD onto HA─PAA

HA─PAA (100mg) was dissolved in 50mL of double deionized water and treated with 50mg of EDC and 50mg of NHS for 45 min, in order to activate the carbonyl groups of HA─PAA. Separately, 300mg of HP-β-CD was dissolved in 10mL of double deionized water and added dropwise into the HA─PAA solution. The reaction mixture was maintained at room temperature under constant stirring for 8 hours. The product formed was dialyzed in tubing (Mw cut off of 12,000, avg flat width 33mm, diameter 1.3in) (Sigma-Aldrich Pty. Ltd. Johannesburg, South Africa) against water for 2 days and freeze dried on a Bulk Tray Dryer (Labconco Corporation, Kansas city, Mo, USA).

3.2.4. Preparation of ACV-loaded HA─PAA─HP-β-CD Nanoparticles

HA─PAA─HP-β-CD ACV-loaded nanoparticles were prepared by completely dissolving HA─PAA─HP-β-CD complex (600mg) into 100mL of double deionized water. Acyclovir (150mg) was suspended in 30mL of DCM, then sonicated for two minute and poured to the reaction mixture to encapsulate ACV to the complex, then moderately stirred to remove DCM. The solution was centrifuged (3500rpm) for 10 minutes to remove un-incorporated ACV drug. The final clear solution obtained was prepared for drying.

3.2.5. Preparation of Solid Nanoparticles through the Nano-Sprayer Drying Process

ACV-loaded solid nanoparticles were prepared using a Nano Spray Dryer B-90 (Buchi, Switzerland) technique. To gain solid nanoparticles, the clear solution obtained from ACV-loaded HA─PAA─HP-β-CD solution was filtered through a 0.45µm filter. For the purpose of this study, a spray cap membrane of 4.0µm in size was used with 60Hz ultrasonic frequency for the actuator. Additional spray drying parameters were set according to **Table 3.1**. The solid nanoparticles produced were collected and weighed to determine the yield.

Table 3.1: Parameters used for the preparation of the nanoparticles

Temperature (^{o}C)	Pressure (nbar)	Pump	Spray (%)
85	26–32	4	85

3.2.6. Determination of the Chemical Transitions of the Polymeric Complexes and Polymeric Complex Nanoparticles

The solid nanoparticles produced from the Nano Spray Dryer B-90 (Buchi, Switzerland) and all other native polymers were analysed using FT-IR spectrometry (PerkinElmer Spectrum 100). The FT-IR spectra of the product and native polymers were recorded in the range of 4000-550cm^{-1} and used to identify the presence and the absence of specific functional groups.

3.2.7. Determination of the Thermal Transitions of the Polymeric Complexes and Polymeric Complex Nanoparticles

Differential scanning calorimetry (DSC) (Mettler Toledo, Schwerzernback, Switzerland) was used to reveal the thermal properties of the ACV-loaded nanoparticles and all the native polymers used to form the loaded nanoparticles. 5–10mg dried samples were weighed into aluminium pans under nitrogen atmosphere (Afrox, Germiston, Gauteng, South Africa) with 200mL/min flow rate acting as the purge gas to decrease oxidation. The sample was then heated from 25^{o}C to 300^{o}C at the rate of 10^{o}C/min.

3.2.8. Determination of Thermal Decomposition of the Polymeric Complexes and Polymeric Complex Nanoparticles

The thermal decomposition analysis of the newly formed polymeric complex nanoparticle system and all native polymers was determined using a TGA 400 thermogravimetric analyser (PerkinElmer Inc., MA, USA). Samples of 10–20mg were placed in a ceramic pan under nitrogen atmosphere. The thermograms were obtained and they revealed the thermal decomposition properties of the polymers.

3.2.9. Determination of Chemical Interaction of the Polymeric Complexes and Polymeric Complex Nanoparticles

The X-ray patterns of the newly formed polymeric nanoparticle system and all the native polymers were determined using X-ray diffraction (XRD) (MiniFlex 600, Rigaku, Japan) and nickel-filtered Cu Kα radiation (a voltage of 40 kV and a current of 30 mA). The X-ray diffractogram were attained at the scanning rate of 5^{o}/min with the scanning scope of 2θ from 5^{o}C to 90^{o}C at room temperature.

3.2.10. Determination of the Surface and Structural Morphology of the Polymeric Complex Nanoparticles

3.2.10.1. Scanning electron microscopy

Scanning electron microscopy (SEM) FEI Quanta 400F (Hillsboro, OR. USA) was used to examine the surface morphology of the ACV-loaded HA─PAA─HP-β-CD nanoparticles. The sample was sputter coated using gold isotope while being mounted on the aluminium spud, with an EPI coater (SPI Modele sputter-coater and control unit, hester, PA, USA). After coating the nanoparticles for 60s, under constant nitrogen gas conditions, the sample was analysed using a FEI Quanta 400F (Hillsboro, OR., USA) electron microscopy. To produce high image resolution of the particles, an electron acceleration charge of 20 kV was used.

3.2.10.2. Transmission electron microscopy

Transmission electron microscopy (TEM) (Joel 100 EX, Japan) was utilized to examine the structural morphology of the ACV-loaded HA─PAA─HP-β-CD nanoparticles. The nanoparticles were re-suspended in methanol (0.5mg/mL) and a pipette was used to place a drop of the suspension on a 200 mesh thick formvar copper grid (TABB Laboratories Equipment, Berks, UK). The nanoparticles were allowed to be adsorbed on the surface of the copper grid in order to determine precise images.

3.2.11. Determination of the Particle Size Distribution and Zeta Potential of the Polymeric Complex Nanoparticles

Size analysis was used to quantify the average particle size. In order to ascertain that the spray-dried nanoparticles were within the expected size range of less than 500nm, the Zetasize NanoZS instrument (Malvern Instruments Ltd, Malvern, United Kingdom) was utilized. Briefly, the particle size was determined after the Nano Spray Dryer B-90 (Buchi, Switzerland) process. The dried particles were re-dispersed in water and subjected to a sonication (ultra-sound) for 2 minutes (6mm probe, 20 kHz, 50 W), for determination of their average size and zeta potential.

3.2.12. Determination of the Yield and Entrapment Efficiency of the Polymeric Complex Nanoparticles

3.2.12.1. Nanoparticle yield

The percentage yield of the product was determined from the weight of the native polymer plus the weight of the drug used in the formulation and the weight of the product (ACV-loaded nanoparticles) and calculated using Equation 3.1:

$$\text{Percentage yield} = \frac{\text{Practical yield}}{\text{Theoretical yield}} \text{ x } 100 \qquad \text{(Equation 3.1)}$$

3.2.12.2. Nanoparticle encapsulation efficiency and drug loading

A dried powder sample (100mg) of ACV-loaded HA─PAA─HP-β-CD was precisely weighed, and subsequently dissolved in NaOH (pH 10) solution over 24 hours. The solution was analysed using an Ultra-performance Liquid Chromatographic (UPLC) method as described in **Section 3.2.15** below. The encapsulation efficiency and drug loading were determined using Equations 3.2 and 3.3 (Schafroth *et al.,* 2012).

$$\text{Encapsulation efficiency} = \frac{\text{the dru g within nanoparticle}}{\text{initial drug amount}} \text{ x } 100 \qquad \text{(Equation 3.2)}$$

$$\text{Drug loading} = \frac{\text{the amount of drug in nanoparticles}}{\text{amount of nanoparticle}} \text{ x } 100 \qquad \text{(Equation 3.3)}$$

3.2.13. Solubility Determination of ACV

A Shake Flask Method was used to determine and compare the solubility of ACV in a comparator product, and ACV formulated as ACV-loaded nanoparticles. A quantity of 100mg of each formulation was placed into a stopped bottle containing 50mL buffer solution of pH 6.8. The solutions in the bottles were maintained in a shaking water bath for 24 hours at 37^{o}C at 75rpm (Waman *et al.,* 2014). The sample contents were filtered through a 0.22µm membrane filter, after suitable dilution with the mobile phase; then the amount of ACV in the solutions were quantified via UPLC as described in **section 3.2.15** below.

3.2.14. *In Vitro* Release Studies of ACV from the Polymeric Complex Nanoparticles vs. a Comparator Product

ACV-loaded polymeric nanoparticles (2000mg) containing 200mg ACV and a comparator product containing 200mg of ACV were separately dispensed in 15mL of pH 6.8 phosphate buffer (0.5M KH_2PO_4/H_2PO_4). The dispensed solutions were then introduced into the dialysis bags (Mw cut off of 12,000, avg flat width 33mm, diameter 1.3in., Sigma Aldrich), which were hydrated in double deionized water for 3 hours prior used to remove glycerol and sulphide. The tubing's were tightly sealed at both ends, and were separately suspended in 900mL of phosphate buffered saline (PBS), pH 6.8 in USP dissolution apparatus II vessels. To prevent floatation of the tubing's because of the unstable hydrodynamics above the paddles, stainless ring-mesh assemblies were used. Samples (0.05mL) were withdrawn at various time intervals and replaced with equal amounts of fresh PBS (pH 6.8) phosphate buffer to maintain sink conditions. The ACV content was quantified using UPLC method as described in **section 3.2.15**. The ACV release study was undertaken over 8 hours, since ACV has half live 3 to 4 hours for a person with a normal kidney functioning.

3.2.15. Ultra Performance Liquid Chromatographic Determination of ACV

For determination of ACV solubility, loading and release, a UPLC method was developed on a Waters® ACQUITY™LC system (Waters®, Milford, MA, USA) coupled with a photodiode array detector (PAD), and Empower® Pro Software (Waters®, Milford, MA, USA) using an Aquity UPLC® BEH Shield RP_{18} column having a pore size of 1.7µm. Indapamide (IP) was used as an internal standard for the calibration. A mobile phase made of methanol: water: orthophosphoric acid (750: 249: 1) was employed with a gradient method which enabled accurate detection of the ACV with run time of 4.559 minutes and the internal standard at 6.509 minutes. The mobile phase flow rate was set at 0.05mL/min with an average pressure of 4100psi. The samples were pre-filtered with a 0.22µm syringe before injection into the

column. A temperature of 27±0.5^{o}C was managed in the sample and column. Measurements were undertaken at a wavelength of 252nm.

The stock solutions of ACV and IP, ranging from 0-0.05mg.mL^{-1}, were prepared using the mobile phase of methanol: water: orthophosphoric acid (750: 249: 1) for preparing the calibration curve.

3.2.16. *Ex Vivo* Permeability Studies of ACV from the Polymeric Complex Nanoparticles vs. a Comparator product

A static Franz diffusion cell (Logan Instruments Corp., New Jersey, and USA) (shown in **Figure 3.1b**) was used to comparatively determine the permeation of ACV from the formulated polymeric nanoparticulate system and the comparator product through Large White Pig intestinal epithelium. For the use of epithelium, a full ethic application was not required as the epithelium were obtained from pigs already euthanized for other purposes; letter from the AESC committee is located in Appendix D. The harvested tissues were immediately immersed in phosphate buffer solution (pH 7.4) and transported to the laboratory within 1 hour. The tissues were cut into 5cm strips and sandwiched between the receptor chamber and donor chamber for the diffusion cells. The tissue was held together with a clamp and the whole system was fixed on the magnetic stirrer, hence the solution (PBS pH 7.4 of 12mL) in the receptor compartment was constantly mixed using a magnetic stirrer bar. The donor chamber contained 3mL of ACV (1.13mg/mL) loaded in the nanoparticles.

Before starting the permeation study, the serosa layer was removed from the pig GIT tissue **(Figure 3.1a**). A sample solution was withdrawn and immediately replaced with the equal fresh solution at every pre-determined time interval for the duration of 8 hours. The UPLC method as described in **section 3.2.15** was used to determine the concentration of ACV in the donor compartment solution and receiver compartment. The calculated membrane exposure was found to be 1.77cm^{2} (Boonen *et al.,* 2010).

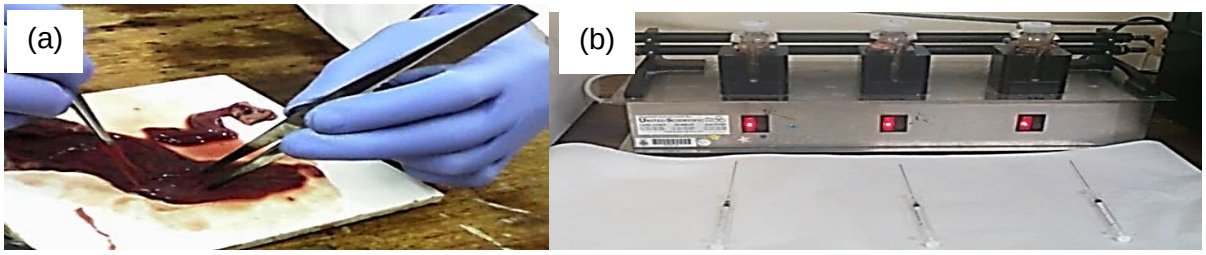

Figure 3.1: (a) The removal of the serosa layer from the interstitial tissue and (b) Static Franz diffusion cell used to undertake the permeation study.

3.2.16.1. Determination of pig intestinal epithelium integrity

For *ex vivo* studies, the confirmation of tissue's integrity is very significant, since any compromised tissue integrity during handling will result inaccurate permeation results. The intestinal tissue integrity was evaluated prior to and after the experimental procedure through ionic conductivity using a SevenMulti S40 pH/electrical conductivity meter (Mttler-Toledo, Zurich, Switzerland) (Davies *et al.,* 2004).

3.2.16.2. Calculation of the resistance reduction factor and permeation enhancement ratio

The damage ratio (or Resistance Reduction Factor, RF) was calculated according to Equation 3.4 below.

$$\mathrm{RT} = \frac{\mathrm{R0}}{\mathrm{Rt}} \qquad \text{(Equation 3.4)}$$

Where R0 = Ratio of the initial resistance value at time 0.

Rt = Resistance value of the sample obtained at time t.

Permeation enhancement ratio was given as defined in Equation 3.5 below:

$$\text{Permeation enhancement} = \frac{\text{P treated tissue}}{\text{P untreated tissue}} \qquad \text{(Equation 3.5)}$$

The cumulative amount of drug permeated across the membranes was calculated in accordance to the formula below (Equation 3.6):

$$\text{Cumulative amount of drug permeated} = \frac{\mathrm{Q}}{\mathrm{A}} \quad (\mathrm{mg.cm^{-2}}) \qquad \text{(Equation 3. 6)}$$

Where A = membrane area exposed (cm^2),

Q = amount of substance crossing membrane (mg).

For the flux values (J) across the membranes, the following formula was used:

$$\mathrm{J} = \frac{\mathrm{Q}}{\mathrm{At}} \quad (\mathrm{mg.cm^{-2}.min^{-1}}) \qquad \text{(Equation 3.7)}$$

Where A = membrane area exposed (cm^2),

Q = amount of substance crossing membrane (mg),

t = exposure time (min).

3.3. RESULTS AND DISCUSSION

3.3.1. Chemical Transitions of the Polymeric Complexes and Polymeric Complex Nanoparticles

FT-IR spectra of the complex nanoparticles and the precursor polymers are shown in **Figure 3.3.** The FT-IR spectrum of hyaluronic acid (HA) exhibited the following significant characteristic bands: υ = ~3263cm^{-1} of O─H very light stretching overlapping N─H Stretching (υ = ~3250cm^{-1}), υ = ~1605cm^{-1} stretching of C=O (carbonyls), υ = 1020cm^{-1} stretch of an ether group (C─O─C) (**Table 3.2, Figure 3.3a**). FT-IR spectrum of poly (acrylic acid) (PAA) demonstrated the following characteristic bands of significance: υ = ~3113cm^{-1} O─H stretching, υ = ~2938cm^{-1} for ─CH─, stretching frequency of (alkanes) functionality and υ = ~1696cm^{-1} C=O (carbonyl group) stretch (**Table 3.2, Figure 3.3b**). FT-IR spectrum of the newly formed hyaluronic acid modification (HA─PAA) showed characteristic bands of significance as follows: υ = ~3266cm^{-1} O─H stretch peak, overlapping N─H stretching (υ = ~3250.00cm^{-1}), υ = ~1547cm^{-1} C=O stretch and υ = ~1035cm^{-1} C─O─C stretch of ether groups that links both native polymers (**Table 3.2, Figure3.3c**). This data provided evidence for the formation of HA─PAA complex, whereby we observed the disappearance of a carbonyl functionality of precursor PAA at υ = ~1696cm^{-1} (**Table 3.2, Figure 3.3b**) in the HA─PAA (**Table 3.2, Figure 3.3c**) due its interaction with the –OH of HA (**Table 3.2, Figure 3.3a**) to give the ether band formation (C─O─C). This resulted in the shift of band position from at υ = ~1696cm^{-1} (**Table 3.2, Figure 3.3b**) to υ = ~ 1547cm^{-1} due to the excess surrounding effects resulted from the HA modification (**Figure 3.3c**). The chemical representation for the reaction HA with PAA is showed in **Figure 3.2** below.

.

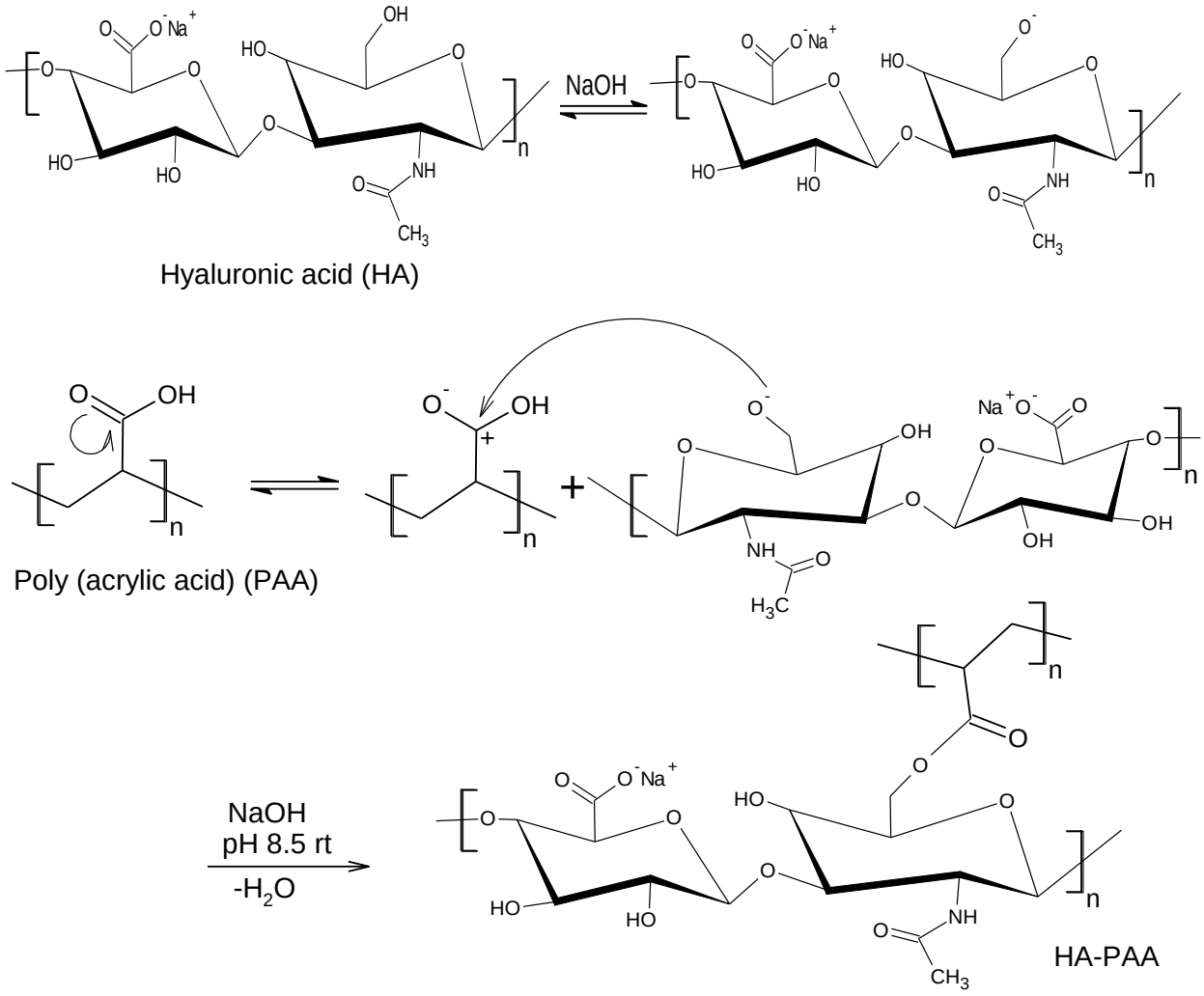

Figure 3.2: The chemical modification reaction of HA with PAA.

The FT-IR spectrum of (2-hydroxypropyl)-β-cyclodextrin (HP-β-CD) exhibited the following characteristic bands of significance: υ = ~3343cm^{-1} O─H stretching, υ = ~2926cm^{-1} ─CH─, stretching (alkanes) and υ = ~1007cm^{-1} (C─O─C) stretch of ether groups (**Table 3.2, Figure 3.3d**). The newly synthesized complex (HA─PAA─HP-β-CD) exhibited the following bands of significance: υ = ~3330cm^{-1} O─H stretch, υ = ~2929cm^{-1} ─CH─ stretch (alkanes), υ = ~1559cm^{-1} C=O stretch and υ = 1023cm^{-1} (C─O─C) stretch (**Table 3.2, Figure 3.3e**). The drug ACV showed characteristic bands of significance as follows: υ = ~3200cm^{-1} for N─H stretching, υ = ~1500cm^{-1} C=O (carbonyl group) and υ = ~1010cm^{-1} for C─O─C stretch of ether.

Table 3.2: FT-IR general function bands assignment for polymeric compounds

Characteristic absorption (cm^{-1})	Function groups	Assignments
3343–3210	O─H Stretch	Alcohol, phenols and carboxylic acid (CO─OH)
3250	N─H symmetric stretch	Secondary amide
3000–2800	C─H Stretch	Alkanes Methylene asymmetrical Methyl symmetrical Methyl asymmetrical
1707─1549	C=O Stretch	Carbonyls Ketones Carboxylic acids
1073─1007	C─O─C Stretch	Ethers

The chemical reaction for the formation of HA─PAA─HP-β-CD complex is shown in **Figure 3.2.1**. Therefore, the newly formed HA─PAA─HP-β-CD complex was confirmed by the disappearance of the intense carbonyl (C=O) functional group of HA─PAA complex at υ = ~1549cm^{-1} (**Table 3.2, Figure 3.3c**) which reacted with hydroxyl (─OH) functional groups of HP-β-CD (**Table 3.2, Figure 3.5d**), which is seen by the decrease absorption intensity at υ = ~3343cm^{-1} of the newly formed Semi-Synthetic Biopolymer Complex (HA─PAA─HP-β-CD) (**Table 3.2, Figure 3.3e**) compared to HP-β-CD (**Table 3.2, Figure 3.3d**).

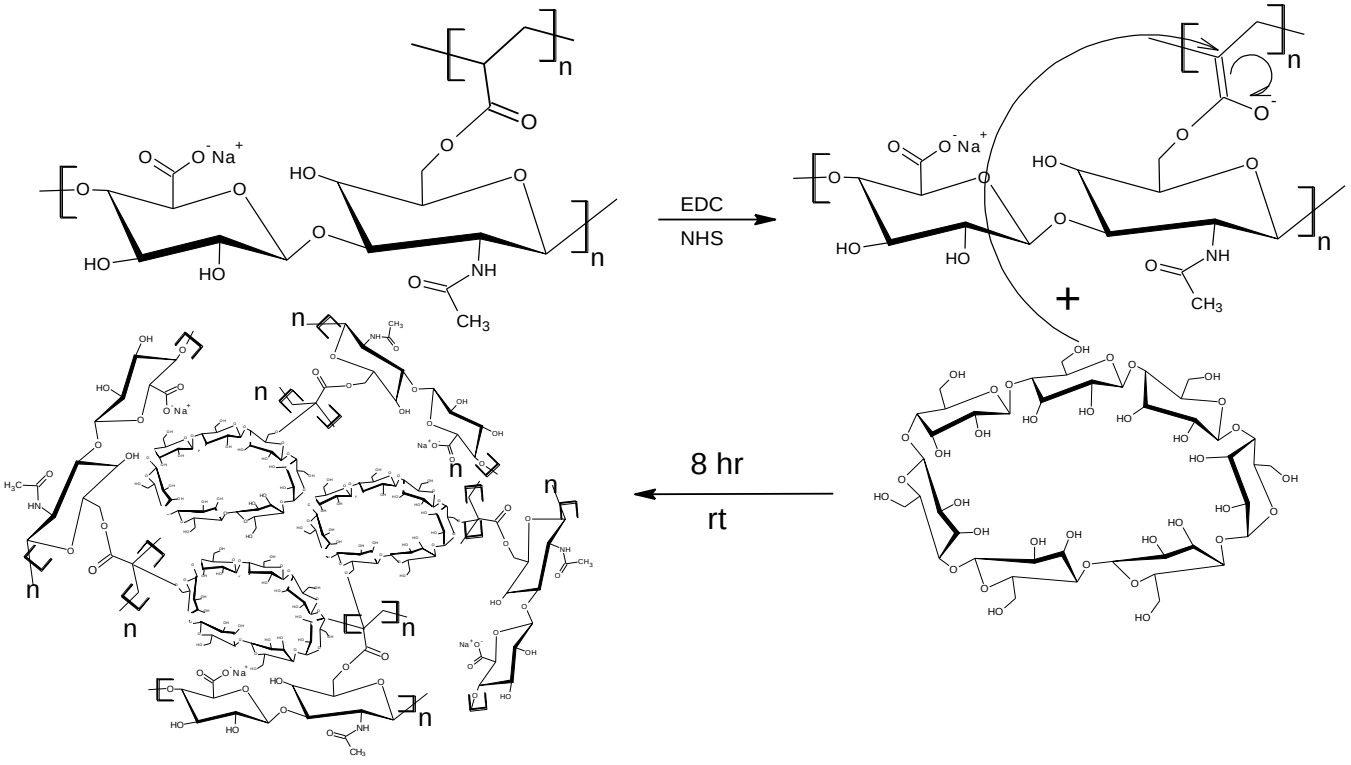

Figure 3.2.1: The chemical conjugation reaction of HA─PAA with HP-β-CD

The ACV-loaded HA–PAA–HP-β-CD nanoparticles demonstrated similar absorption characteristics as the un-loaded polymeric complex, with little evidence of drug absorbed peaks (**Figure 3.3** g). Hence, it was confirmed that the encapsulation of the drug within the core of the formed polymeric complex was evident; however additional tests were done in order to further confirm the presence of the drug under investigation within the nanoparticle polymeric complex.

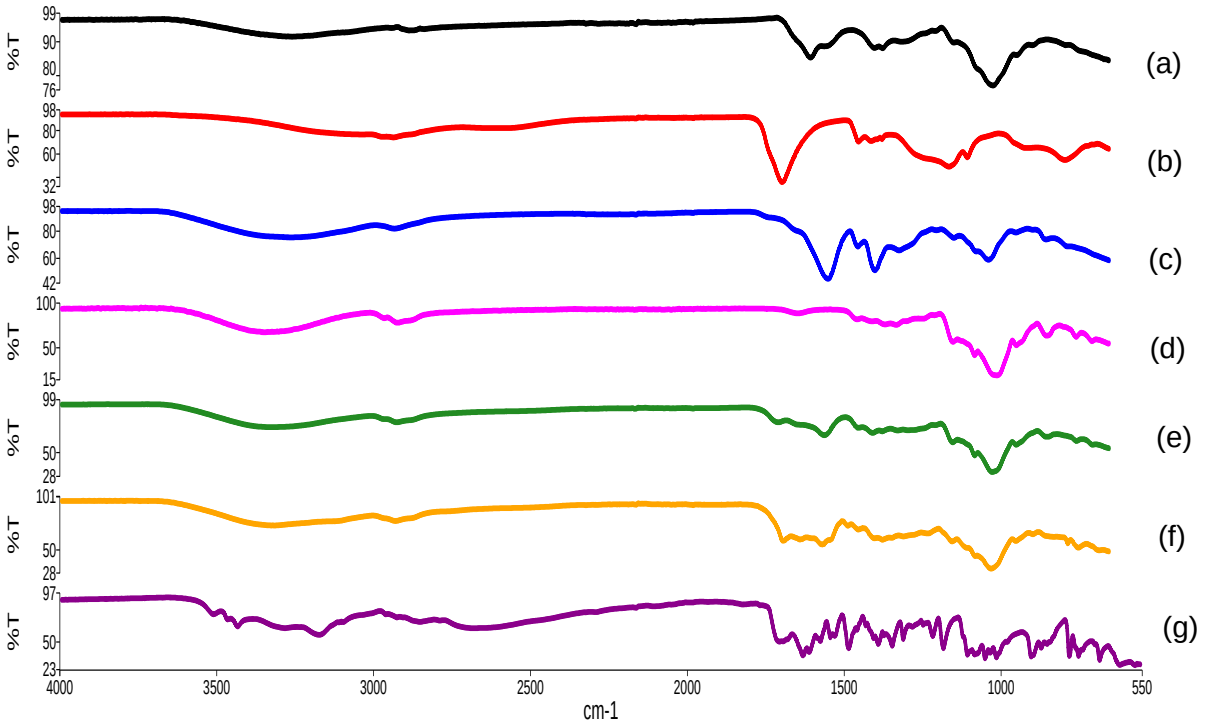

Figure 3.3: FT-IR spectra of (a) Hyaluronic acid (HA), (b) Poly (acrylic acid) (PAA), (c) Modification of Hyaluronic acid with Poly acrylic acid (HA–PAA), (d) (2-hydroxypropyl)-β-cyclodextrin (HP-β-CD), (e) HA–PAA–HP-β-CD, (f) ACV-loaded HA–PAA–HP-β-CD and (g) ACV.

3.3.2. ^{1}H NMR Analysis of the Polymeric Complexes and Polymeric Complex Nanoparticle

^{1}H NMR analysis was used for further structural confirmation of the complex nanoparticles and the precursor polymers. The ^{1}H NMR for HA exhibited the following peaks of significance: at δ = 4.70ppm is the peak for water d_6, at δ = 4.50–3.00ppm are peaks that originated from anhydrous glucose unit (**Figure 3.4a**). The ^{1}H NMR for PAA gave the following peaks of significance: ^{1}H NMR peaks at δ = 4.70ppm for water-d_6, peaks at δ = 2.50–1.00ppm are associated with hydrogen from alkyl, methyl and ethyl functionality (–CH–,–CH_2–) and hydrogen protons peaks at δ = 7.90–7.58ppm in PAA spectrum are possible due to (acrylic acid) residual monomer impurities (**Figure 3.4b**).

The ^{1}H NMR spectrum for the newly formed HA modification (HA─PAA) contains the following peaks of significance: at δ = 4.70ppm is the peak for water-$d_{6,}$ peaks at δ = 4.50–3.00ppm is from anhydrous glucose unit from the modified HA, peaks at δ = 2.50–1.00ppm is from hydrogen of the alkyl, methyl and ethyl functionality (─CH─,─CH_2─) from the PAA use in modification. The solvent D_2O exchange with COOH groups of PAA to give COOD resulting in no proton signal observed for COOH in ^{1}H NMR at δ = 7.90–7.58ppm (**Figure 3.4c**).

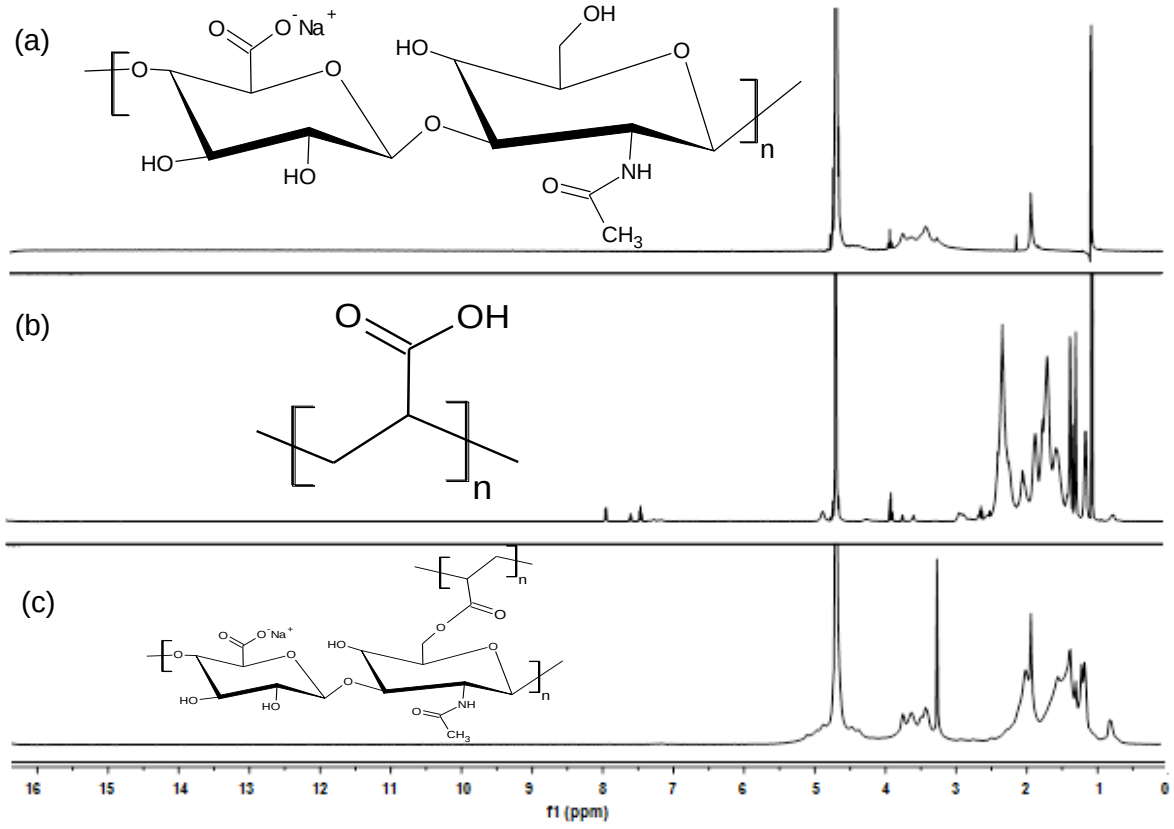

Figure 3.4: ^{1}H NMR spectra of (a) hyaluronic acid (HA), (b) Poly (acrylic acid) (PAA) and (c) HAA─PAA in D_2O.

^{1}H NMR analysis for the newly formed complex (HA─PAA─HP-*β*-CD) confirmed the existence of the anhydrous glucose unit peaks at δ = 4.50–3.00ppm from native polymeric complexes (HA─PAA and HP-*β*-CD) plus the alkyl (methyl, ethyl) functionality at δ = 2.00–1.00ppm (**Figure 3.5c**). Of great significance is the confirmation of the existence of ACV drug (**Figure 3.5d**) within the polymeric complex (**Figure 3.5e**). Therefore, the ^{1}H NMR spectrum of the ACV-loaded HA─PAA─HP-*β*-CD confirmed that ACV integrity was maintained, since all the significant peaks of ACV (**Figure 3.5d**) from the ACV-loaded HA─PAA─HP-*β*-CD nanoparticles (**Figure 3.5e**) can be clearly identified. The maintenance of drug integrity is very significant in order to ensure that the drug chemical intervention in relation to its clinical

functioning had not been interfered with, instead only the drug properties for the desired solubility has been modified.

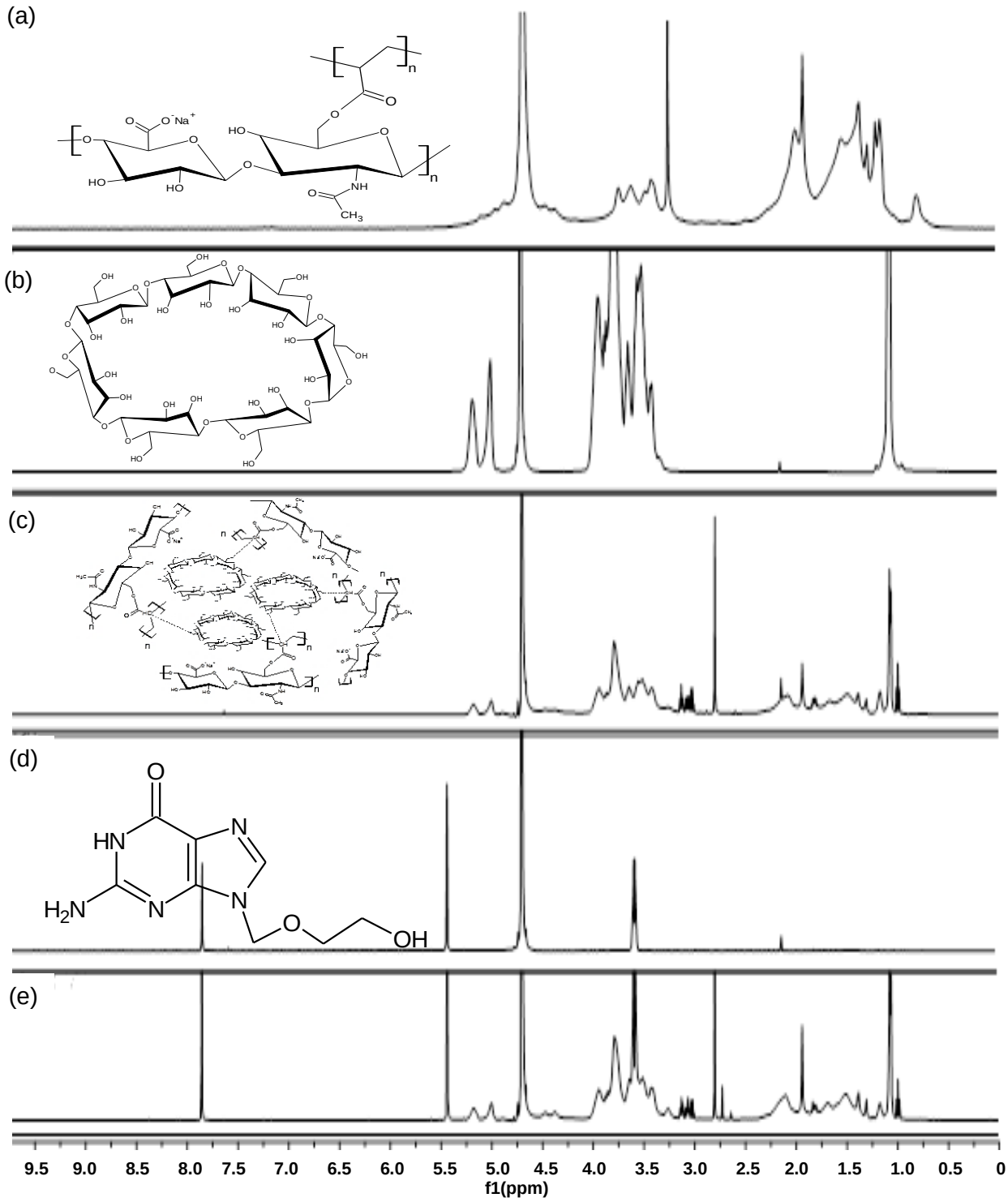

Figure 3.5: ^{1}H NMR spectra of (a) HAA–PAA, (b) HP-β-CD, (c) HA–PAA–HP-β-CD, (d) ACV and (e) ACV-loaded HA–PAA–HP-β-CD in D_2O.

3.3.3. X-ray Diffraction Pattern Analysis of the Polymeric Complexes and Polymeric Complex Nanoparticles

Polymers can exist in various forms: crystalline, semi-crystalline, micro-crystalline or amorphous, with a single polymer possessing the potential to exhibit different forms. X-ray diffraction (XRD) patterns were used to study the characteristic forms of the native polymers used and the newly formed polymeric complexes with drug-loaded nano-complex. **Figure 3.6**; depicts the XRD patterns of the native polymers (PAA and HA) used and the newly formed polymeric complexes (HA–PAA). The XRD pattern B of PAA reveals its being less amorphous in nature compared to HA. The absence of peaks in pattern C also confirmed that the newly formed HA–PAA graft is totally amorphous.

Figure 3.7 depicts the XRD patterns of the precursor polymeric complexes (HA–PAA and HP-β-CD), the newly formed polymeric complex (HA–PAA–HP-β-CD), and the ACV-loaded polymeric complex .Pattern B of HP-β-CD reveals its semi-crystalline form and pattern C of HA–PAA–HP-β-CD highlights that the resultant polymeric complex is semi-crystalline. Hence, XRD pattern D of ACV-loaded HA–PAA–HP-β-CD nanoparticles and pattern C of non-loaded HA–PAA–HP-β-CD polymeric complex were both observed to be similar in shape with minimum difference, as they are both semi-crystalline. The small difference in shape is due to the existence of ACV drug within the complex. The difference in the degree of crystallinity between the HA–PAA, HP-β-CD and HA–PAA–HP-β-CD polymeric complex suggests that there is a strong hydrogen bond interaction between the HA–PAA and HP-β-CD forming HA–PAA–HP-β-CD. **Figure 3.7.1** also confirmed that the drug was encapsulated within the complex, since the complex phase is dominant and the drug phase is less observed.

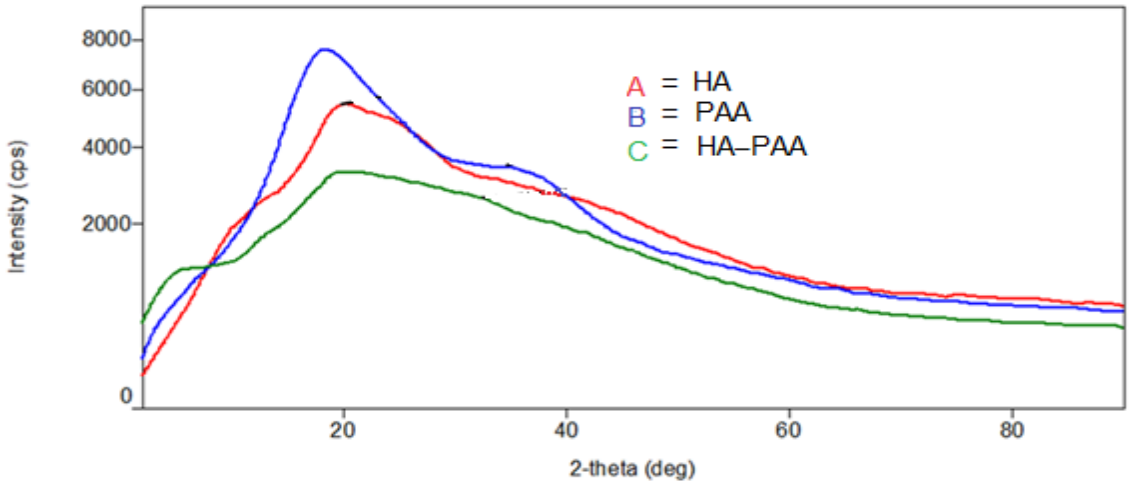

Figure 3.6: The XRD spectra for (a) HA, (b) PAA, and (c) HA–PAA.

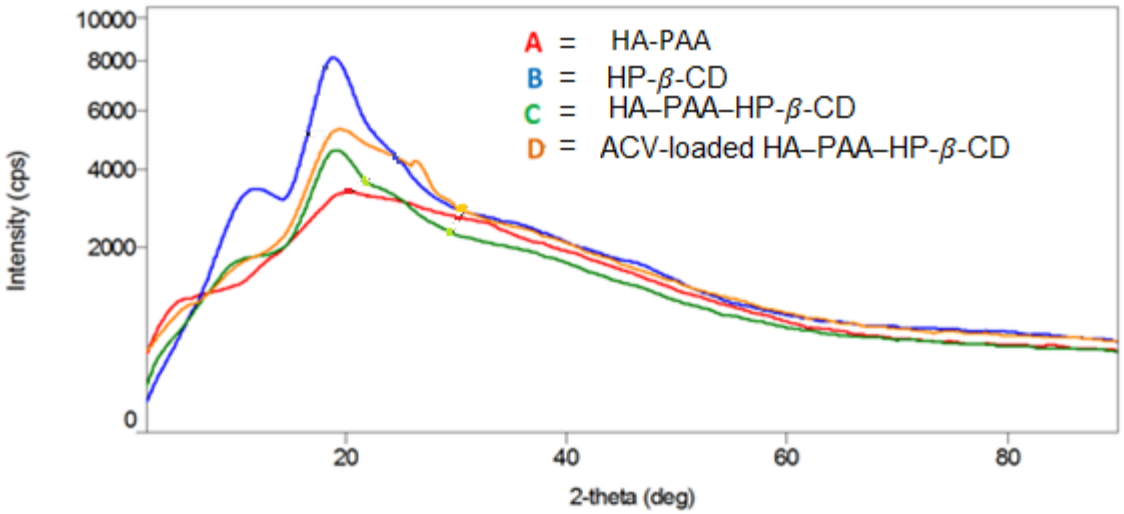

Figure 3.7: The XRD spectra for (a) HA–PAA, (b) HP-β-CD, (c) HA–PAA–HP-β-CD and (d) ACV-loaded HA–PAA–HP-β-CD.

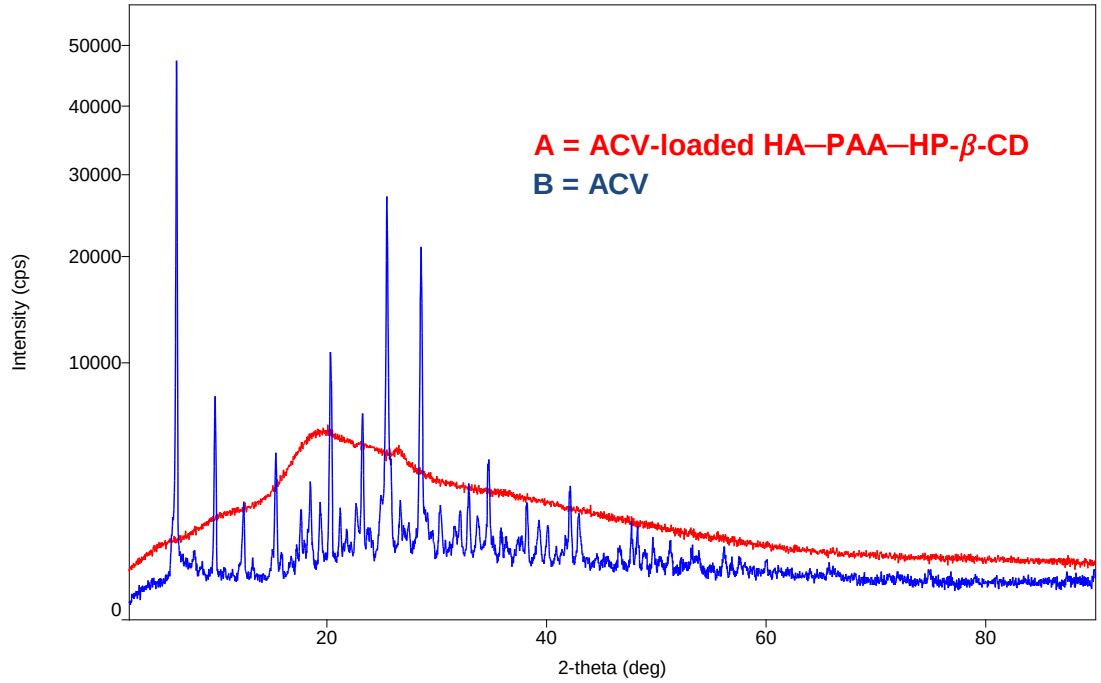

Figure 3.7.1: The XRD spectra for (a) ACV-loaded HA–PAA–HP-β-CD and (b) ACV

3.3.4. Thermal and Thermodynamic Analysis of the Polymeric Complexes and Polymeric Complex Nanoparticles

Differential scanning calorimetry (DSC) analysis was used to determine the thermal events of HA, PAA, HA–PAA, HP-β-CD, HA–PAA–HP-β-CD and ACV-loaded HA–PAA–HP-β-CD polymers measured from 25^{o}C to 300^{o}C (**Figure 3.8 and 3.9). Figure 3.8** reveals thermogram A of HA–PAA, showing an endothermic melting point at 115^{o}C and a very broad crystallization point (exothermic peak) at 240^{o}C before degradation. Thermogram B of HA

demonstrated an endothermic melting point at 110^{o}C with a sharp crystallization point (exothermic peak) at 240^{o}C. Thermogram C of PAA possessed two slightly broad endothermic peaks at 60^{o}C and 240^{o}C before degradation. It is also observed that thermogram A of HA–PAA polymeric complex is more exothermic (more heat is required to break its bonds) compared to the native polymers. This also confirm that the newly formed HA–PAA polymeric complex is more stable compared to the native polymers.

Figure 3.9 also revealed thermal events of HP-β-CD, HA–PAA, HA–PAA–HP-β-CD and ACV-loaded HA–PAA–HP-β-CD. Thermogram B of HA–PAA–HP-β-CD revealed two thermal events which are at 110^{o}C and 220^{o}C, while thermogram C of HP-β-CD reveals one endothermic thermal event at 110^{o}C confirming that these molecules bonds are easily broken.

The thermogram of ACV-loaded HA–PAA–HP-β-CD formulation (thermogram D), reveals that it is also more endothermic (it can easily release the entrapped drug without requiring significant energy or heat) compared to thermogram B of HA–PAA–HP-β-CD, due to the presence of entrapped drug. **Figure 3.9** also revealed a very sharp endothermic meting point of ACV at 260^{o}C.

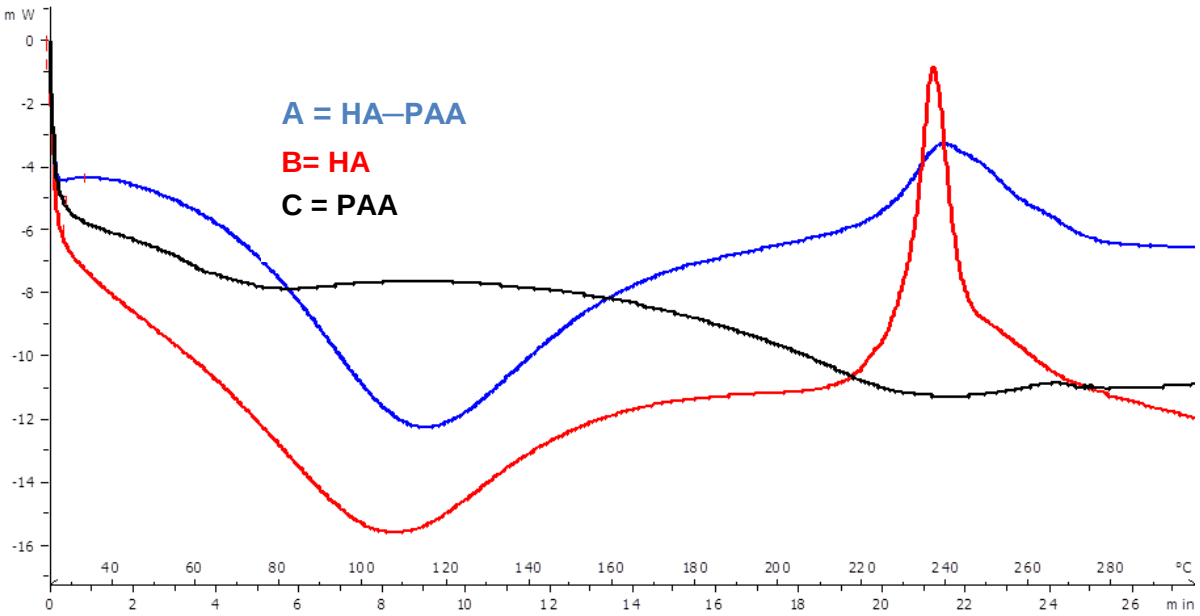

Figure 3.8: DSC thermograms of (a) HA–PAA, (b) HA and (c) PAA, measured from 25^{o}C to 300^{o}C.

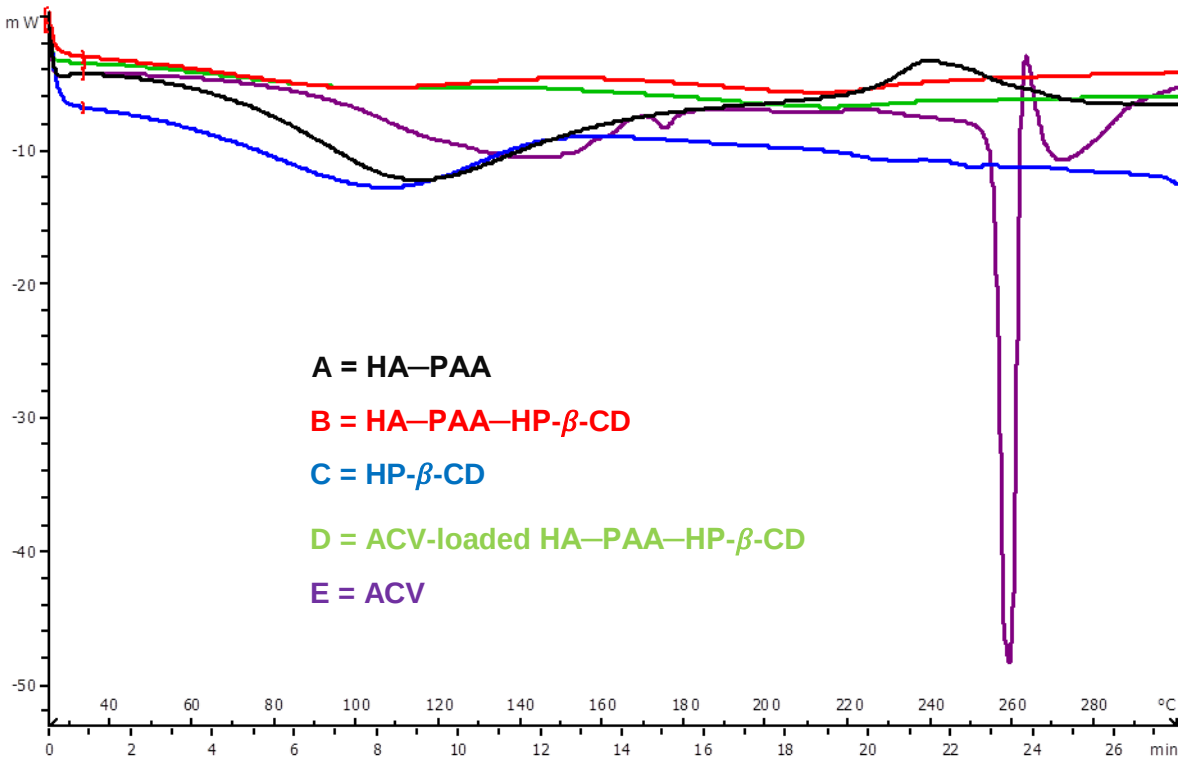

Figure 3.9: DSC thermograms of (a) HA–PAA, (b) HA–PAA–HP-β-CD; (c) HP-β-CD and d) ACV-loaded HA–PAA–HP-β-CD, measured from 25^{o}C to 300^{o}C.

3.3.5. Thermogravimetric Analysis of the Polymeric Complexes and Polymeric Complex Nanoparticles

The thermogravimetric (TGA) analysis which yielded thermograms of PAA, HA, HA–PAA, HA–PAA–HP-β-CD and ACV-loaded HA–PAA–HP-β-CD are depicted in **Figure 3.10 and 3.11**. The thermograms were used to determine the thermal events of the above mentioned polymers, such as their thermal decomposition pattern and thermal stability, which assisted with the identification/confirmation of formation of new polymeric systems.

Different polymers usually possess different thermal decomposition patterns and have varying thermal stabilities. The thermograms (in **Figure 3.10 and 3.11**) confirmed that a comparatively novel polymeric material has been synthesized, supported by varied thermal decomposition patterns. Thermogram A (in **Figure 3.10**) of native PAA, shows two degradation/decomposition events of significance at 220^{o}C and 450^{o}C and thermogram B (in **Figure 3.10**) of native HA, shows three degradation/decomposition events of significance at 90^{o}C, 220^{o}C and 620^{o}C. Thermogram C (in **Figure 3.10**) of the newly formed HA–PAA, shows three degradation/ decomposition events of significance at 90^{o}C, 230^{o}C and 400^{o}C. The difference in decomposition pattern and weight percentage of the native polymer thermograms compared to the formed copolymer thermogram suggests the formation of a composite material.

Figure 3.11 shows thermogram A of native HP-β-CD, possessing one degradation/decomposition of significance at 340^{o}C. Thermogram C (**Figure 3.11**) of the newly formed HA─PAA─HP-β-CD polymeric complex has four degradation events/decompositions of significance which are at 90^{o}C, 230^{o}C, 330^{o}C and 400^{o}C. The variety in thermal events for the HA─PAA─HP-β-CD polymeric complex suggested the formation of a new complex copolymer. The comparative thermograms of the complex copolymer (HA─PAA─HP-β-CD), thermogram C, and thermogram D for the ACV-loaded HA─PAA─HP-β-CD are also shown in **Figure 3.11**. The thermograms decomposition events and weight percentage are slightly different; indicating the effect of the existence of ACV drug within the formed polymeric complex being minimal, due to the small percentage (20%) of the drug within the complex.

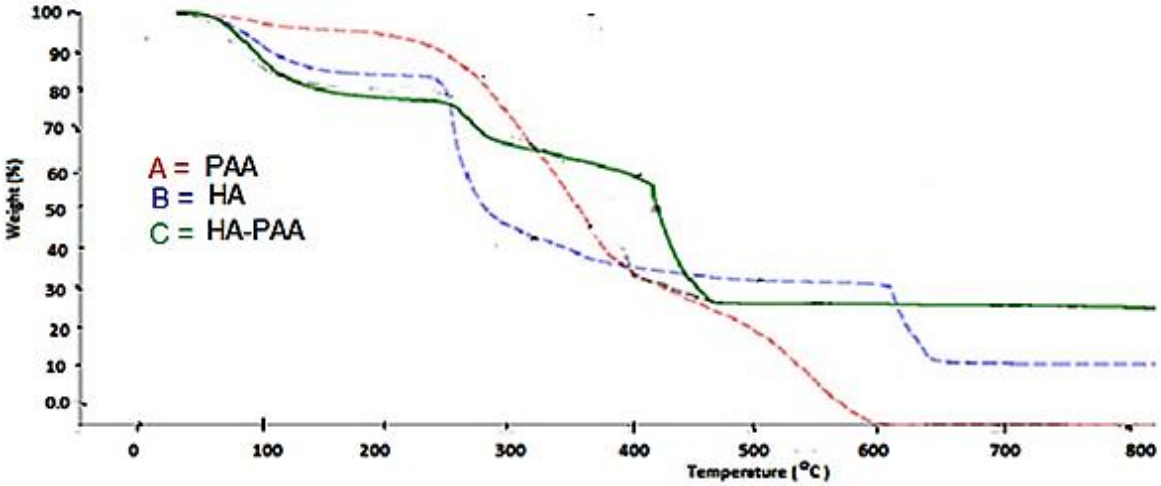

Figure 3.10: The TGA thermogram of (a) Poly acrylic acid PAA, (b) Hyaluronic acid HA and (c) HA─PAA.

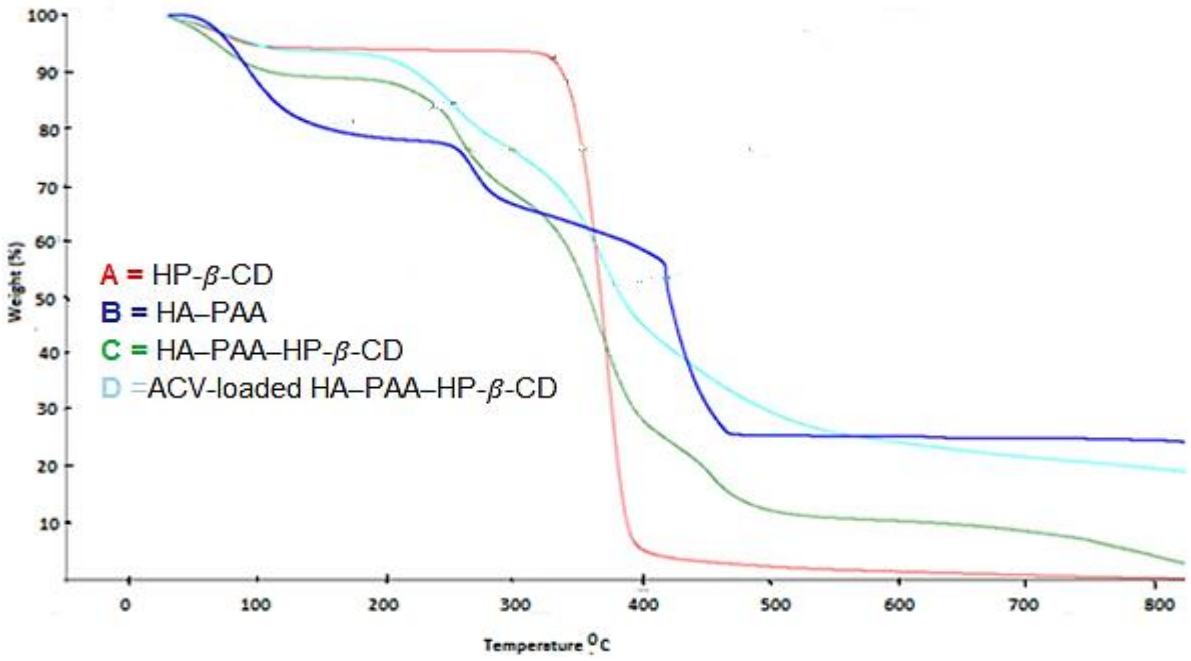

Figure 3.11: The TGA thermograms of (a) HP-β-CD, (b) HA─PAA, (c) HA─PAA─HP-β-CD and (d) ACV-loaded HA─PAA─HP-β-CD.

3.3.6. Morphology and Particle Size Distribution of the ACV-loaded HA─PAA─HP-β-CD Nanoparticles

The cross-sectional morphology of ACV-loaded HA─PAA─HP-β-CD nanoparticles was observed immediately after the nano spray-drying process. The nanoparticles were spherical in shape, as viewed via SEM (**Figure 3.12** (**a and b**)). It was also observed that the nanoparticles were less than 500nm in size. **Figure 3.13,** shows the size distribution of ACV-loaded HA─PAA─HP-β-CD nanoparticles, which revealed the average nanoparticle diameter of 257.9.2nm, the zeta potential of -58.3mV and a particle distribution intensity (PdI) of 0.315. A PdI < 0.5 revealed that there was limited variation of size in the nanoparticle range and the zeta potential signified that the ACV-loaded HA─PAA─HP-β-CD nanoparticles were not easily agglomerating. TEM (in **Figure 3.12** (**c and d**)) also confirmed the spherical shape of the nanoparticles.

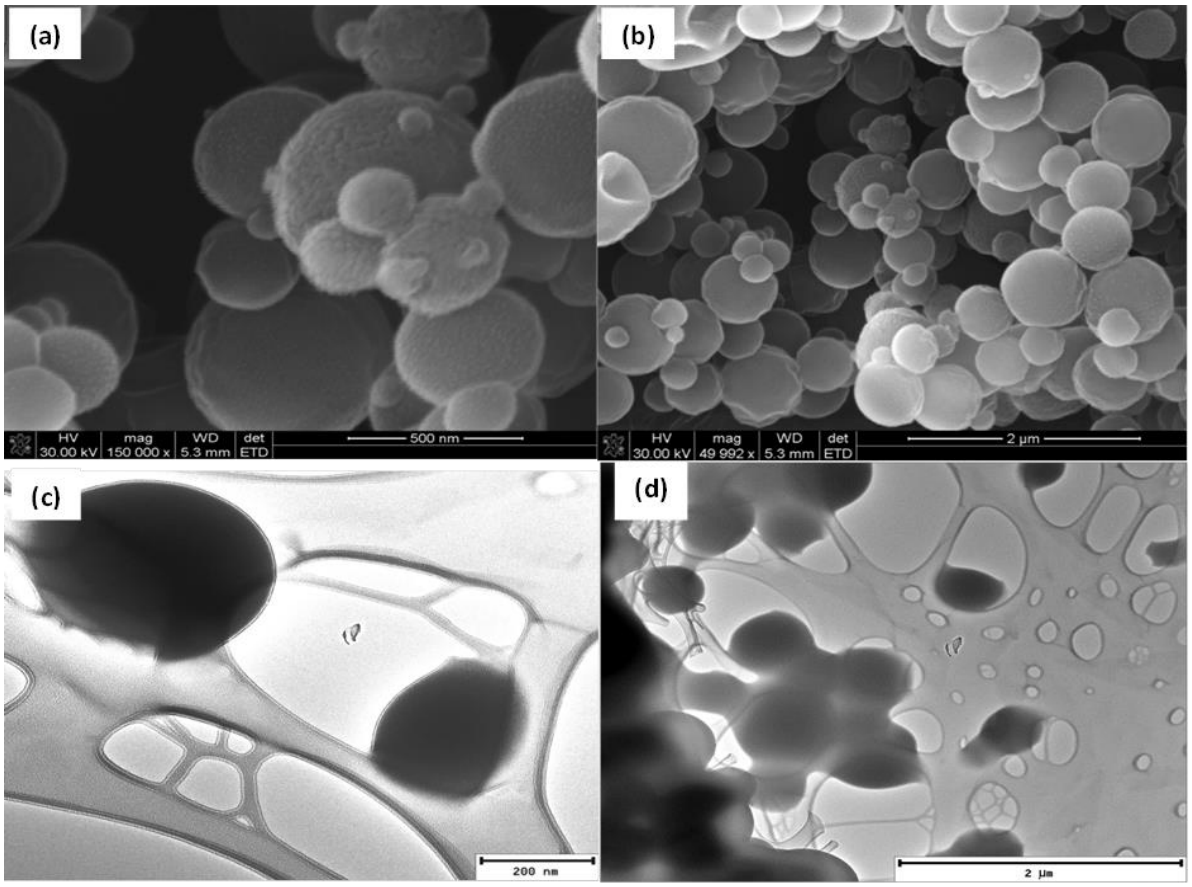

.

Figure 3.12: Images of the prepared nanporticles, SEM (a and b) and TEM (c and d) (The black spots representing the nanoparticles of interest and the surrounding areas representing the copper grid spaces).

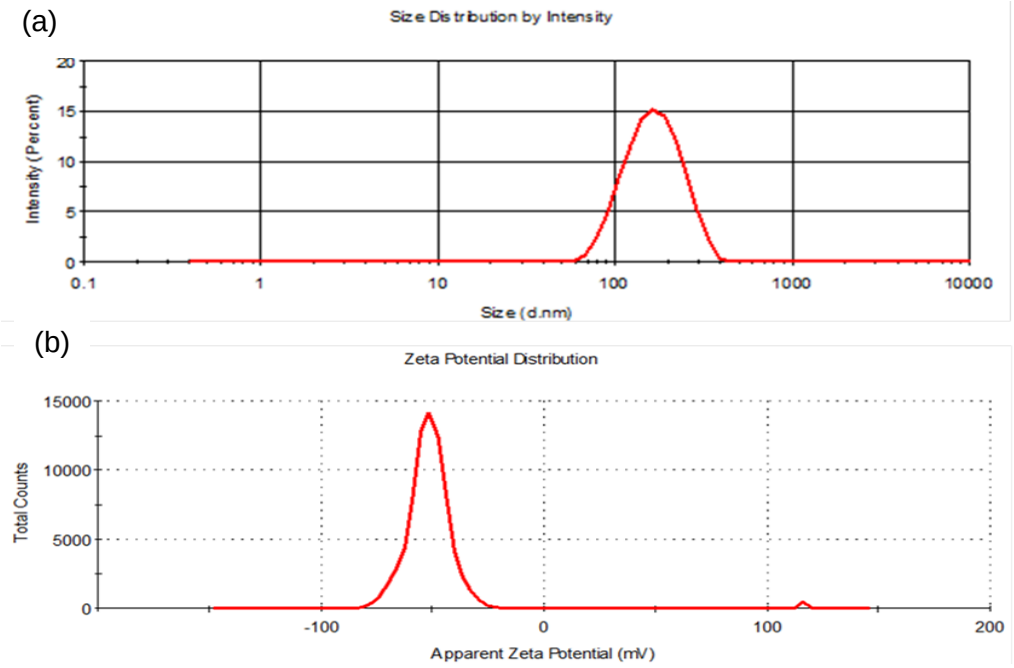

Figure 3.13: (a) Particle size distribution and (b) Average zeta potential distribution profile for ACV-loaded HA–PAA–HP-β-CD nanoparticles.

3.3.7 Chromatographic Analysis for Acyclovir Quantification

Figure 3.14 demonstrated chromatographic separation peaks for ACV and Indapamide (IP), represented as the internal drug standard. A calibration curve was prepared by running the samples after optimization of the verified method.

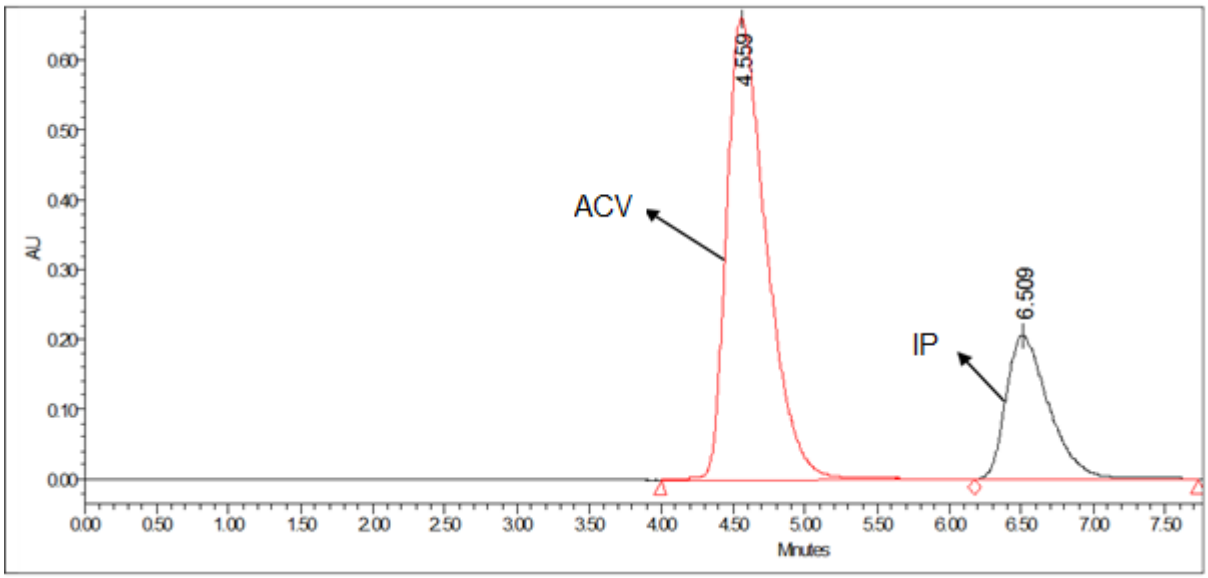

Figure 3.14: Chromatogram showing the separation peaks for ACV and Indapamide.

The area under the curve (AUC) ratio of ACV and IP was plotted against concentration (mg. mL^{-1}). Figure 3.15 displays the calibration curve for ACV quantification in PBS (pH 6.8, 37°C).

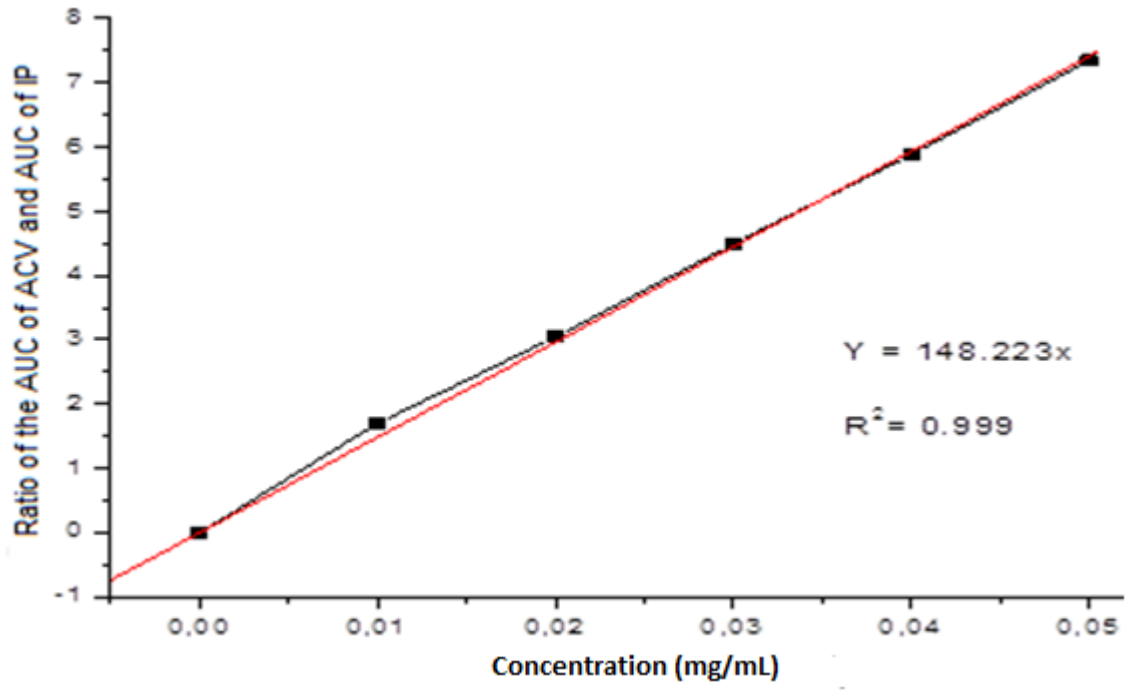

Figure 3.15: Calibration curve for ACV quantification in PBS (pH 6.8), n=3.

3.3.8. Solubility Analysis of Acyclovir from the Polymeric Complex Nanoparticles vs. a Comparator Product

Solubility analysis demonstrated that the concentration of ACV in water was enhanced in the presence of HA─PAA─HP-β-CD. After 24 hours (as per the method undertaken in **section 3.2.13**), 59% of ACV from the comparator product was dissolved in water compared to 90% of ACV from polymeric nanoparticle complex. Therefore, the incorporation of ACV into the HA─PAA─HP-β-CD complex improved its solubility.

3.3.8.1. The mechanism of solubility

The prepared SSBC contains two main components, which enable it to physically interact easier with poorly soluble drugs. The complex contains a hydrophobic component (mainly hydrocarbon heads, which repel water) and a hydrophilic component rendering it an amphiphilic complex. Hence, an entity with a given degree of hydrophobicity will attract similar hydrophobic structures. The poorly water soluble drug was attracted to the inner core of the complex since it contains long polymeric hydrocarbon chains from the modified PAA, the drug will be mainly within HP-β-CD cycle while the hydrophilic component of the complex stabilizes the formed complexation in an aqueous environment (**Figure 3.16** shows the interaction of the drug with the polymeric complex). The drug absorption peaks were not observed in the FT-IR spectra, confirming the existence of the drug within the HP-β-CD complex, thereby hindering its absorption. The complex HA─PAA is amphiphilic, hence the conjugation of an additional amphiphilic HP-β-CD further enhance the oral absorption properties of the drug loaded complex, while maintaining its integrity as proven from ^{1}HNMR in **section 3.3.2, Figure 3.5**.

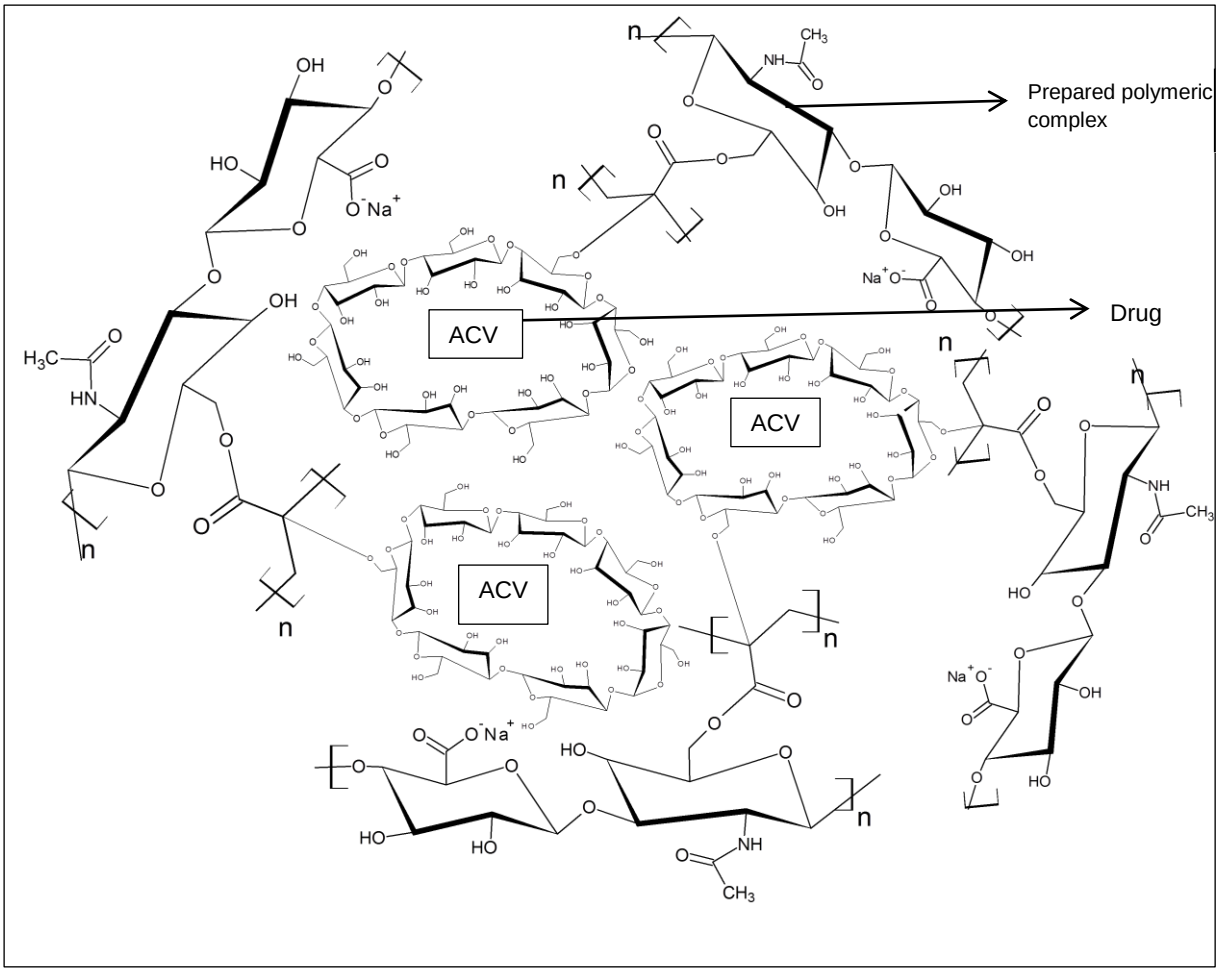

Figure 3.16: Schematic representation of the drug interaction with the polymeric complex.

3.3.9. *In Vitro* Release/Diffusion Studies of ACV from the Polymeric Complex Nanoparticles vs. a Comparator Product

In vitro drug release studies are critical in determining the rate and extent of drug absorption, which in turn affect the therapeutic efficacy of the drug. Absorption of the drug is influenced by its release from the dosage form, its solubility and subsequently permeability into the systemic circulation among other factors (Horter and Dressman, 2001). The influence of the solubility of the drug on the rate of release was observed with respect to the drug incorporated. As the aqueous solubility increases, the rate of drug release increases proportionally. However, the mechanism of release is greatly influenced by the properties of the polymer employed. **Figure 3.17** shows the release of ACV from three formulations. ACV-loaded HA─PAA-HP─β-CD nanoparticles demonstrated rapid release of ACV, as the complex is freely soluble in water. At 5 hours, approximately 70% of ACV was released from HA─PAA─HP-β-CD polymeric nanoparticles complex, while only 30% of ACV was released from the comparator product, as well as for pure ACV (without any excipient) in accordance to the method employed in **section 3.2.14.** This confirms the influence of the

physicochemical properties of HA–PAA–HP-β-CD polymeric complex on the drug, resulting in an increased solubility during the release.

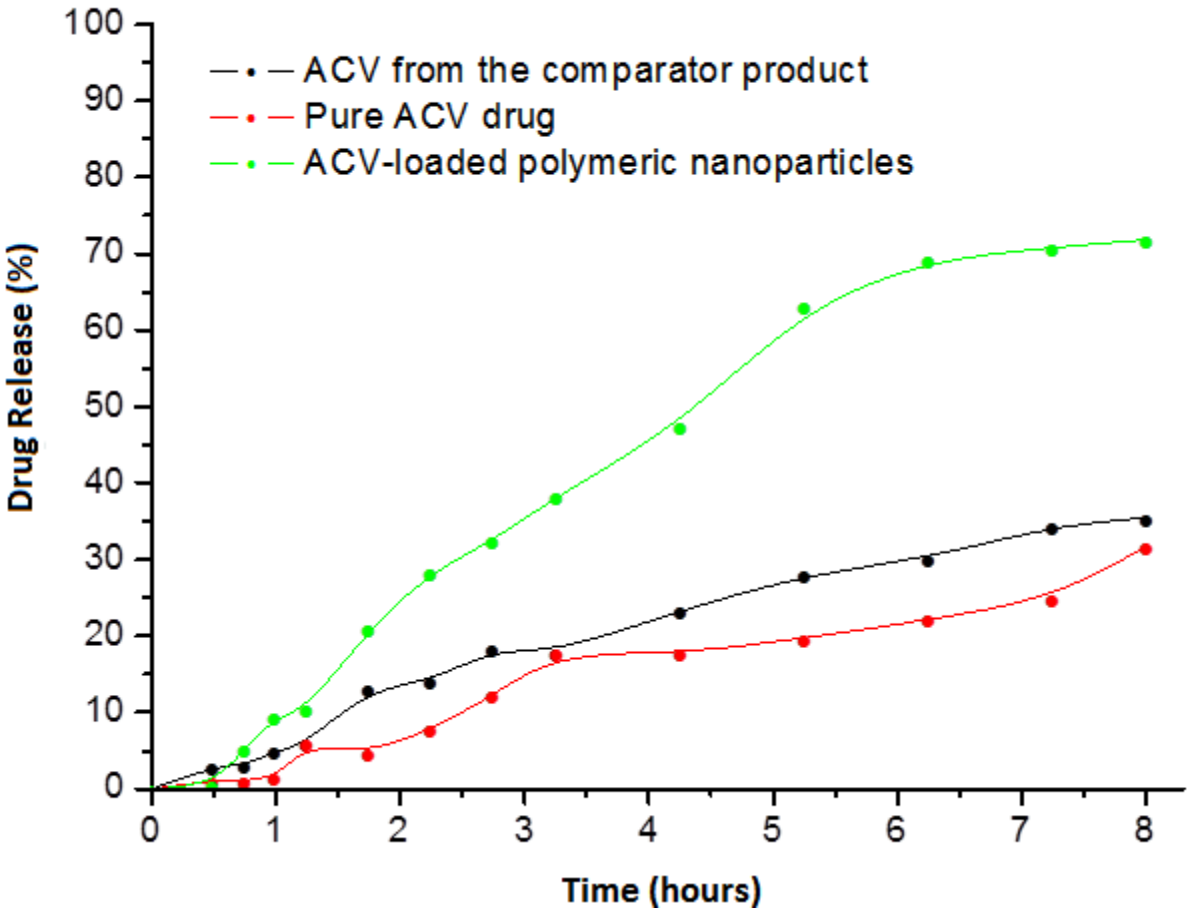

Figure 3.17: Comparative drug release\diffusion profiles for ACV (SD 28.70, **SD 14.40** and SD 13.95), n=3.

Literature has reported a number of different methods that can be used to compare dissolution profiles (Fernandes et al., 2006; Ferraz et al., 2007; Polli et al., 1997; Anderson et al., 1999). The fit factor method was utilized in this study, since it is the most widely accepted method defined by two approaches: f_1 (the difference factor) and f_2 (the similarity factor) given by Equation 3.8 and Equation 3.9:

$$f_1 = \left(\left[\sum_{t=1}^{n} |R_t - T_t|\right] \Big/ \left[\sum_{t=1}^{n} |R_t|\right]\right) \mathrm{X}\ 100 \qquad \text{(Equation 3.8)}$$

And

$$f_2 = 50\ \times \log\left(\left[1 + \frac{1}{n}\sum_{t=1}^{n}(R_t - T_t)^2\right]^{-0.5} X\ 100\right) \qquad \text{(Equation 3.9)}$$

Where factor f_1 represents the average percentage difference over all time points in the amount of the newly developed ACV-loaded polymeric nanoparticle formulation dissolution, compared to the comparator product (ACV existing in the market). R_t represents the percentage of dissolved ACV from the comparator at time t and T_t is the percentage of dissolution of the newly developed ACV-loaded polymeric nanoparticle formulation. The number of time points is represented by n. Therefore, if f_1 is zero, the two formulations are identical, but f_1 increase proportionally with dissimilarity between the newly formulated ACV-loaded polymeric nanoparticles formulations and the comparator product. However, f_2 is between 0 and 100, whereby 100 signifies that the newly developed polymeric nanoparticle formulation and the comparator product are identical. The calculated fit factors in our investigation were found to be f_1 = 104.02 and f_2 = 31.83. Therefore, as confirmed from the calculations, the 2 profiles vary in their release profiles, due to the unique behaviour of the nanoparticle complex.

3.3.10. *Ex Vivo* Acyclovir Permeation Studies

The cumulative amount of ACV permeated from the HA─PAA─HP-β-CD polymeric nanoparticles complex and the comparator product, across the intestinal tissue gradient, is represented in **Figure 3.18**. The HA─PAA-HP-β-CD polymeric nanoparticles complex significantly enhanced the cumulative values of ACV compared to the ACV from the comparator product ($p < 0.05$, where $p = 0.0004$), due to the smaller size of the polymeric nanoparticles (<500nm), which enhances intestinal mucosal permeation and internalization of particles (Francis et *al*., 2004), further altering ACV physicochemical properties through polymeric encapsulation. **Table 3.3** shows the overall flux values for each formulation.

Table 3.3: The overall flux values and accumulation amount for each formulation after 8 hours

Formulations	**Flux ($mg.cm^{-2}.min^{-1}$)**	**Total accumulation ($mg.cm^{-2}$) after 8 hours**
Polymeric nanoparticles	3.0316×10^{-3}	1.4552
Comparator product	2.0023×10^{-3}	1.1027

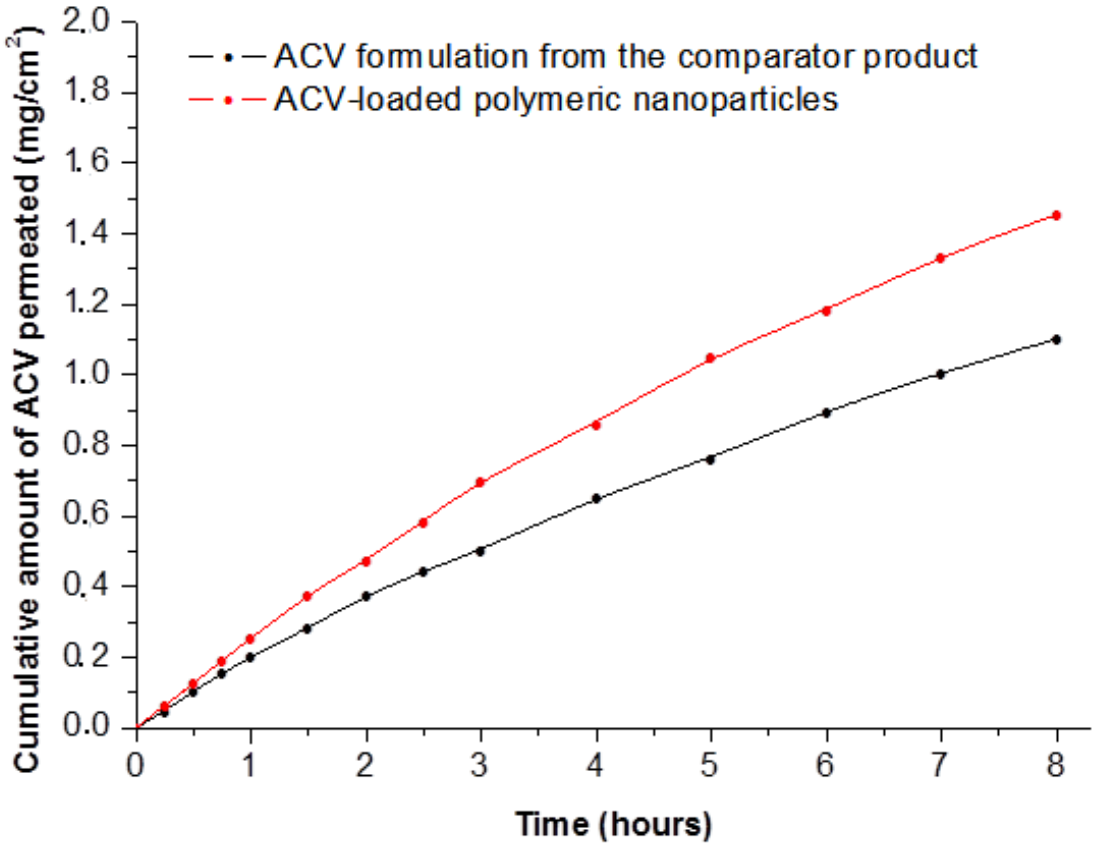

Figure 3.18: The cumulative values of ACV-loaded HA–PAA–HP-β-CD and ACV from the comparator product (37^{o}C) (**SD 0.00942** and SD 0.01044), n=3.

3.4. CONCLUDING REMARKS

It was reported that ACV has poor bioavailability (15-20) after oral administration, due to its poor absorption across the intestinal epithelium. A SSBC (HA–PAA–HP-β-CD polymeric complex) was synthesized and characterized in an effort to improve ACV permeation and solubility. *In vitro* release/diffusion studies of ACV-loaded HA–PAA–HP-β-CD were conducted in order to determine the possibility that the HA–PAA–HP-β-CD nanoparticles may have on the permeability and solubility of ACV in comparison with the conventional commercial dosage of ACV that is currently available on the market. The loading of ACV into the HA–PAA–HP-β-CD polymeric complex caused a significant increase in its permeation across the intestinal epithelium ($p < 0.05$), compared to the comparator product of ACV. *In vitro* data confirmed a marked improvement in drug release characteristics, in comparison to the commercially available product. This could be significantly attributed to the smaller particle size of the complex, enabling it to easily permeate through the intestinal epithelium in the GIT and easily dissolve in aqueous medium.

CHAPTER FOUR
EXPERIMENTAL DESIGN AND STATISTICAL OPTIMIZATION OF THE DRUG-LOADED SEMI-SYNTHETIC BIOPOLYMER COMPLEX

4.1. INTRODUCTION

Spray-drying methods have recently gained huge attention as continuous single-step drying process to convert liquids to solid powders. These methods are significant because particles are obtained with controlled shape and size. Nanomedicine had also added to the demand of spray-drying methods for conversion of liquids to solid powders in the invention of nano-size particles with narrow distribution and good yield (Heng *et al.,* 2011; Lee *et al.,* 2011). The potential of spray-dried nanoparticles has not yet been fully explored. This was observed from the results obtained from the Web of Science online database for a search on “Nano” and “Spray-drying”.

Most of existing spray drying systems have limitations, such as not able to produce nano-scale particles due to limited collection efficiency for particles < 2µm (Schmid *et al.,* 2009; Chan and Kwok, 2011; Heng *et al.,* 2011) and the overall yield is limited to the laboratory scale since these systems need a minimum of 30mL liquid for it to begin a run (Arpagaus *et al.,* 2010; Li *et al.,* 2010; Schmid *et al.,* 2009). To try and minimize or to overcome some of these limitations, a Nano Spray Dryer B-90 was employed. The Nano Spray Dryer B-90 is the fourth and most recent generation of BUCHI laboratory-scale spray dryer instrument (Buchi, Switzerland), following the Mini Spray Dryer B-290, B-191 and B-190 models (Arpagaus *et al.,* 2010; Buchi, 2010).

The operation principle of the Nano Spray Dryer B-90 is based on the actuator causing the vibration of a tiny steel membrane (spray mesh) in a tiny spray cap driven on a piezoelectric crystal. There are different membrane sizes that can be used. The average droplet size is controlled by different spray cap sizes (4.0µm, 5.5µm and 7.0µm). Hence, a sample is fed in a form of liquid or dispersion through a peristaltic pump at a specific flow rate. To eject and vibrate the vapour of droplets, the spray mesh is triggered by the actuator that moves in an ultrasonic frequency creating many precise droplet sizes. The drying chamber contains a drying gas which enters through the laminar flow at the top and sets the inlet temperature by heat. The fine droplets produced are progressively dried to powder (solid particles). These powders are deposited at the surface of the electrode, since the particles are electrostatically charged. During the filtering of the gas, the outlet is measured and the drying gas exits the spray dryer. Connected to the Nano Spray Dryer B-90 apparatus is the inert Loop B-295

functioning as a cooling unit. For the safe operation of solvents an inert gas (N_2) was used to avoid any explosive gas mixture. The electrical field carbon dioxide gas is supplied for the separation of particles at 1.5 bar (Schafroth *et al.,* 2012).

These nano-size systems have the potential to enhance dissolution rates of drug with some hydrophobic characteristics and since particle size is reduced, it creates a larger surface area (Chan *et al.,* 2011; Heng *et al*., 2011;Li *et al.,* 2010; Schmid *et al.,* 2009). Hence, there is a great need for producing nano-carriers for their potential use in improvement of bioavailability and the enabling of targeted drug delivery systems (Li *et al.,* 2010; Lee *et al.,* 2011). The Nano Spray Dryer B-90 was utilized in the design and optimization of the ACV-loaded nanoparticle formulation in this study.

The trial and error approach had been used in designing drug carrier systems, but this method is time consuming because it involves variation of one variable at a time in the formulation. Hence, the success of this method mainly depends on factors such as, intuition, knowledge base and previous experience (Singh *et al.,* 2005). Design of Experiments (DoE) permits the experimental data to fit statistical equations and explores these models during formulation optimization and predicts performance. Different experimental data can be connected through DoE, resulting in data from fewer experiments. This method is a useful scientific tool (Lewis *et al.,* 1999, Singh *et al.,* 2005, Furnaletto *et al.,* 2006).

For the design of the drug-loaded Semi-Synthetic Biopolymer Complex (SSBC) nanoparticles, two variables of interest were identified as concluded in **Chapter 3**. Hence, this **Chapter** seeks to develop drug-loaded SSBC nanoparticles by employing a suitable experimental design with optimal drug entrapment, size and solubility, resulting in an improved oral bioavailability.

A Face-Centred Central Composite Design (FCCCD) was selected. The FCCCD contains an embedded 2^n (where n = number of factors) factorial design with an additional group of star and central points. The star points help in the estimation of the interaction and curvature of the response surface. Hence, response surface plots are also obtained during experimental data optimization which is a graphic representation of the mathematic data obtained for the experimental design. These plots show the relationship between variables for single outcomes (Singh *et al.,* 2005).

The aim of this **Chapter** was to highlight the statistical optimization of the drug-loaded SSBC nanoparticles which was developed in **Chapter 3**. This was carried out by preparing the

drug-loaded polymeric solution and dry the solution using the Nano Spray Dryer B-90 with varied parameters according to the FCCCD generated. The preparation of nanoparticles was undertaken in accordance with the methods developed during the preliminary experimentation phase and was loaded with the model drug (ACV). In order to prepare an optimized drug-loaded system, the size, solubility, drug entrapment and permeation of the different formulations were investigated.

4.2. MATERIALS AND METHODS

4.2.1. Materials

The materials employed in this study were as described in **Chapter 3**, **Section 3.2.1** of this dissertation.

4.2.2. The Face-Centred Central Composite Design for Formulation Optimization

A two factor, three level (3^2) Face-Centred Central Composite Design (FCCCD) was used for the optimization of the prepared ACV-loaded HA─PAA─HP-β-CD nanoparticles. The effect of the independent variables [Nanospray solution concentration (mg/mL) and Encapsulation time (hours)] were explored using the two factor, three level (3^2) FCCCD. The two independent variables were selected because of their noticeable significance during the preliminary preparation of the ACV-loaded HA─PAA─HP-β-CD nanoparticles described in **Chapter 3**. As outline in **Table 4.1**, the maximum drug entrapment, solubility, flux values and minimum zeta size were the expected dependent responses.

Table 4.1: Variables and responses of the preparation of SSBC optimization

Independent Variables	**Levels**	
	Lower	**Upper**
Nanospray solution concentration (mg/mL)	0.75	2.50
Encapsulation time (hours)	2	8
Responses	**Objective**	
Zeta size (nm)	Minimize	
Drug entrapment	Maximize	
Solubility (%)	Maximize	
Flux ($mg.cm^{-2}.min^{-1}$)	Maximize	

4.2.3. Preparation of Face-Centred Central Composite Design Template

The polymeric complex for ACV-loading was prepared as outlined in **Chapter 3**, **section 3.2.2 and 3.2.3**. The loading of ACV and the preparation of ACV-loaded HA─PAA─HP-β-CD nanoparticles were generated according to the FCCCD template, producing 13 formulations.

The encapsulation times and the nanospray solution concentrations for the 13 formulations were prepared as outline in **Table 4.2**. The resulting formulations were characterized and the outcomes were evaluated using a MINITAB® design software, with the purpose of obtaining an optimized formulation.

Table 4.2: Generated formulations for the optimization of ACV-loaded nanoparticles

Formulation number	Nanospray solution concentration (mg/mL)	Encapsulation time (hours)
F1	2.50	2
F2	1.625	2
F3	0.75	2
F4	0.75	8
F5	1.625	5
F6	2.50	8
F7	1.625	5
F8	1.625	5
F9	1.625	5
F10	1.625	5
F11	1.625	8
F12	2.50	5
F13	0.75	5

4.2.4. Preparation of Powder Nanoparticles through Nano-Spray Drying

The Nano Spray Dryer B-90 (Buchi, Switzerland) was used to produce ACV-loaded HA–PAA–HP-β-CD powder nanoparticles (**Figure 4.1**) for all formulations. Briefly, a clear solution was attained, with ACV-loaded HA–PAA–HP-β-CD formulation process and filtered before spray-drying process (0.45µm Millipore filter). For the purpose of this study, a 4.0µm spray cap membrane was used with 60Hz ultrasonic frequency for the actuator. Supplementary spray drying parameters were set in accordance to **section 3.2.5, Table 3.1**.

Figure 4.1: Collection of powder ACV-loaded HA–PAA–HP-β-CD nanoparticles.

4.2.5. Determination of ACV-loaded HA─PAA─HP─β-CD Nanoparticle Size Distribution

The particle sizes of all prepared 13 formulations were determined immediately after the Nano spray-drying process. The Zetasize NanoZS (Malvern Instruments Ltd, Malvern, United Kingdom) instrument was used to quantify the average particle size from each formulation. Briefly, dried powder particles were re-dispersed in water and subjected to a sonication (ultra-sound) for 2 minutes (6mm probe, 20 kHz, 50 W), then their average size was determined.

4.2.6. Morphological Determination of the ACV-loaded HA─PAA─HP-β-CD Nanoparticles

The morphology of the prepared nanoparticles was confirmed using scanning electron microscopy (SEM) (FEI company, Hillsboro, Oregon, USA). Prior to visualization, the prepared nanoparticles were sputter-coated with an isotope of gold, for high refractive imaging.

4.2.7. Determination of Drug Entrapment for ACV-loaded HA─PAA─HP-β-CD Nanoparticles

For each ACV-loaded HA─PAA─HP-β-CD nanoparticle formulation, 50mg was dissolved in 50mL of NaOH (pH 10) solution for 24 hours. Thereafter, the ACV content in each dissolved formulation was determined using UPLC analysis, as verified and described in **Chapter 3, section 3.2.15**.

4.2.8. Determination of the Solubility of ACV-loaded HA─PAA─HP-β-CD Nanoparticles

A Shake Flask Method was used to determine the solubility of the formulations. Each formulation (50mg) was placed into a stopped bottle containing 50mL of buffer solution of pH 6.8. The solutions in the bottles were maintained in a shaking water bath for 24 hours at 37^{o}C at 75 rev.min^{-1} (Waman *et al.,* 2014). Thereafter the sample contents were filtered through a 0.22µm membrane filter, after suitable dilution with the mobile phase. The amount of ACV in the formulations was quantified using UPLC analysis, as mentioned in **Chapter 3**, **section 3.2.15**.

4.2.9. *Ex Vivo* Drug Permeation Studies for ACV-loaded HA─PAA─HP-β-CD Nanoparticles

The tissue preparation and the *ex vivo* drug permeation were implemented as outlined in **Chapter 3 section 3.2.16**. At predetermined time intervals (15, 30, 60, 90, 120, 150, 180,

240, 300, 360, 420 and 480 minutes), samples were drawn from the acceptor compartment and replaced with a fresh equal amount of the PBS (pH 7.4). The drug content from each formulation was analysed using a UPLC analysis. The cumulative amount of the drug permeated and the average flux values (J) of each formulation was calculated as outlined in **Chapter 3, section 3.2.16.1 (Equation 3.6 and Equation 3.7).**

4.2.10. *In Vitro* Cytotoxicity Testing of the ACV-loaded Polymeric Nanoparticles using Caco-2 Cell Lines

The small intestinal lumen surface area is lined with an epithelial cell monolayer, isolating the systemic circulation from the intestinal lumen, which prevents the invasion of bacteria and toxic compounds from the GI tract. Intestinal epithelial cells can be disturbed or damaged by toxic compounds or toxicity generated during digestion. Disturbance or damage in the intestinal epithelial tissues can weaken its protective role. Thus, the possible cytotoxicity of ACV-loaded polymeric nanoparticles was investigated in an intestinal cell line using Caco-2 intestinal cells (Cellonex, South Africa).

4.2.10.1. Cell culturing using caco-2 cell lines

Caco-2 cell lines (Cellonex, South Africa) were grown in culture flasks containing solution Dulbecco's Modified Eagle Medium (DMEM), supplemented with 10% fetal bovine serum with 4.0mM L-Glutamine and sodium pyruvate, with added 50µL Amphotericin (Sigma-Aldrich; St. Louise, MO, USA). Cells were maintained in an incubator (RS Biotech Galaxy, Irvine, UK) under humidified atmosphere of 5% CO_2 at 37°C during cell growth. Cells were grown until they reached 60–90% confluence. The medium was discarded in the cultured flask, adding Trypsin-EDTA (3mL) and incubated for 3–4 minutes to detach the cells. Then fresh medium (3mL) was added in the culture flask after cell detachment and centrifuged at 2000rpm for 2 minutes. The supernatant was discarded and cells were suspended in the fresh medium (10mL) and poured into two flasks. When necessary, cells were frozen in a 1:1 mixture of cryoprotective medium (15%v/v DMSO) at –80^{o}C.

4.2.10.2. Cell counting utilizing trypan blue solution assay and a haemocytometer

After detachment of cells and removal of the supernatant as described in **section 4.2.10.1**, cells were suspended in flesh media (3mL). Briefly, Trypan blue solution (30µL) was added to the suspended cells (10µL). The disposable haemocytometer chamber was filled with a mixture of trypan blue solution added to the suspended cells. Light microscopy (Olympus CKS microscope, Olympus, Japan) was used to examine the chamber for cell counting. Trypan blue solution stains only dead cells and excludes living cells. By counting unstained

cell (living cells) and stained cells (death cells), the number of cells in the sample was determined.

4.2.10.3. *In vitro* cytotoxicity evaluation utilizing 3-4,5-Dimethylthiazol-2-yl)-2,5-Diphenyltetrazolium bromide assay

Cytotoxicity of the ACV-loaded polymeric nanoparticles in Caco-2 cell lines was evaluated utilizing 3-(4,5-dimethylthiazol-2-yl)-2,5-diphenyltetrazolium bromide assay. Briefly, 96 well plates were seeded with Caco-2 cells at a density of $2x10^4$ cells/well. After culturing the cells in 96 well plates for 24 hours in the incubator (RS Biotech Galaxy, Irvine, UK) under humidified atmospheric conditions of 5% CO_2 at 37^{o}C, the culture was removed from the incubator in to a laminar flow unit. Thereafter, different concentrations of the prepared ACV-loaded polymeric nanoparticles solutions (50, 100, 200, 400 and 1000µg/mL) of equal volumes were added to the initial culture media. The cells were again incubated for further 24 hours at 37^{o}C. The medium was removed at the end of the 24-hour incubation, and 100µL of MTT 3-(4,5-dimethylthiazol-2-yl)-2,5-diphenyltetrazolium bromide solution (diluted in a culture media with a final concentration of 0.5 mg/mL) was added to the wells, with a further incubation of 4 hours to allow the conversion of MTT to formazan by mitochondrial dehydrogenase. After a 4-hour incubation period, the culture was removed from the incubator and the formazan formed crystals which were dissolved by adding MTT solubilizing solution equal to the original culture medium volume. All absorbance measured at a wavelength of 570nm. The background absorbance of the multiwall plates was measured at 690nm and was subtracted from the 570nm measurement. The resulting measurements were presented as relative cell viability (mean±standard deviation). Equation 4.1 was used to calculate the relative cell viability:

$$\text{Relative cell viability} = \frac{\text{OD (sample)} - \text{OD (blank)}}{\text{OD(control)} - \text{OD (blank)}} \qquad \text{(Equation 4.1)}$$

4.3. RESULTS AND DISCUSSION

4.3.1. Assessment of Particle Surface Morphology and Particle Size

It was observed by undertaking SEM studies, that the ACV-loaded HA–PAA–HP-β-CD nanoparticulate formulations were spherical in structure. **Figure 4.2** shows an exemplary representation of the formulations. The average sizes of the varying formulations are outlined in **Table 4.3**. It was noted that, as the nanospray solution concentration was decreased, and by increasing the encapsulation time, particles appeared smaller and more spherically defined. The reasoning for this occurring is due to an increased encapsulation time, leading

to greater complexation of the polymer and drug, resulting in uniformly produced nanoparticles.

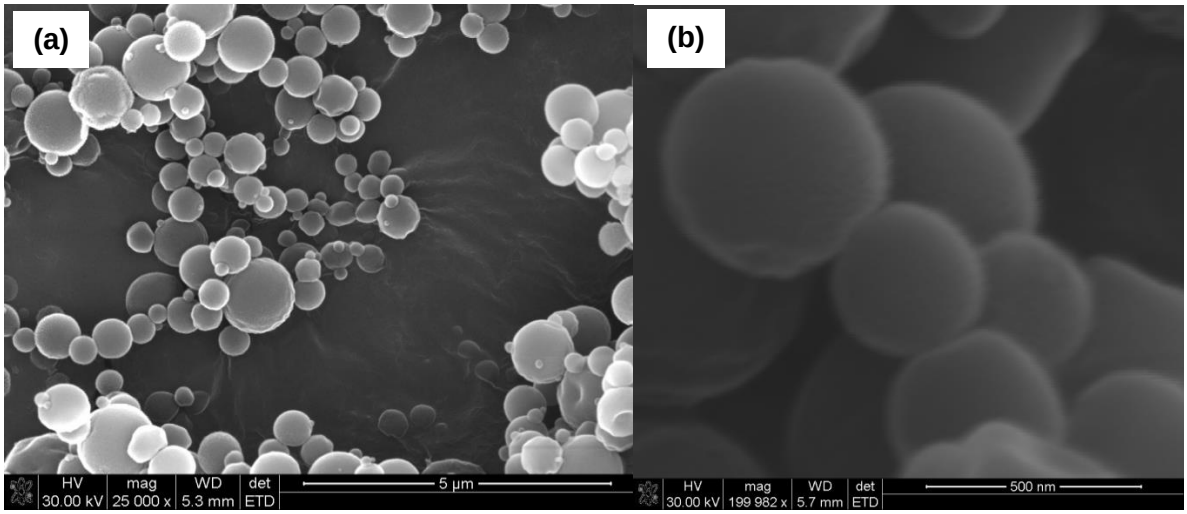

Figure 4.2: The representative SEM image of the ACV-loaded HA–PAA–HP-β-CD nanoparticles where (a) Image is taken at 25 000 x magnification and (b) Image is taken at 199 992 x magnification.

Table 4.3: The experimental responses of the ACV-loaded HA-PAA-HP-β-CD nanoparticles

Formulation	Nanospray solution concentration(mg/mL)	Encapsulation time (hours)	Average Size (nm)	Drug Entrapment in 50mg of formulation	Solubility (%)	Flux (values in 8 hrs.)
F1	2.50	2	280.0	9.67mg (19.34%)	90.49	$206x10^{-5}$
F2	1.625	2	192.6	9.20mg (18.40%)	90.63	$216 x10^{-5}$
F3	0.75	2	185.2	10.05mg (20.10%)	97.58	$185 x10^{-5}$
F4	0.75	8	207.1	11.87mg (23.56%)	90.16	$239 x10^{-5}$
F5	1.625	5	257.8	11.30mg (22.60%)	82.73	$239 x10^{-5}$
F6	2.50	8	207.0	11.81mg (23.62%)	82.05	$216 x10^{-5}$
F7	1.625	5	266.5	11.79mg (23.58%)	83.35	$248 x10^{-5}$
F8	1.625	5	266.9	11.82mg (23.64%)	84.32	$241 x10^{-5}$
F9	1.625	5	272.6	11.92mg (23.84%)	85.13	$233 x10^{-5}$
F10	1.625	5	266.1	11.52mg (23.04%)	81.85	$239 x10^{-5}$
F11	1.625	8	254.3	12.14mg (24.28%)	83.46	$249 x10^{-5}$
F12	2.50	5	185.6	11.89mg (23.78%)	72.31	$216 x10^{-5}$
F13	0.75	5	174.0	12.47mg (24.94%)	73.96	$246 x10^{-5}$

Drug entrapment for each formulation is outlined in **Table 4.3**. It was observed that, percentage drug entrapment is dependent on the encapsulation time and nanospray solution concentration. Hence, the lowest concentration and moderate time duration resulted in the highest drug entrapment. This could be attributed to sufficient time given to the drug to interact with the complex in a concentrated solution medium.

4.3.2. *Ex Vivo* Permeation Studies using ACV-loaded HA–PAA–HP-*β*-CD Nanoparticles

The *ex vivo* permeation rate of the fabricated ACV-loaded HA–PAA–HP-*β*-CD nanoparticles were evaluated prior to *in vivo* study. For all the formulations, the average flux values were calculated as outline in **Table 4.3**. The cumulative amount of ACV permeated against time from the *ex vivo* study for all 13 formulations were plotted as displayed in **Figure 4.3**. The ACV-loaded HA–PAA–HP-*β*-CD nanoparticles formulation profiles are displayed in **Figure 4.3** a, b and c, representing formulations 1-5, 6-9 and 10-13, respectively. The overall highest permeation concentration out of 13 formulations was observed to be formulation 5, while formulation 3 was observed to have the least permeation concentration. Formulation 5,7,8,9 and 10 exhibited nearly similar permeation rates after 8 hours, with formulation 5 possessing slightly higher permeation after 24 hours.

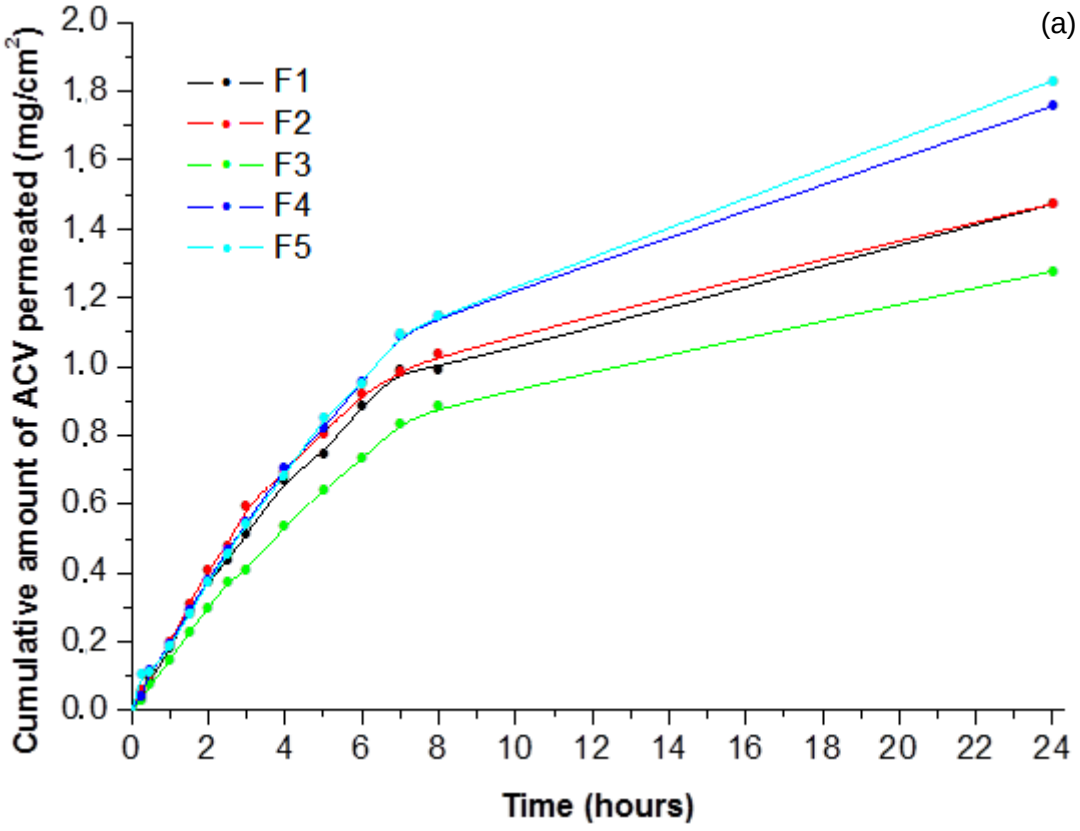

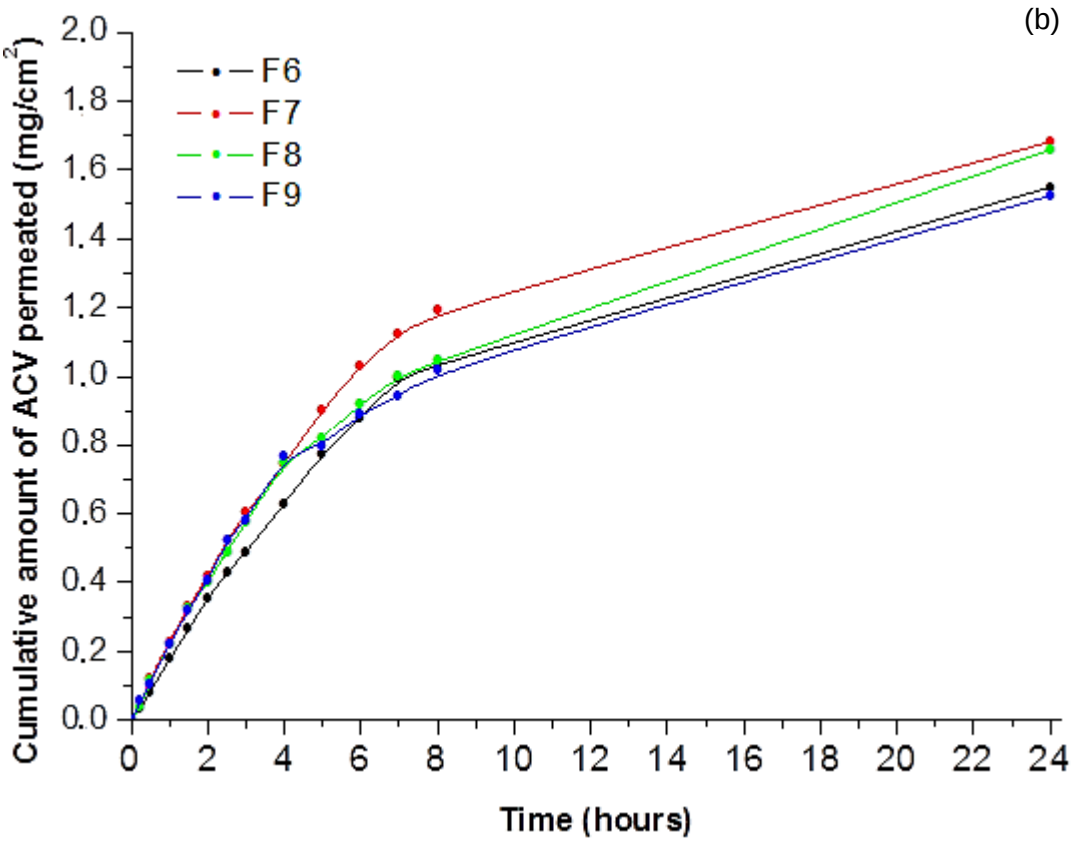

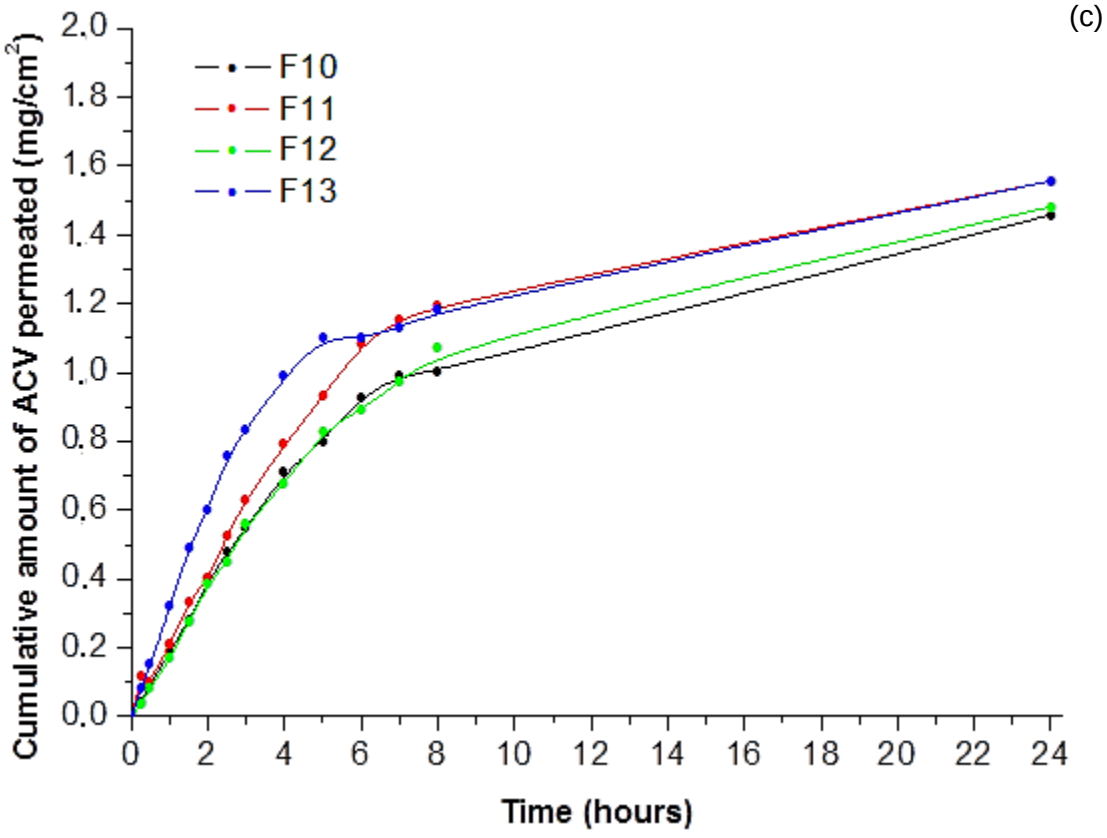

Figure 4.3: The cumulative amount of ACV permeated for (a) formulations 1-5, (b) formulations 6-9 and (c) formulations 10-13, n=3.

4.3.3. Analysis of the Face-Centred Central Composite Design for Nanoparticle Formulation Optimization

Residual plots were used to differentiate between predicted and observed values of particles; with independent variables on the x-axis and residual plots on the y-axis. These plots were mainly employed to investigate regression models. A linear regression model is scientifically acceptable for data that has indiscriminate residuals plot points which are dispersed around the horizontal axis, in comparison to a non-linear model. **Figure 4.4** displays the residual plot of particles size (nm). A near-straight line was observed in a normal probability plot of the residuals signifying a normal distribution analysis. Further, an indiscriminate dispersion of residuals around zero is observed in the residual versus the fitted value scattered plot as expected. A bell shape was obtained in the histogram of the residuals plot, indicating a uniformed distribution of predicted results.

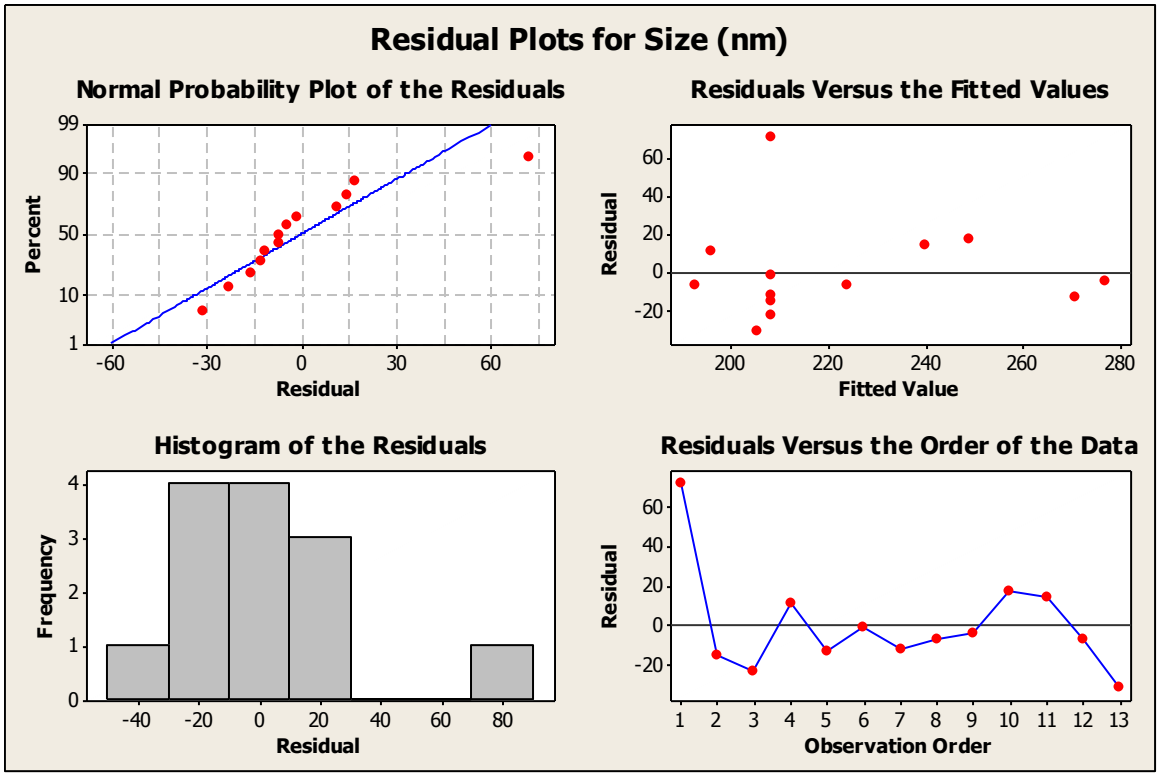

Figure 4.4: Residual plots for formulations representing particle size (nm).

The three-dimensional response surface plots are depicted in **Figure 4.5**; they represent the relationship between the dependent and independent variables of the formulations. As depicted in **Figure 4.5a**. it was observed that solubility increases with an increased encapsulation time and the nanospray concentration solution displayed quadratic effects on the solubility. Solubility increased with increase nanospray concentration solution (until ~2mg/mL) thereafter slightly decreasing in nature.

(a)

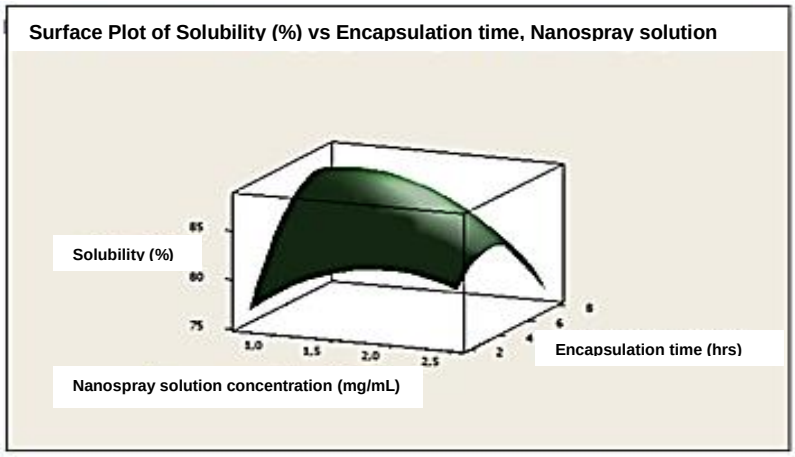

(b)

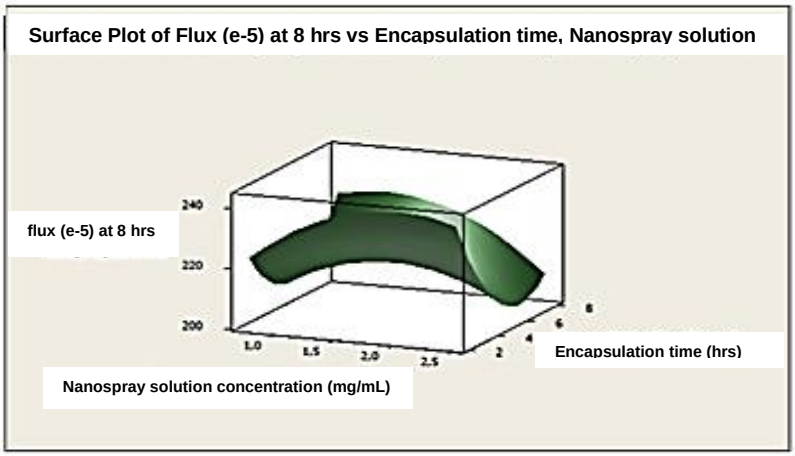

(c)

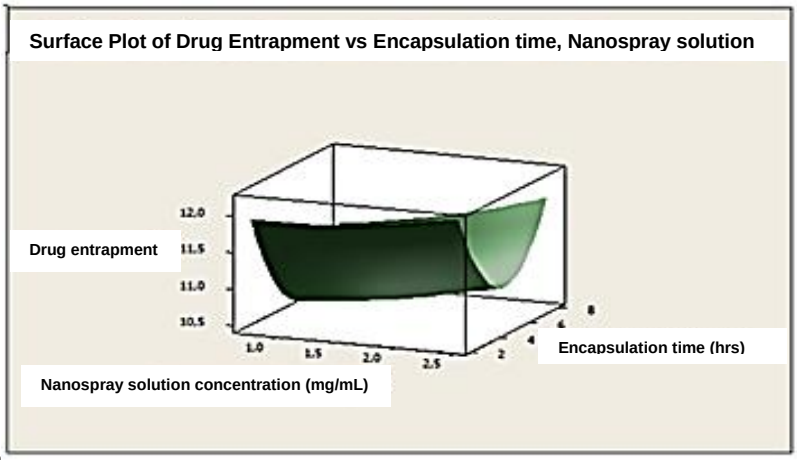

n

Figure 4.5: Response surface plots correlating (a) solubility with nanospray solution concentration and encapsulation time, (b) flux ($x10^{-5}$) with nanospray solution concentration and encapsulation, (c) drug entrapment with nanospray solution concentration and encapsulation time.

As depicted in **Figure 4.5** b, the flux gradually increases with the nanospray concentration solution, thereafter remaining constant in the region of 2mg/mL. The encapsulation time demonstrates a vertical parabolic effect on the response solubility. As depicted in **Figure 4.5**

c, drug entrapment slightly increases with an increase in nanospray solution concentration, with a vertical parabolic effect also observed in response to solubility.

4.4. RESPONSE OPTIMIZATION OF THE ACV-LOADED HA–PAA–HP-β-CD NANOPARTICLES

The statistical software (Minitab®, V14, Minitab Inc®, PA, USA) was used for each variable to determine its optimum parameters. The formulations were optimized, in accordance to the measured responses, being drug entrapment, solubility, as well as flux and size, as displayed in **Figure 4.6**.

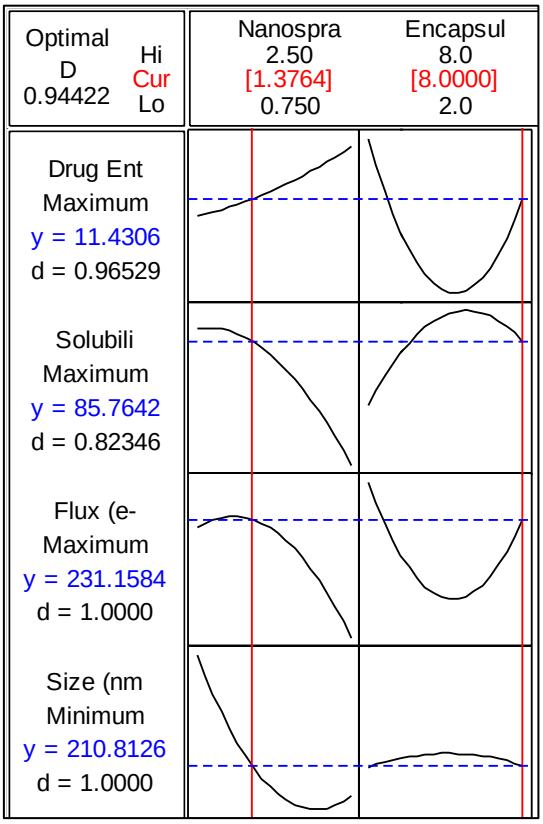

Figure 4.6: Optimization plots displaying factorial levels and desirability values for the chosen optimized ACV-loaded HA–PAA–HP-β-CD Nanoparticle Formulations.

4.4.1. Fabrication and Characterization of the Optimized Formulation

Fabrication of the polymeric complex was described in **Chapter 3 Section 3.2.2 and 3.2.3**, with optimization undertaken as outlined in **Figure 4.6.**

4.4.2. Morphology and Size Distribution Analysis of the Optimized Formulation

The cross-sectional morphology of the optimized polymeric nanoparticulate formulation was observed immediately after the Nano Spray Drying process. It was found that the nanoparticles were spherical in shape as viewed using SEM analysis. The average size

distribution of the optimized polymeric nanoparticle formulation was found to be in the region of 209.50nm and a zeta potential of -51mV was observed, with a PdI of 0.330. A PdI value less than 0.50, revealed minimum particle size variation, with a particle charge preventing agglomeration.

4.4.3. Assessment of Drug Entrapment and Solubility for the Optimized Formulation

Drug entrapment for the optimized ACV-loaded polymeric nanoparticle formulation was predicted to be 11.23mg (22.46%), while the experimental value was 10.00mg in 50.00mg of the formulation (equivalent to 20.00%). During solubility experiments, it was found that the solubility or the concentration of ACV in the buffer was 83% after 24 hours (as per the method in **section 3.2.13**). The flux value was calculated to be 205.03×10^{-5}.

Table 4.4 displays the predicted values of the optimized ACV-loaded polymeric nanoparticle formulation, in comparison to the experimental values of the four responses.

Table 4.4: Measured responses of the experimental verses the predicted values

Measured response	Predicted values	Experimental values	Desirability (%)
Drug Entrapment	11.23mg (22.46%)	10mg (20.00%)	89.05
Solubility	85.7642%	83%	96.78
Flux ($x10^{-5}$)	231.1584	205.03	88.70
Size (nm)	210.8126	209.50	99.38

4.4.4. *In Vitro* Assessment of the Optimized Formulation

As mentioned in **Chapter 3**, *In vitro* drug release studies essential for determining the rate and extent of drug absorption, which in turn affects the therapeutic efficacy of the drug. Absorption of the drug is influenced by its release from the dosage form, its solubility and subsequently permeability into the systemic circulation among other factors (Horter and Dressman, 2001). The rate of ACV release from the novel HA─PAA─HP-β-CD polymeric complex was studied. The mechanism of drug release is mostly influenced by the properties of the polymer employed. **Figure 4.7,** illustrated the release of ACV from the ACV-loaded HA─PAA─HP-β-CD nanoparticulate formulation. Results revealed that, at 7 hours, approximately 75% of ACV was released from HA─PAA─HP-β-CD polymeric nanoparticle complex in accordance to the method employed in **Section 3.2.14.** This confirms the influence of the physicochemical properties of HA─PAA─HP-β-CD polymeric complex on the drug, resulting in an increased solubility with enhanced drug release.

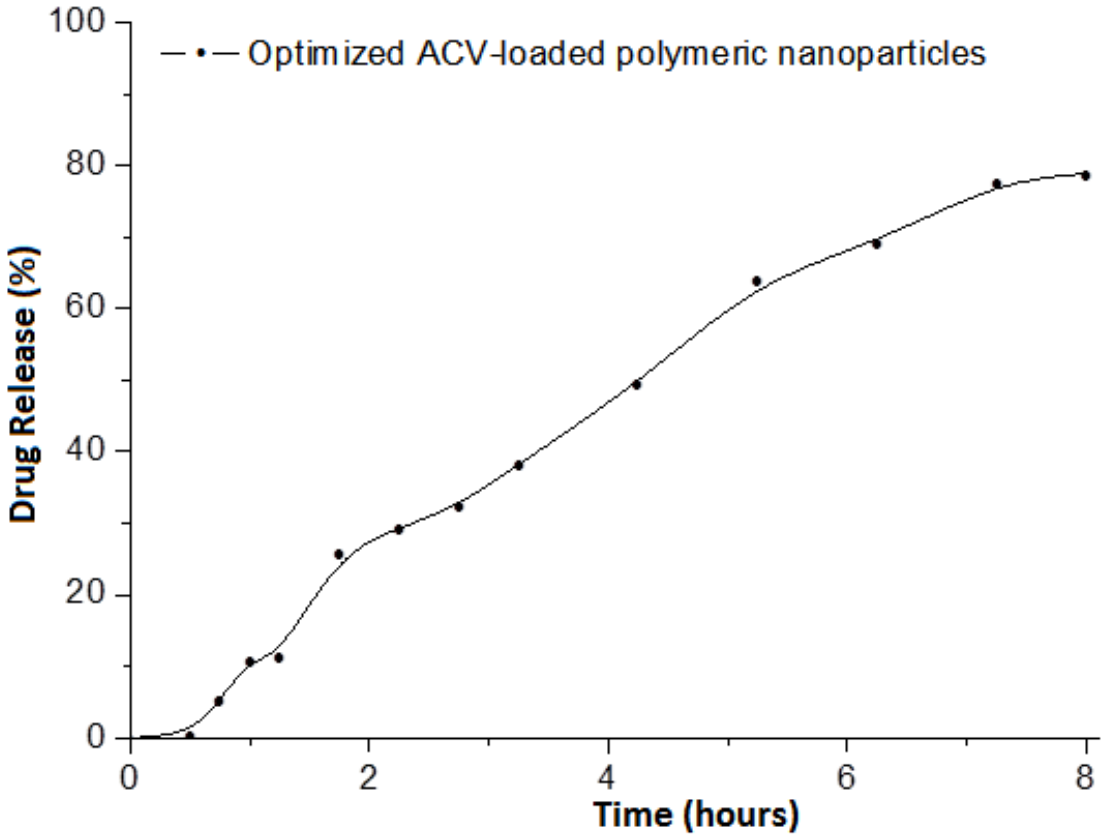

Figure 4.7: Percentage release of ACV for the optimized nanoparticle formulation (SD 3.23), n=3.

4.4.5. *Ex Vivo* drug Release of ACV from the Optimized Formulation

The cumulative amount of ACV permeated from the optimized drug-loaded HA–PAA–HP-β-CD nanoparticle complex across the pig intestinal tissue, is reflected in **Figure 4.8**. As concluded in **Chapter 3**, this polymeric complex demonstrated significant results for increased drug permeability, due to uniform reduced particle size.

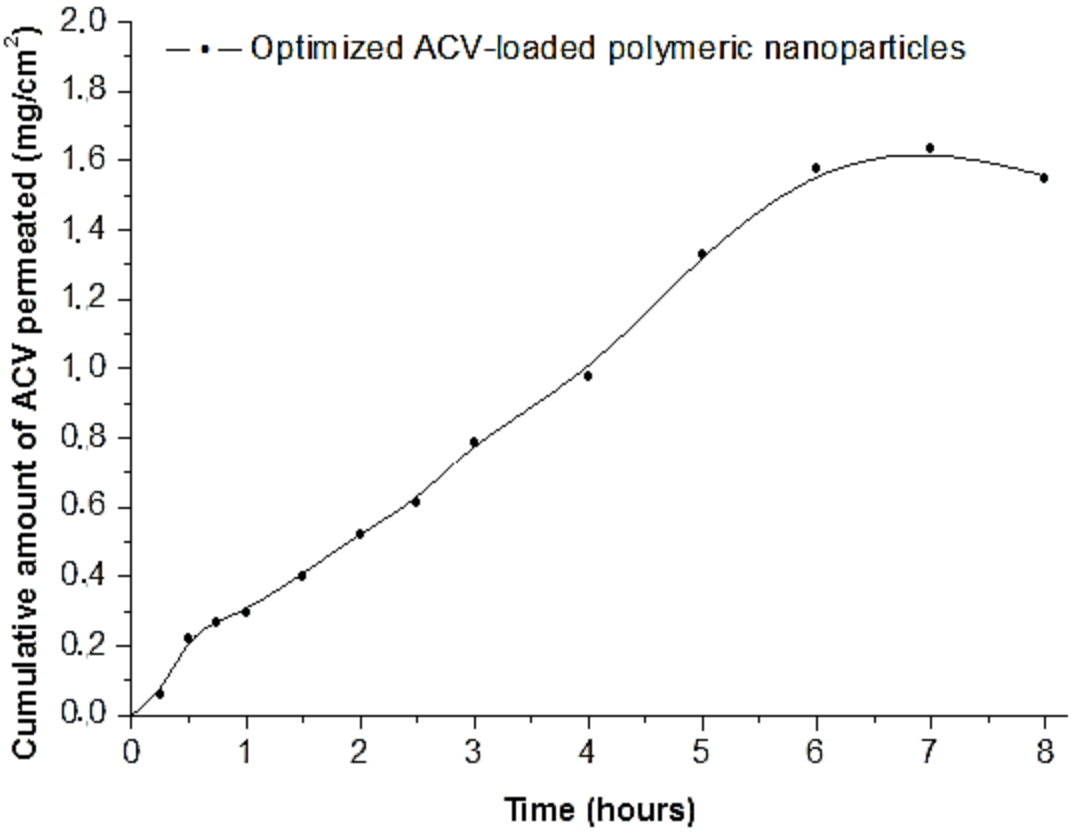

Figure 4.8: Cumulative drug permeation graph of ACV from the optimized polymeric nanoparticulate formulation (SD 0.059), n=3.

4.4.6. Cytotoxicity Analysis of ACV-loaded Polymeric Nanoparticles

The cytotoxicity of ACV-loaded polymeric nanoparticulate formulation was investigated using Caco-2 cells. Cells were incubated in ACV-loaded polymeric nanoparticle medium (50 to 1000ug/mL) for 24 hours, using a MTT assay to investigate the cytotoxicity effects. **Figure 4.9** demonstrates that there were no significant differences in relative viability of the ACV-loaded polymeric nanoparticles compared to the control. The synthesized novel ACV-loaded polymeric nanoparticle formulation thus demonstrated no noticeable toxic effects on the intestinal epithelium tissue.

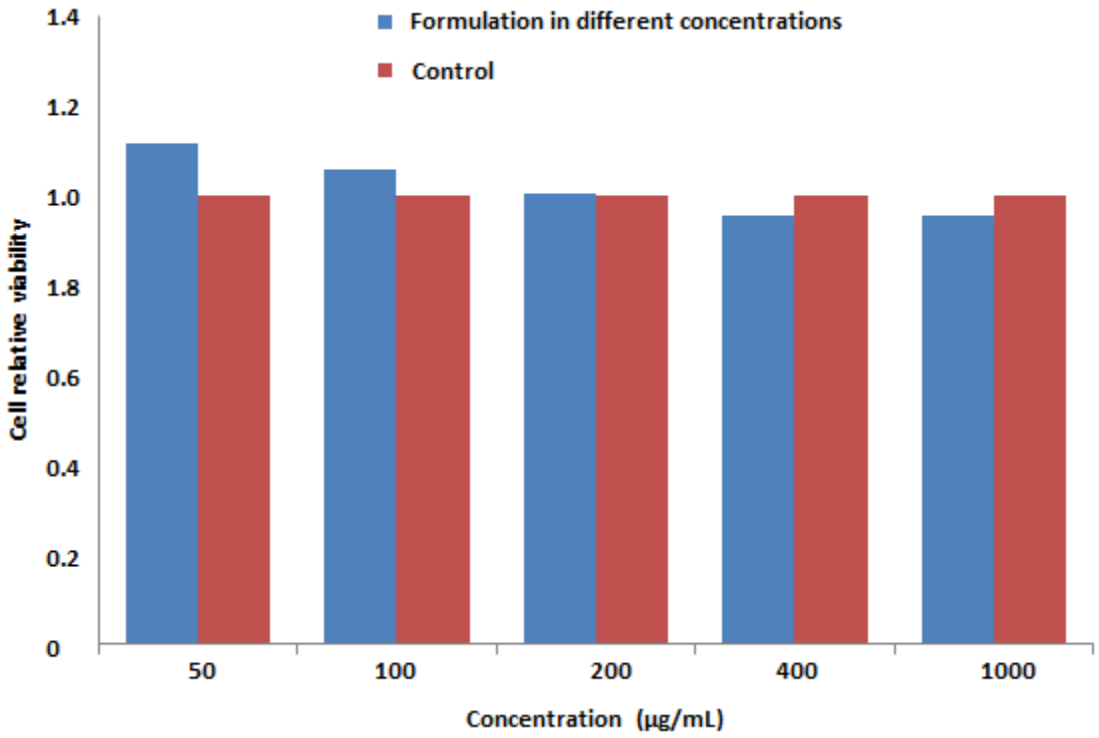

Figure 4.9: Cytotoxicity cell culture test.

4.5. CONCLUDING REMARKS

The novel ACV-loaded polymeric nanoparticle formulation was optimized and synthesized in accordance to the FCCCD. The effects observed from the independent variables on the measured responses were examined, determining the predicted responses and experimental input for the optimized ACV-loaded polymeric nanoparticle formulation. The experimental design proved to be scientifically suitable and the prepared optimized formulation was tested and characterized in accordance to previously verified techniques. The optimized formulation confirmed the improved intestinal solubility and permeation of the drug under investigation, demonstrating no significant toxicity on Caco-2 cell lines. Due to these positive results, the optimized ACV-loaded polymeric nanoparticles under investigation was successfully evaluated *in vitro* and *ex vivo*, thus progressing to the final stage of this research where the optimized polymeric nanoparticles are evaluated *in vivo*, using a Large White Pig model, which discussed in detail in **Chapter 5**.

CHAPTER FIVE

IN VIVO ASSESSMENT OF THE DRUG-LOADED SEMI-SYNTHETIC BIOPOLYMER COMPLEX IN THE LARGE WHITE PIG MODEL

5.1. INTRODUCTION

In vitro drug release studies are conducted in an attempt to partially simulate *in vivo* conditions; however, drug carriers are not exposed to the complete functionality of an *in vivo* environment. *In vivo* drug release studies are of great significance, providing pharamacokinetic data which is most reliable and quantifiable (Lachman, 1992; Quimby, 2002; Festing and Wilkinson, 2007; Stokes and Marsman, 2014).

The *in vivo* release studies utilizing animals are of great importance in order to study the pathogenic and potential therapeutic strategies of the human disease (Gerlach, 1996). Hence, it of great significance and benefit to select an appropriate animal model for a particular study that will closely mimic the conditions and effects in humans.

For the purpose of this study, Large White Pig model was selected to evaluate the release rate of the prepared novel optimized ACV-loaded polymeric nanoparticle drug delivery system in comparison to the current existing ACV conventional dosage form that is available in the market. The Large White Pig animal model was selected since they have similar buccal tissue and gastrointestinal anatomy and physiology as humans. In addition, pigs have minimal cost of maintenance and they are a good model for studies that require frequent blood collection sampling (Oberle *et al.,* 1994; Anderson *et al.,* 2002; Dorkoosh *et al.,* 2002; Brunet *et al.,* 2006). The digestive characteristics of pigs also allows acceptable parallel comparison to humans, hence, pigs are the best model for *in vivo* studies employing oral drug therapeutic technologies (Patel, 2005; Cooppan, 2010; Kolawole *et al.,* 2010; Ndesendo *et al.,* 2011; Shaikh, 2012; Moodley, 2013; Bawa *et al.,* 2013).

This **Chapter** critically evaluates the pharmacokinetic behaviour of the optimized ACV-loaded polymeric nanoparticles, in comparison to the current commercially available ACV dosage formulation. The polymeric nanoparticulate formulation was administered in a capsule, which was further enteric coated to avoid acid degradation in the stomach.

5.2. MATERIALS AND METHODS

5.2.1. Materials

UPLC grade solvents were used for UPLC-MS/MS analysis, employing analytical grade reagents of 99.99% purity. Methanol was purchased from Microsep (Johannesburg, South Africa). Heparin sodium 1000 i.u/mL (Boden^{PTY}, Intramed, Port Elizabeth, South Africa), Acrodisc$^{@}$ 13mm 0.22µm filters and french gauge double lumen 35cm catheters (SA-17752) was obtained from Life science (Johannesburg, South Africa). ACQUITY UPLC C18 columns (1.7µm, 2.1x100mm) was purchased from Water Corporation (Milford, MA, USA). White Large Pigs were obtained from the Central Animal Services (CAS) from the University of the Witwatersrand. All other reagents were of standard analytical grade, and was used as procured.

5.2.2. Ethics Clearance for the Use of Animals in this Study

In vivo assessment of innovative polymeric oral drug delivery systems in Large White Pigs was approved by the Animal Ethics Screening Committee (AESC), from the University of the Witwatersrand with Ethics Clearance Number 2014/38/C (Appendix C)

5.2.3. Experimental Procedures Undertaken During *In Vivo* Evaluation

Prior to oral dosing of the ACV-loaded polymeric nanoparticles formulation and commercial product, pigs were weighed on a day-to-day basis. In order to keep record of any weight changes that had occurred, the animals were weighed during the study for possible interferes with the standard procedures of the study. For any pig that was found to have lost body weight > 10%, the CAS at the University of the Witwatersrand was obliged to remove the animal from the study. All animals were regularly observed for any behavioural changes and any signs of pain or reluctance to move around.

This study compared the prepared novel optimized ACV-loaded polymeric nanoparticle formulation with the ACV conventional dosage currently on the market in terms of their kinetic release. During this experimentation, a placebo (drug free) formulation was also administered orally as a reference system (control) in order to observe any behavioural variations in the drug dosed and non-drug dosed animals. A total of 18 Large White Pigs were divided into groups of 3, each containing 6 Large White Pigs as described below:

Group 1 (Test): Contained 6 Large White Pigs, in which 5 were orally administered with the optimized novel ACV-loaded polymeric nanoparticle formulation (containing ACV = 200mg),

using an intragastric tube, with 1 pig not administered any formulation. This group was used to obtain pharmacokinetic data for comparison purposes.

Group 2 (Conventional dosage form): Contained 6 Large White Pigs, in which 5 were orally administered with ACV conventional dosage formulation (containing ACV = 200mg) through an intragastric tube, with one pig not been administered anything. This group was also utilized to obtain pharmacokinetic results, which would allow comparison between the optimized novel ACV-loaded polymeric formulation and the conventional ACV dosage that is currently available on the market.

Group 3 (Control): Contained 6 Large White Pigs, in which 5 were orally administered with a drug-free formulation through an intragastric tube with 1 pig not being administered with any formulation.

Figure 5.1 is a schematic representation of the animal experimentation design using a Large White Pig model. Pigs were anaesthetized by injecting Anklet® (Ketamine 11mg/kg) and Dormice® 0.3mg/kg, which was maintained under Isoform® and medical oxygen gas for 30 minutes. Under the influence of anaesthesia, the novel optimized ACV-loaded polymeric nanoparticle formulation and the ACV convention dosage were administered via intragastric dosing, with a three day wash out period in between. Blood samples were drawn from the catheterized jugular vein into heparinized tubes at pre-determined time intervals. All blood samples were centrifuged at 5000rpm for 10 minutes. The separated plasma was removed and stored at –80^{o}C until further analysis (Patel, 2005; Cooppan, 2010; Kolawole *et al.,* 2010; Ndesendo *et al.,* 2011; Shaikh, 2012; Bawa *et al.,* 2013; Moodley, 2013).

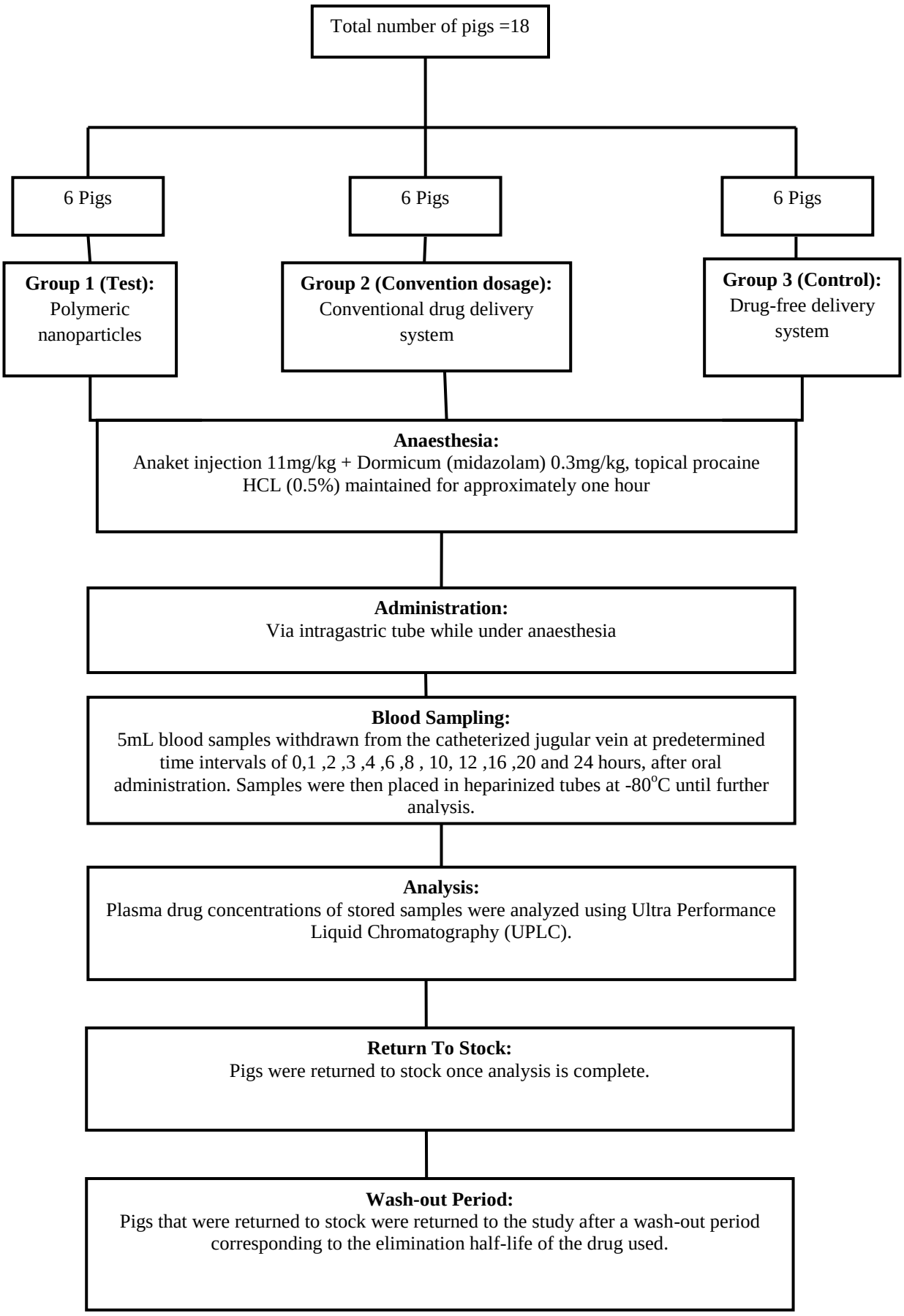

Figure 5.1: Schematic of the experimental design employed for *in vivo* drug release studies

5.2.4. Surgical Attachment of a Catheter into the Jugular Vein for Blood Sampling

5.2.4.1. Surgical preparation of Large White Pigs

All Large White Pigs were anaesthetized using Midazolam 0.3mg/kg, topical procaine and ketamine HCL 11mg/kg. The anaesthesia in pigs was maintained by medical oxygen (100%) and isoflurane gas (2%) for approximately 30-60 minutes (Likenhoker *et al*., 2010) to allow enough time for the surgical implantation of the catheter into the left jugular vein (Kolawole *et al.,* 2010*)*.

5.2.4.2. Surgical implantation of the catheter into the jugular vein

The surgical implantation of catheters into the pigs left jugular vein was undertaken after 10 days of habituation. The surgical insertion of the 7 gauge double lumen 40cm catheter (CS-28702, Arrow Deutchland GmbH, and Erding, Germany) into left jugular vein was carried. The jugular vein was exposed by an incision made to the left lateral part of the neck. The jugular vein was isolated by blunt segmentation and a two-lumen 10cm central venous catheter was inserted into the lumen of the vein. A technique called purse suture was used to fasten the inserted catheter into the wall of the vein. 25cm length of the catheter remaining after insertion was tunnelled subcutaneously to an exit point towards the cranial position, at the dorsal aspect of the scapula, which was stitched to avoid detachment. The external injection ports of the catheter were sutured to the skin to prevent excess bending. Blood samples were taken with heparinised saline (5000IU heparin in 1L of 0.9% saline). Buprenorphine 0.05mg/kg and Carpofen 4mg/kg intramuscularly were administered to manage the pain and inflammation. After surgery, all pigs were observed critically to ensure full recovery from anaesthesia. Prior to oral dosing, all pigs were allowed complete recovery for a period of 10 days.

5.2.5. Capsule Enteric-Coating Method

5.2.5.1. Preparation of the coating dispersion

For preparation of a Eudragit® L 100 dispersion, 2.3g of a polysorbate 80 solution (33%$^{v}/_{v}$), 4.6g of triethyl citrate (plasticiser) and 1.9g of glyceryl monostreorate were added to 100mL deionized water solution. The mixture was stirred for 10 minutes in a high speed mixture until a fine, homogenous dispersion was obtained. Finally, the dispersion was gently added to 80g of Eudragit® dispersion in deionized water (30%$^{w}/_{v}$) to form an enteric coating solution.

5.2.5.2. Methodology for enteric coating of the capsule

The method of capsule enteric coating was adapted from the ProCoater method (Gill and Prausnitz, 2007). Briefly, an empty Gelatine Capsule size 00 was filled with the prepared sterilized novel optimized ACV-loaded polymeric nanoparticle formulation and sealed. The prepared enteric coating solution was gently poured in the Coating Tray, to avoiding bubble formation. The filled capsules were loaded into a capsule coating holder, thereafter the entire capsule body plus a portion of the capsule cap were dipped into the prepared enteric coating solution. A dipping and withdrawal operation of 10 times was performed within a total of 25 to 30 minutes.

5.2.6. Optimized Nanoparticle Formulation Administration to the Large White Pigs

Pigs were fasted overnight and the following day prior to dosing. All pigs were sequentially anaesthetized by injecting Ketamine HCL (40mg/Kg) through the implanted catheter. The anaesthesia was maintained using topical procaine and oxygen. Once the pig was stable on anaesthesia, an intragastric tube was inserted all the way into the stomach while the pig was lifted in an upright manner and the tube size was limited to the weight of the pig. The enteric coated capsule containing the novel optimized ACV-loaded polymeric nanoparticle formulation was administered through the intragastric tube and a small amount of water (~30mL) was utilized to flush down the capsule. After administration, the pig was taken back to its pen, and was observed until full recovery and consciousness was obtained.

5.2.7. Convention Dosage Formulation Administration to the Large White Pigs

The administration of the ACV conventional dosage that is current available in the market was as described in **section 5.2.6.**

5.2.8. Collection of Blood samples, Measurements and Drug Extraction

5.2.8.1. Blood sample treatment and handling after collection

There was no need for any form of anaesthesia or restraint during blood sampling from the catheters. Hence, blood was sampled in order to determine the concentration of ACV that reached the systemic circulation of the pig at a certain time interval. Sterilized syringes were used for the collection of blood samples from the inserted catheter into the jugular vein. The collected blood was placed in EDTA tubes (BD Vacutainers, Franklin Lakes, NJ, USA) to avoid contamination. After administration of the formulation, blood was collected at 0, 1, 2, 3, 4, 6, 8, 10, 12, 16, 20 and 24-hour time points, as seen in **Figure 5.2.** The sampled blood

was centrifuged at 5000rpm for 15 minutes to obtain plasma and stored it in a –80^{o}C. The obtained plasma was analysed using UPLC techniques.

Figure 5.2: Blood sampling procedures undertaken after dosing of the nanopolymeric and commercial ACV formulations.

5.2.8.2. Drug extraction method from the plasma samples

Protein has to be removed from the blood prior to injecting the sample into the UPLC for analysis. There are two commonly used extraction methods to remove protein from the blood, which are: Liquid-liquid extraction and solid phase extraction. For this study, Liquid-liquid extraction method was established to be the best method to remove proteins, whereby propan-2-ol and dichloromethane were used as deproteinizing agents of choice for this procedure.

*5.2.8.2.1***.** *Mechanism of removal of ACV from plasma*

After obtaining the optimized ratio of protein removal according to **Section 5.2.8.2***,* the frozen plasma sample was thawed and poured in a tube. The ratio of propan-2-ol: dichloromethane (1200µL:400µL) was pipetted into the centrifuge tube and 400µL of blood plasma was added into the tube, in accordance with the ratio obtained in **Section *5.2.8.2.***. To ensure proper mixing with the blood, samples were vortexed (Vortex-Genie 2, Scientific Industries Inc., Bohemia , NY , USA) for 15 minutes. In order to remove the precipitated protein, samples were centrifuged at 1500rpm for 10 minutes (Model TG16-WS, Shanghai Luxiangyi Centrifuge Instrument Co., Ltd., Shanghai, China). Eppendorf microtubes (Eppendorf AG, Hamburg, Germany) were used to hold the supernatant, which were then placed in a vacuum

oven (60^{o}C). Samples were then filtered using a 0.2µm filter (GHP Acrodisc filter, Pall Life Sciences, NY, USA). Indapamide (IP) was used as an internal standard and 100µL of a 0.1mg/mL solution was added to each sample before analysis.

5.3. THE UTILIZATION OF UPLC FOR DRUG ANALYSIS

The concentration of the ACV drug under investigation from pig blood plasma was determined using UPLC analysis technique. In this study, Waters, UPLC system (Waters, Milford, MA, USA) with a PDA detector was utilized. However, separation occurs in the UPLC® BEH Shield RP_{18} column having a pore size of 1.7µm. A method for separating ACV from pig plasma was developed, involving the appropriate selection of the flow rate, injection volume, wavelength and mobile phases.

5.3.1. Preparation of the Mobile Phase and Washing Solutions

Double deionised water (Milli-Q Gradient, Millipore, MA, USA, electrical conductivity 18.2MΩ.cm at 25˚C) was used for all solution preparation. Prior to use, all solutions were filtered under vacuum using Durapore® membrane filters (0.22µm) to avoid column blockage that may lead to instrument failure. The appropriate mobile phase was found to be methanol: water: orthophosphoric acid in a ratio of 75:29:1. The washing solution consisted of 90% $^{v}/_{v}$ acetonitrile (Strong wash) and 10% $^{v}/_{v}$ acetonitrile (weak wash).

5.3.2. Construction of the Calibration Curve for the Analysis of ACV Release from the Nanoparticle Formulation

A standard stock solution of 0.1mg/mL ACV was prepared, by first dissolving ACV (10mg) in 15mL of 0.1N sodium hydroxide, with the solution made to 100mL with the mobile phase. A sequence of working solutions were prepared by spiking blank plasma with working standard solutions to obtain concentrations of 0.025, 0.020, 0.015, 0.010 and 0.005mg/mL. The calibration curve was constructed from the peak ratio of drug/internal standard versus the prepared working solution concentrations.

5.4. VALIDATION OF ULTRA PERFORMANCE LIQUID CHROMATOGRAPH (UPLC) ASSAY IN DETERMINATION OF ACV CONCENTRATION IN PIG PLASMA

5.4.1. Selectivity Analysis of the UPLC Technique

The selectivity of the instrumental assay was done by comparing the chromatograms of plasma obtained from the six pigs and the prepared mobile phase on UPLC to those spiked with ACV and the internal standard. Therefore, it would be easier to identify and eliminate interfering peaks.

5.4.2. Drug Recovery Test Utilizing the UPLC Technique

A drug recovery test was performed by comparing the area ratio (analyte/IS) peak obtained from the blank plasma that was spiked with different concentrations of analytes and with constant concentration of the internal standard before and after drug extraction procedures (Iriarte *et al.,* 2009; Samanidou *et al.,* 2009).

5.4.3. Calibration Curve Linearity Analysis

The linearity was validated from the plotted calibration curve obtained from the calculated ratio of analyte/IS peak area versus analyte. Working concentrations were prepared by spiking the blank plasma with the working solutions prior to extraction (Samanidou *et al.,* 2009; Iriarte *et al.,* 2009). Therefore the plot was drawn to validate the linearity of the chromatographic assay and all measurements were performed in triplicate.

5.4.4. The Degree of Detection and Quantification

The degree of detection and quantification were determined in accordance to the following 2 Equations (Samanidou *et al.,* 2009).

Limit of quantification = $10\sigma/S$ (Equation 5.1)
Limit of detection = $3.3\sigma/S$ (Equation 5.2)
Where:

σ = standard deviation (SD)

S = Calibration curve.

5.4.5. Chromatographic Assays Accuracy and Precision

The precision and accuracy of the chromatographic assay was determined by preparing 3 different analyte concentrations (low, middle and high concentration). Hence, precision was taken as the percentage relative standard deviation (RSD) observed in the three different prepared analyte concentrations and accuracy was taken as a measure of deviation from the true value (RE). In three different days, the prepared analyte concentrations were tested (Samanidou *et al.,* 2009, Iriarte *et al.,* 2009).

5.5. RESULTS AND DISCUSSION

5.5.1. Assessment of Bleeding and Flushing Prior to Formulation Administration

The Large White Pigs showed no sign of distress, prior to surgical procedures. Following surgical procedures, the animals showed no sign of unusual behaviour as the anaesthesia

wore off. Due to the successful habituation, blood sampling procedures in the Large White Pig was quicker, less time consuming and easier. Therefore, the additional 7 days of flushing and bleeding prior to formulation administration was successful.

5.5.2. The Large White Pig Behaviour after Formulation Administration

The oral administration of formulations to the Large White Pigs showed no sign of hostility. Hence, no signs of distress or pain were observed after oral administration of the formulations. Normal behaviour in terms of appetite and activities were displayed by all pigs after oral administration of the formulations. All pigs involved during experimentation survived the entire duration of the study and were additionally observed for 7 days after the study was completed.

5.5.3. Assessment of Liquid-liquid Extraction Method and UPLC Chromatographic Separation of ACV in Plasma

The liquid-liquid extraction method was the favoured method of drug extraction. The sample to be separated using UPLC analysis was prepared by spiking blank plasma with ACV and IP. In order for drug to combine into the mixture, the sample was vortexed. The extraction method was undertaken as described in section **5.2.8.2.** The extracted solution was injected into the UPLC for analysis and was perceived that the separation method was adequate since the drug peak was separated adequately. **Figure 5.3** Is a UPLC chromatographic representation of ACV drug after plasma extraction.

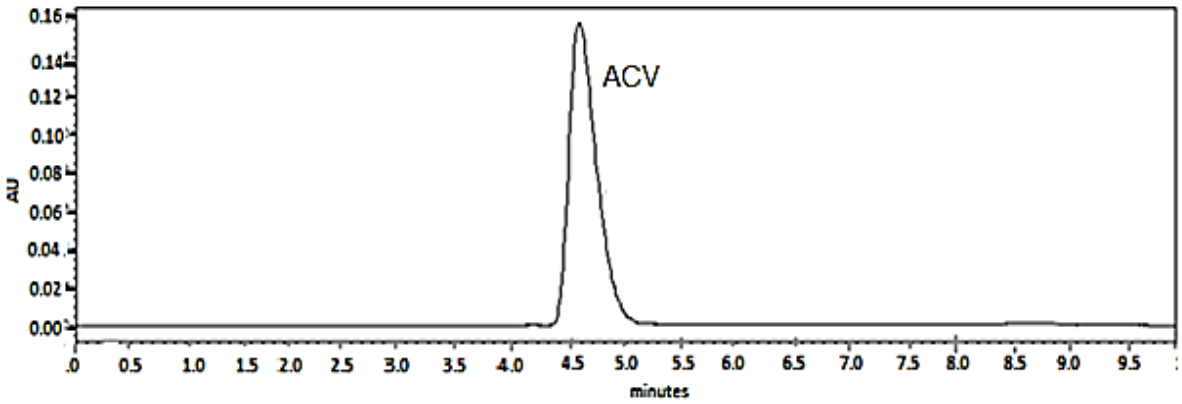

Figure 5.3: Chromatogram displaying the spiked plasma separation of ACV drug after extraction.

5.5.3.1. UPLC analysis validation of plasma: recovery, limit of detection and linearity

Drug recovery was found to be 89% and 90% for ACV and IP, respectively, from the selected extraction method. Drug recovery was calculated in percentage by comparing the drug peak

area generated using the mobile phase as the dissolving medium with that of the plasma method with the same concentration. As previously mentioned, the limit of detection is calculated as the concentration of the analyte that produced a signal, equating to three times the standard deviation of the signal from the blank. In addition, the error limit of detection is described as three times the standard deviation obtained from the blank or three times the height of the baseline of the blank. The calculated limit of detection was found to be 50ng/mL.

5.5.3.2. Determination of calibration curve for the analysis of ACV drug in pig plasma

The chromatographic separation method for ACV and IP proved to be ideal as observed in **Figure 5.4**, displaying two separate chromatogram peaks. IP was selected as an internal standard since this drug peak does not interfere or overlap with the ACV peak. Hence, the spiked internal standard (IP) and analyte (ACV) in plasma eluted within 8 minutes with a retention time (R_t) of 6.20 minutes for the internal standard and 4.60 minutes for the analyte (ACV). The internal standard (IP) and analyte (ACV) peaks that were obtained from UPLC analysis were distinct as displayed in **Figure 5.4.**

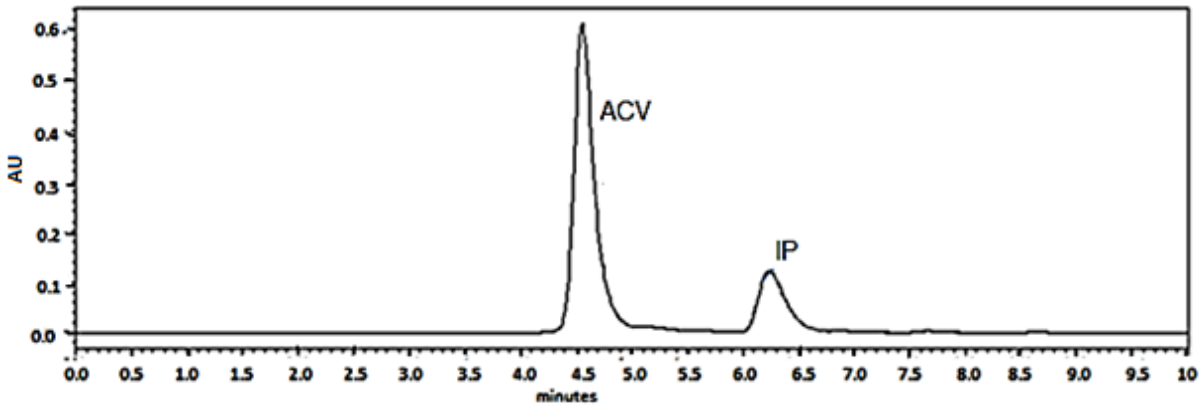

Figure 5.4: Chromatogram depicting the separation of ACV and IP after plasma extraction.

A concentration range between 0-2500ng/mL for the drug was selected for the calibration curve. **Figure 5.5,** represents the calibration curve obtained from pig plasma spiked with ACV and IP.

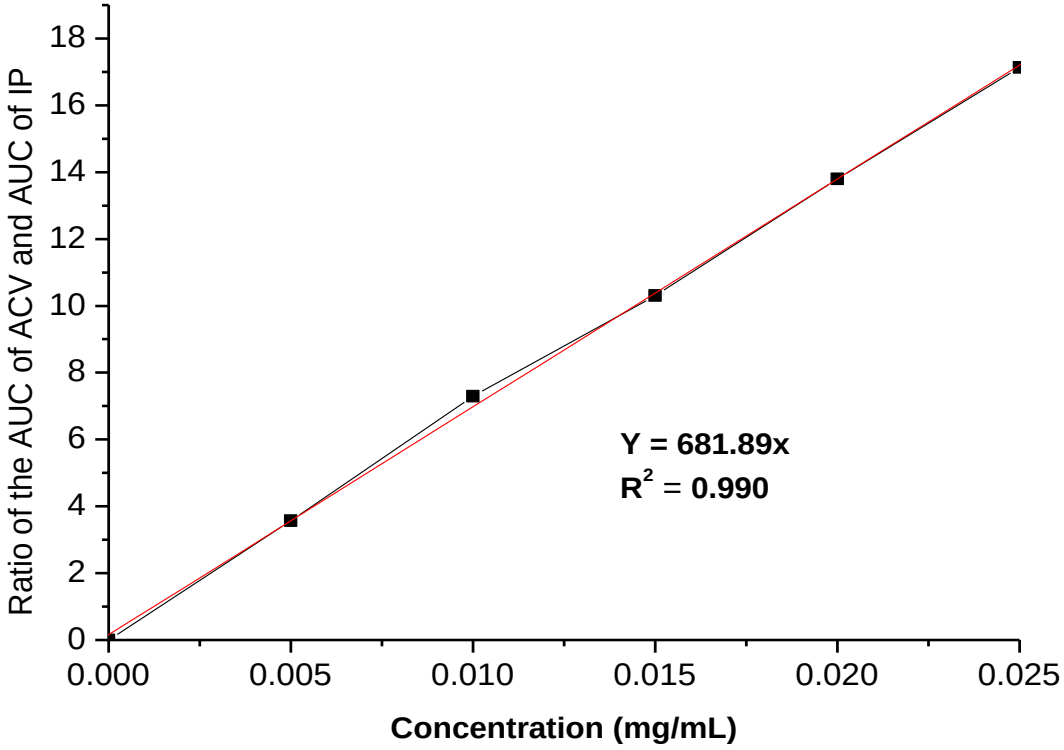

Figure 5.5: ACV calibration curve in plasma, n=3.

5.5.4. Assessment of *In Vivo* ACV Drug Release from the Optimized Nanoparticle Formulation and the Comparator Product

ACV is a pH sensitive drug, hence capsules were enteric coated to avoid acidic conditions of the stomach (pH 1.2) and only release the active ingredient in the small intestine (pH 5.5-6.8). As previously mentioned, ACV is poorly soluble in pH of 6.8 (2.25mg/mL) compared to acidic conditions (pH 1.2) (18.3mg/mL) (Chaudhary and Verma, 2014). Therefore, the novel optimized ACV-loaded polymeric nanoparticle formulation was enteric coated to avoid the stomachs acidic conditions and to only dissociate in small intestine.

The *in vivo* drug release studies were conducted in order to compare the drug release from the ACV conventional dosage (the comparator product) and the optimized ACV-loaded polymeric nanoparticle formulation.

5.5.4.1. Pharmacokinetics analysis of acyclovir in a Large White Pig Model

Figure 5.6 represents a graph, illustrating the comparative differences in the drug profiles of ACV from the comparator product (conventional dosage) and ACV-loaded polymeric nanoparticle formulation respectively, in pig blood plasma. For the ACV conventional dosage (comparator product), an initial significant rise of ACV concentration, with a plasma

concentration of ~256ng/mL was noted after ~2.5 hours from the analysed samples of pig plasma. It can be confirmed that the conventional dosage highest drug release was at 3 hours (T_{max}), with a peak plasma concentration of ~400ng/mL (C_{max}).

A rapid reduction in plasma concentration of ACV from the conventional dosage was observed from 6 hours until 24 hours. For optimized ACV-loaded polymeric nanoparticles, an initial significant rapid increase in ACV concentration with a C_{max} = ~850ng/mL was noted at T_{max} = 8 hours, followed by nearly constant ACV release up to 16 hours. The sustained release observed from the optimized ACV-loaded polymeric nanoparticle concentration curve from 8 to 16 hours may be due to the drug been carried into the deeper layers of the mucosa after passing through the epithelium, followed by slow drug release from the polymeric nanoparticles. For both drug release profiles, plasma levels subsequently decreased up to 24 hours. The low therapeutic levels of ACV drug noted in the conventional dosage formulation compared to the optimized ACV-loaded polymeric nanoparticle formulation may be due to the poor *in vivo* absorption, and distribution characteristics of the drug.

Studies demonstrate that after oral administration, ACV has an average oral bioavailability of ~10-20%, and approximately 80% of oral dose is excreted through faeces (Bangaru *et al*., 2000), thereby confirming the low C_{max} concentration (~400ng/mL) of ACV from the comparator product. ACV has an average half-life of 3 hours in an adult with normal renal function (Wagstaff, 1994). A huge improvement in systemic levels of ACV was observed from the optimized ACV-loaded nanoparticle formulation illustrated in **Figure 5.6** by the highest increased C_{max}= ~850ng/mL, compared to the conventional ACV dosage C_{max}= ~400ng/mL.

ACV is a guanine analogue used to treat herpes zoster (Kharla and Singhal, 2015). Herpes zoster is a disease that results from reactivation of latent varicella-zoster virus (VZV) and is mainly found in old aged group people (Harpaz *et al.,* 2008). The 50% inhibitory concentration (IC_{50}) of ACV in an *in vitro* study for different clinical VZV, isolates the range from ~280ng/mL to ~1410µg/mL. Therefore, the optimised optimized ACV-loaded polymeric nanoparticles have a C_{max} that is safe within the IC_{50} range.
The optimized ACV-loaded polymeric nanoparticle formulation has thus proved substantial efficacy in comparison to the commercially available ACV dosage formulation, with significantly improved solubility and permeation, thereby reducing the frequency of administration of ACV.

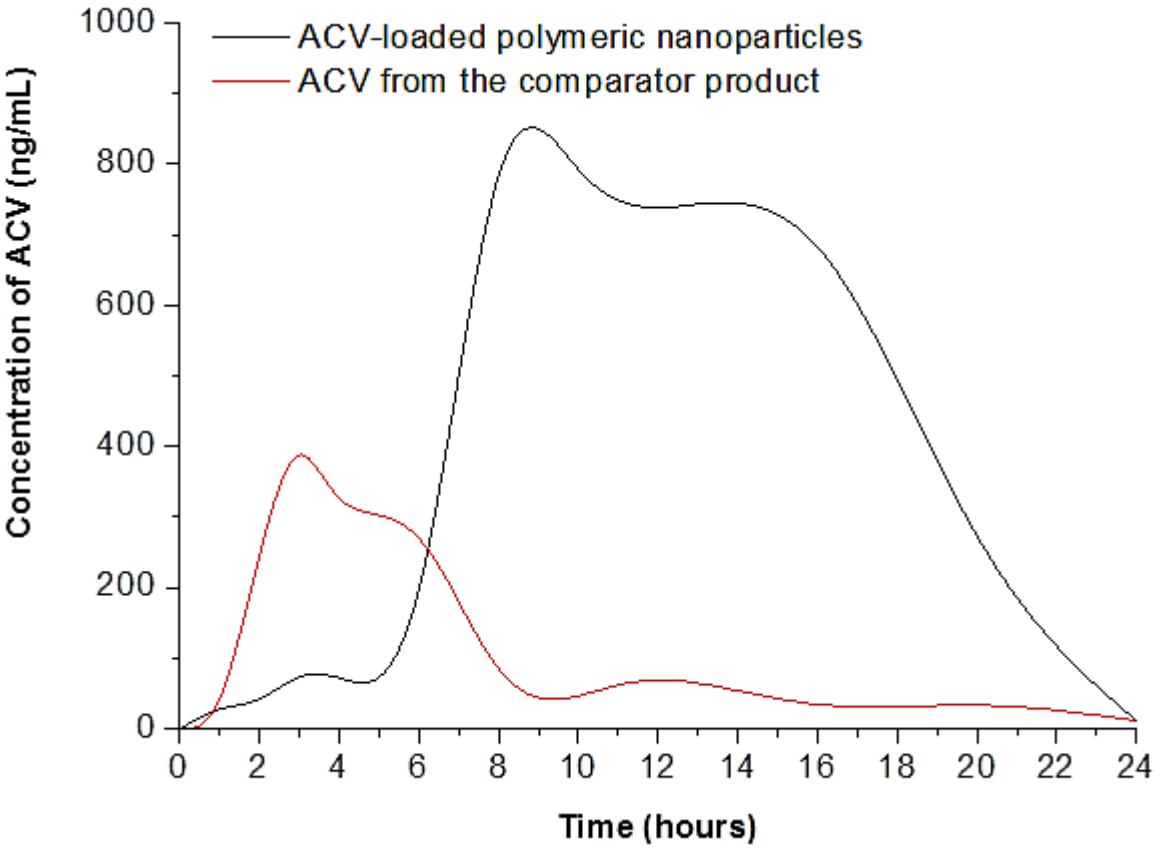

Figure 5.6: Comparative plasma drug concentration profiles of the optimized ACV-loaded nanoparticle formulation, in comparison to the conventional ACV dosage over a 24 hour duration, n=3.

The area under the plasma curve (AUC) was calculated for both formulations, to determine the comparative systemic exposure of ACV. In this study, a linear trapezoidal method was used to calculate the area under the concentration-time curve (AUC) (Rowland and Tozer, 1995) given by Equation 5.3:

$$\text{AUC}_{\text{Linear}} = \frac{1}{2}(C1 + C2)(t2 - t1)$$
$$= \frac{1}{2}(C1 + C2)\Delta t \qquad \text{(Equation 5.3)}$$

Where C1 = Concentration1, C2 = Concentration 2 and Δt = Time difference

The calculated area under the plasma profile curve (AUC) of the optimized ACV-loaded polymeric nanoparticles was found to be 10301ng.h/mL, and the calculated area under the plasma profile curve for the comparator product was calculated as ~2468ng.h/mL. The bioavailability (F) of the optimized ACV-loaded polymeric nanoparticles, relative to the comparator product is given by Equation 5.4:

Bioavailability (F) = $\frac{F1}{F2} = \frac{AUC1}{AUC2}$ (Equation 5.4)

Assuming volume 1 = volume 2 and dose1= dose 2; where:

F1 = bioavailability of optimized ACV-loaded polymeric nanoparticles

F2 = bioavailability of the comparator product formulation and

AUC1 = area under the plasma profile curve (AUC) of the optimized ACV-loaded polymeric nanoparticles

AUC2 = area under the plasma profile curve (AUC) for the comparator product

The relative bioavailability of the optimized ACV-loaded polymeric nanoparticles relative to the comparator product formulation was enhanced by a factor of ~4.17. The improved systemic exposure of ACV, leading to the increased relative bioavailability of the optimized ACV-loaded polymeric nanoparticle formulation compared to the comparator product formulation was the consequence of the reduced average particle size of the optimized ACV-loaded nanoparticles (Kharia and Singhai, 2015). Another reason of the substantial improvement, may be as a result of increased solubility of ACV that was encapsulated in the formulated complex, resulting in an increased amount of ACV available for cell membrane/systemic absorption. The absorption enhancer complexed within the formulation, further assisted ACV uptake, thereby increasing the overall bioavailability of the polymeric formulation.

5.6. CONCLUDING REMARKS

The purpose of this *in vivo* drug release study was to evaluate ACV release proficiency from the optimized ACV-loaded polymeric nanoparticle formulation compared to the ACV conventional dosage. The ACV-loaded polymeric nanoparticles, demonstrated superior results in comparison to the commercially available ACV formulation on the market. After drug collection, UPLC proved to be the best technique for the analysis of ACV from pig plasma. The optimized ACV-loaded polymeric nanoparticle formulation depicted an improved release profile of ACV, with an increased AUC calculated from the polymeric nanoparticles, in relation to the conventional ACV product.

CHAPTER SIX
CONCLUSIONS AND RECOMMENDATIONS

6.1. CONCLUSIONS

A novel Semi-Synthetic Biopolymer Complex (SSBC) for the improvement of oral solubility and intestinal permeation of ACV was designed, developed and characterized. During preliminary studies, hyaluronic acid (HA), poly acrylic acid (PAA) and an oral permeation enhancer HP-β-CD were identified as suitable components for the formation of a novel SSBC (HA─PAA─HP-β-CD). ACV was used as a model drug, formulating nanoparticles, through modification and coupling techniques. Nanoparticles from ACV-loaded HA─PAA─HP-β-CD polymeric complex were prepared using emulsion technique, thereafter subjected to spray-drying, to obtain uniformly produced nanoparticles. A Face-Centred Central Composite Design (FCCCD) was chosen for experimental evaluation, in order to obtain an optimized formulation with variables attained in pre-formulation studies. The optimized formulation was mathematically determined and the effects of the independent variables were assessed from dependent response variables.

The optimized novel SSBC was evaluated *in vivo* using a Large White Pig model. The polymeric nanoparticle formulation displayed significant results, which substantially surpassed the comparator ACV formulation on the market, thereby demonstrating major enhancement in solubility and permeability of ACV.

6.2. RECOMMENDATIONS

The developed novel SSBC is not entirely limited to the enhancement of solubility and permeability of ACV. This polymeric complex can be applicable to any hydrophobic and poorly permeable drugs in order to improve their oral bioavailability. Therefore, further research on this polymeric system can be undertaken on a variety of hydrophobic drugs, in order to validate this complex as a universal drug-solubility and permeation enhancer for hydrophobic and poorly permeable drugs. There is also a requirement to investigate other types of cyclodextrin properties and use these polymers as nano-based formulations.

The *in vivo* study provided significant results concerning the pharmacokinetic analysis of the polymeric complex under investigation. These results could have been enhanced if a proper diet was provided to this animal model, which in this instance may have possibly accelerated enzymatic alterations of ACV in the polymeric and commercially available formulations. Pilot human bio-studies are recommended and depending on the study results, Wits enterprise will market the product to pharmaceutical companies leading to commercializing the product.

REFERENCES

1. Abbad, S., Zhang, Z., Waddad, A., Ayman, Y., Munyendo, W.L.L., Lv, H., Zhou, J., 2015. Chitosan-Modified Cationic Amino Acid Nanopartcles as a Novel Oral Delivery System for insulin. J. Biomed. Nanotechnol. 11, 486-499.
2. Adikwu, M.U., 2009. Biopolymers in Drug Delivery: Recent Advances and Challenges. Bentham Science Publishers.
3. Ahmad, A., Pandey, R., Sharma, S., Khuller, G.K., 2006. Pharmacokinetic and pharmacodynamic behavior of antitubercular drugs encapsulated in alginate nanoparticles at two doses. Int. J. Antimicrob. Agents. 5, 420–427.
4. Alarcon, C.D.H., Pennadam, S., Alexander, C., 2005. Stimuli responsive polymers for biomedical applications. Chem. Soc. Rev. 34, 276–285.
5. Alenso, M.J., Losa, C., Calvo, P., Vila-Jato, J.L., 1991. Approaches to improve the association of amikacin sulphate to poly-(cyanoacrylate) nanoparticles. Int. J. Pharm. 68, 69-76.
6. Allemann, E., Leroux, J., Gurny, R., 1998. Polymeric nano- and microparticles for the oral delivery of peptides and peptidomimetics. Adv. Drug. Deliv. Rev. 34, 171–189.
7. Arnal, J., Gonzalez-alvarez, I., Bermejo, M., Amidon, G.L., Junginger, H.E., Kopp, S., Midha, K.K., Shah, V.P., Stavchansky, S., Dressman, J.B., Barends, D.M., 2008. Biowaiver Monographs for Immediate Release Solid Oral Dosage Form: Aciclovir. J. Pharm. Sci. 97, 5061-5073.
8. Amidi, M., Mastrobatista, E., Jiskoot, W., Hennink, W.E., 2010. Chitosan-based delivery systems for protein therapeutics and antigens. Adv Drug Deliv Rev. 662, 59-82.
9. Anderson, D.L., Bartholomeusz, F.D., Kirkwood, I.D., Chatterton, B.E., Summersides G., Penglis, S., Kuchel, T., Sansom, L., 2002. Liquid Gastric Emptying in the Pig: Effect of Concentration of Inhaled Isoflurane. J. Nucl. Med. 43, 968-971.
10. Anderson, N.H., Bauer, M., Boussac, N., KhanMalek, R., Munden, P., Sardaro, S., 1999. An evaluation of fit factors and dissolution efficiency for the comparison of in vitro dissolution profiles. J. Pharma. Biomed. Anal. 17, 811–822.
11. Arai, K., Kinumaki, T., Fujita, T., 1968. Toxicity of chitosan. Bull. Tokai Reg. Fish. Lab. 43, 89–94.
12. Arnal, J., Gonzalez-alvarez, I., Bermejo, M., Amidon, G.L., Junginger, H.E., Kopp, S., Midha, K.K., Shah, V.P., Stavchansky, S., Dressman, J.B., Barends, D.M., 2008. Biowaiver Monographs for Immediate Release Solid Oral Dosage Form: Aciclovir. J. Pharm. Sci.. 97, 5061-5073.

13. Arpagaus, C., Meuri, M., 2010. Laboratory scale spray drying of inhalable particles: a review. Respiratory Drug Delivery, VCU. 469-473.
14. Athawale, V.D., Rathi, S.C., 1999. Graft polymerization: starch as a model substrate. J. Macromol. Sci-Rev. Macromol. Chem. Phys. 39, 445-480.
15. Bala, I., Hariharan, S., Kumar, R.M., 2004. PLGA Nanoparticles in Drug Delivery: The State of the Art. Critical Reviews™ in Terapeutic Drug Carrier Systems. 21, 387–422.
16. Bangaru, R.A., Bansal, Y.K., Rao, A.R., Gandhi, T.P., 2000. Rapid, simple and sensitive high-performance liquid chromatographic method for detection and determination of acyclovir in human plasma and its use in bioavailability studies. J. Chromatogr. B Biomed. Sci. Appl. 739, 231-237.
17. Bangaru, R.A., Bansal, Y.K., Rao, A.R.M., Gandhi, T.P., 2000. Rapid, simple and sensitive high-performance liquid chromatographic method for detection and determination of acyclovir in human plasma and its use in bioavailability studies. J. Chromatogr. B Analyt. Technol. Biomed. Life Sci. 739, 231–237.
18. Banna, G.L., Collovà, E., Gebbia, V., Lipari, H., Giuffrida, P., Cavallaro, S., Condorelli R., Buscarino, C., Tralongo, P., Ferraù, F., 2010. Anticancer oral therapy: Emerging related issues. Cancer Treat. Rev. 36, 595–605.
19. Battaed, H.A.J., Tregear, G.W., 1967. Graft copolymers. Interscience. New York,NY.
20. Bawa, P., Pillay, V., Choonara, Y.E., du Toit, L.C., 2009. Stimuli-responsive polymers and their applications in drug delivery. Biomed. Mater. 4, 1-15.
21. Bawa, P., Choonara, Y.E., du Toit, L.C., Kumar, P., Ndesendo, V.M.K., Meyer, L.C.R., Pillay, V., 2013. A novel stimuli-synchronized alloy-treated matrix for space-defined gastrointestinal delivery of mesalamine in the Large White pig model. J. Control. Release. 66, 234–245.
22. Behnken design: An alternative for the optimization of analytical methods. Analytica Chimica. Acta. 597, 179-186
23. Boonen, J., Baert, B., Roche, N., Burvenich, C., De Spiegeleer, B., 2010. Transdermal behaviour of the N-alkylamide spilanthol (affinin) from Spilanthes acmella (Compositae) extracts. J. Ethnopharmacol. 127, 77–84.
24. Borges, O., Cordeiro-da-Silva, A., Romeijn, S.G., 2006. Uptake studies in rat Peyer's patches, cytotoxicity and release studies of alginate coated chitosan nanoparticles for mucosal vaccination. J. Control. Release. 114, 348–358.
25. Bowman, k., Leong, K.W., 2006. Chitosan nanoparticles for oral drug and gene delivery. Int. J. Nanomedicine. 1, 117-128.
26. Braga, A.S., Catirs, A.B.C.E.B., Vaz, L.G., Spadaro, A.C.C., 2005. Quantitative analysis of potentially toxic metals in alginates for dental use. Rev. Ciênc. Farm. Básica. Apl. 26, 125–130.

27. Brunet, B., Doucet, C., Venisse, N., 2006. Validation of Large White Pig as an animal model for the study of cannabinoids metabolism: Application to the study of THC distribution in tissues. Forensic Sci. Int. 161, 169–174.
28. BÜCHI Labortechnik AG. Nano Spray Dryer B-90 Brochure, 11592236 en 1012. 2010. Flawil, Switzerland, available on www.buchi.com.
29. Burlant, W.J., Hoffmann, A.S., 1960. Block and graft copolymers. Rheinhold Pub Corp, New York, NY.
30. Bussière, P., Peyroux, J., Chadeyron, G., Therias, S., 2013. Influence of functional nanoparticles on the photostability of polymer materials: Recent progress and further applications. Polym. Degrad. Stab. 98, 2411-2418.
31. Cakmak, G., Togan, L., Uguz, C., Severcan, F., 2003. FT-IR spectroscopic analysis of rainbow trout liver exposed to nonylphenol. Appl. Spectrosc. 57, 835-841.
32. Camilleri, M., Colemont, L.J., Phillips, S.F., Brown, M.L., Thomforde, G.M., Chapman N., Zinsmeister, A.R., 1989. Human gastric emptying and colonic filling of solids characterized by a new method. Am. J. Physiol. 257-284.
33. Cascone, M.G., Sim, B., Sandra, D., 1995. Blends of synthetic and natural polymers as drug delivery systems for growth hormone. Biomaterials. 16, 569-574.
34. Cascone, M.G., 1997. Dynamic–mechanical properties of bioartificial polymeric materials. Polym. Int. 43, 55–69.
35. Chan, H.K., Kwok, P.C.L., 2011. Production methods for nanodrug particles using the bottom-up approach. Adv. Drug Deliv. Rev. 63, 406-416.
36. Chan, J.M., Valencia, P.M., Zhang, L., Langer, R., Farokhzad, O.C., 2010. Polymeric Nanoparticles for Drug Delivery. Methods Mol. Biol. 624, 163-75.
37. Charles, F.,Camilleri, M., Phillips, S.F., Thomforde, G.M., Forstrom, L.A., 1995. Scintigraphy of the whole gut: clinical evaluation of transit disorders. Mayo Clin. Proc. 70, 113.
38. Chaudhary, B., Verma, S., 2014. Preparation and Evaluation of Novel In Situ Gels Containing Acyclovir for the Treatment of Oral Herpes Simplex Virus Infections. ScientificWorldJournal. 2014, 1-7.
39. Chaudhury, A., Das, S., 2011. Recent Advancement of Chitosan-Based Nanoparticles for Oral Controlled Delivery of Insulin and Other Therapeutic Agents. AAPS PharmSciTech. 12, 10-20.
40. Cheow, S.W., Hadinoto, K., 2011. Factors affecting drug encapsulation and stability of lipid–polymer hybridnanoparticles. Colloids and Surfaces B: Biointerfaces. 85, 214–220.

41. Chiang, W., Hu, C., 1996. The improvement in flame retardance and mechanical properties of polypropylene/FR blends by acylic acid graft copolymerization. Eur. Polym. J. 32, 385-39.
42. Cho, C.G., Lee, K., 2002. Preparation of starch graft copolymer by emulsion polymerization. Carbohydr. Polymw. 48, 125-130.
43. Chouhan, P., Saini, T.R., 2014. Hydroxypropyl-β-cyclodextrin: A Novel Transungual Permeation Enhancer for Development of Topical Drug Delivery System for Onychomycosis. J. Drug. Deliv. 1-7.
44. Christian, W., Schwendeman, S.P., 2008. Principles of encapsulating hydrophobic drugs in PLA/PLGA microparticles. Int. J. Pharm. 2, 298-327
45. Cooppan, S., 2010. A once daily multi-unit system for the site-specific delivery of multiple drug regimens, M Pharm Dissertation, Department of Pharmacy and Pharmacology, University of the Witwatersrand.
46. Corti, G., Maestrelli, F., Cirri, M., Furlanetto, S., Mura, P., 2006. Development and evaluation of an in vitro method for prediction of human drug absorption I. Assessment of artificial membrane composition. Eur. J. Pharm. Sci. 27, 346–53.
47. Costa, N.L., 2009. Short-term stress: the case of transport and slaughter. J. Anim. Sci. 8, 241-252.
48. Cunliffe, D., Pennadam, S., Alexander, C., 2004. Synthetic and biological polymers-merging the interface. Eur. Polym. J. 40, 5–25.
49. Davies, D.J., Ward, R.J., Heylings, J.R., 2004. Multi-species assessment of electrical resistance as a skin integrity marker for in vitro percutaneous absorption studies. Toxicol. In Vitro. 18, 351–358
50. Degen, L.P., Phillips, S.F., 1996. Variability of gastrointestinal transit in healthy women and men. Gut. 39, 299-305.
51. Desai, M.P., Labhasetwar, V., Amidon, G.L., Levy, R.J., 1996. Gastrointestinal uptake of biodegradable microparticles: effect of particle size. Pharm. Res. 13, 1838–1845.
52. Deming, T.J., 1997. Facile synthesis of block copolypeptides of defined architecture. Nature. 390, 386–389.
53. Deng, L., Wang, G., Ren, J., Zhang, B., Yan, J., Li, W., Khashab, N.M., 2012. Enzymatically triggered multifunctional delivery system based on hyaluronic acid micelles. RSC Advances. 2, 12909–12914.
54. Dhakar, R.C., Maurya, S.D., Aggarawal, S., Kumar, G., Tilak, V.K., 2010. Design and evaluation of SRM microspheres of metformin hydrochloride. IJCP. 1:1-5.
55. Dorkoosh, F.A., Verhoef, J.C., Borchard, G., Rafiee-Tehrani, M., Verheijden, J.H.M., Junginger, H.E., 2002. Intestinal absorption of human insulin in pigs using delivery systems based on superporous hydrogel polymers. Int. J. Pharm. 247, 47-55.

56. Ferguson, E.L., Alshame, A.M., Thomas, D.W., 2010. Evaluation of hyaluronic acid-protein conjugates for polymer masked-unmasked protein therapy. Int. J. Pharm. 402, 95-102.
57. Ferraz, H.G., Carpentieri, L.N., Watanabe, S.P., 2007. Dissolution Profile Evaluation of Solid Pharmaceutical Forms Containing Chloramphenicol Marketed in Brazil. Braz. arch. biol. technol. 50, 57–65.
58. Fernandes, C., Junqueira, R.G., Campos, L., Pianetti, G.A., 2006. Dissolution test for lamivudine tablets: Optimization and statistical analysis. J. Pharm. Biomed. Anal. 42, 601–606.
59. Fernandez, M., Sepulveda., Aranguiz, T., von Plessing, C., 2003. Technique validation by liquid chromatographyfor the determination of acyclovir in plasma. J. Chromatogr. B Analyt. Technol. Biomed. Life Sci. 791, 357–363.
60. Fernandez-Urruuno, R., Calvo, P., Reminan-Lopez, C., Vila-Jato, J.L., Alonso, M.J., 1999. Enhancement of nasal obsorption of insulin using chitosan nanoparticles. Pharm. Res. 16, 1576-81.
61. Festing, S., Wilkinson, R., 2007. The ethics of animal research. Talking Point on the use of animals in scientific research. EMBO Reports. 8, 526-530.
62. Francis, M.F., Cristea, M., Winnik, F.M., 2004. Polymeric micelles for oral drug delivery: Why and how. Pure Appl. Chem. 76, 1321-1335.
63. Furnaletto, S., Cirri, M., Maestrelli, F., Corti, G., Mura, P., 2006. Study of formulation variables influencing the drug release rate from matrix tablets by experimental design. Eur. J. Pharm. Biopharm. 62, 77-84.
64. George, M., Abraham, T.E., 2006. Polyionic hydrocolloids for the intestinal delivery of protein drugs: alginate and chitosan—a review. J. Control. Release. 114, 1–14.
65. Gerlach, M., Riederer, P., 1996. Animal models of Parkinson's disease: an empirical comparison with the phenomenology of the disease in man. J. Neural. Transm. 103, 987-1041.
66. Gill, H.S., Prausnitz, M.R., 2007. Coating formulations for microneedles. Pharm. Res. 24, 1369–1380.
67. Giusti, P., Lazzeri, L., Lelli, L., 1993. Bioartificial polymeric materials: a new method to design biomaterials by using both biological and synthetic polymers. TRIP. 1, 261–267.
68. Grandin, T., 1997. Assessment of stress during handling and transport. J. Anim. Sci. 75, 249-257.
69. Grandin, T., 2007. Livestock handling and transport, CABI Publishing, Oxford.
70. Guihen, E., 2013. Nanoparticles in modern separation science. Trends Analyt. Chem. 46, 1-14.

71. Gumustas, M., Kurbanoglu, S., Uslu, B., Ozkan, S.A., 2013. UPLC versus HPLC on Drug Analysis: Advantageous, Applications and Their Validation Parameters. Chromatographia. 76, 1365–1427
72. Han, H.S., Lee, J., Kim, H.R., Chae, S.Y., Kim, M., Saravanakumar, G., Yoon, H.Y., You, D.Y., Ko, H., Kim, K., Kwon, I.C., Park, J.C., Park, J.H., 2013. Robust PEGylated hyaluronic acid nanoparticles as the carrier of doxorubicin: Mineralization and its effect on tumor targetability in vivo. J. Control. Release. 168, 105–114.
73. Hans, M.L., Lowman, A.M., 2002. Biodegradable nanoparticles for drug delivery and targeting. Curr. Opin. Solid State Mater Sci. 6, 319–327.
74. Harpaz,, R., Ortega-Sanchez, I.R., Seward, J.F., 2008. Advisory Committee on Immunization Practices Centers for Disease Control and Prevention. Prevention of herpes zoster: recommendations of the Advisory Committee on Immunization Practices (ACIP). MMWR. Recomm. Rep. 57, 1-30.
75. Hawker, C.J., Bosman, A.W., Harth, E., 2001. New polymer synthesis by nitroxide mediated living radical polymerizations. Chem. Rev. 101, 3661–3688.
76. He, Y.Z.B., Inoue, Y., 2004. Hydrogen bonds in polymer blends. Prog. Polym. Sci. 29, 1021-1051.
77. Helliwell, M., 1993. The use of bioadhesives in targeted delivery within the gastrointestinal tract. Adv. Drug Deliv. Rev. 11, 221-251.
78. Heng, D., Lee, S.H., Ng, W.K., Tan, R.B.H., 2011. The Nano Spray Dryer B-90. Expert. Opin. Drug. Deliv. 8, 965-972.
79. Hoffmann, B., Volkmer, E., Kokott, A., Augat, P., Ohnmacht, M., Sedlmayr, N., Schieker, M., Claes, L., Mutschler, W., Ziegler, G., 2009. Characterisation of new bioadhesive system based on polysaccharides with the potential to be used as bone gue. J. Mater Sci: Mater Med. 20, 2001–2009.
80. Holkar, G., Daphal, V., Yadav, R., Rokade, M.D., 2012. Method Validation and Quantitative Determination of Antiviral Drug Acyclovir in Human Plasma by a LCMS/MS. Int. J. 4, 11-17
81. Horter, D., Dressman, J.B., 2001. Influence of physicochemical properties on dissolution of drugs in the gastrointestinal tract. Adv. Drug Deliv. Rev. 46, 75-87.
82. Hsu, S.T., Pan, T.C., 2007. Adsorption of paraquat using methacrylic acid-modificaion rice husk. Bioresour Technol. 98, 3617-3621.
83. Hu, Y., Jiang, X., Ding, Y., Ge, H., Yuan, Y., Yang, C., 2002. Synthesis and characterization of chitosan–poly (acrylic acid) nanoparticles. Biomaterials. 23, 3193–3201.
84. Husseini, G.A., Pitt, G.W., 2008. Micelles and nanoparticles for ultrasonic drug and gene delivery. Adv. Drug Deliv. Rev. 60, 1137–1152.

85. Illum, L., Farrai, N.F., Davis, S.S., 1994. Chitosan as a novel nasal delivery system for peptide drugs. Pharm. Res. 11, 1186-1189.
86. Iwanaga., Y., Wen, J., Thollander, M.S., Kost, L.J., Thomforde, G.M., Allen, R.G., Phillips, S.F., 1998. Scintigraphic measurement of regional gastrointestinal transit in the dog. Am. J. Physiol. 275, 904-910.
87. Iriarte, G., Gonzalez, O., Ferreirós, N., Maguregui, M.I., Alonso, R.M., Jiménez, R.M., 2009. Validation of a fast liquid chromatography-UV method for the analysis of drugs used in combined cardiovascular therapy. J. Chromatogr. B Analyt. Technol. Biomed. Life Sci. 877, 3045-3053.
88. Jani, P., Halbert, G.W., Langridge, J., Florence, A.T., 1990. Nanoparticle uptake by the rat gastrointestinal mucosa: quantitation and particle size dependency. J. Pharm. Pharmacol. 42, 821–826.
89. Jankowski, A., Jankowska, A.L., Lamparczyk, H., 1998. Determinationand pharmacokinetics of acyclovir after ingestion of suspension form. Journal of Pharmaceuticaland Biomedical Analysis. 18, 249–254.
90. Jerkovich, A.D., Mellors, J.S., Jorgensen, J.W., 2003. The use of micrometer-sized particles in ultrahigh pressure liquid chromatography. LC-GC North Americ.
91. Joshi, A.J., Patel, R.P., 2012. Role of biodegrable polymer in drug delivery. Int. J. Curr. Pharm. Res. 4, 74-81.
92. Kakran, M., Li, L., Muller, R.H., 2012. Overcoming the Challenge of Poor Drug Solubility. I,S,P.E. 32, 1-7.
93. Khan, T.A., Khiang, P.K., 2002. Reporting Degree of Deacetylation Values of Chitosan: The Influence of Analytical Methods. J. Pharm. Pharm. Sci. 205-212.
94. Khokale, A.S., Patil, P.M., 2014. Stability-indicating Spectrophotometric Method of Acyclovir in Bulk and Pharmaceutical Dosage Form. W.J.P.P.S. 3, 1235-1245
95. Kharia, A.A., Singhai, A.K., 2015. Development and optimisation of mucoadhesive nanoparticles of acyclovir using design of experiments approach. J. Microencapsul. 32, 521–532.
96. Khotimchenko, Y.S., Khotimchenko, M.Y., 2004. Healing and preventive effects of calcium alginate on carbon tetrachloride induced liver injury in rats. Mar. Drugs. 2, 108–122.
97. Kingsley, J.D., Dou, H., Morehead, J., Rabinow, B., Gendelman, H.E., Destache, C.J., 2006. Nanotechnology: A Focus on Nanoparticles as a Drug Delivery System. J. Neuroimmune Pharmaco. 1, 340–350.
98. Kogan, G., Soltés, L., Stern, R., Gemeiner, P., 2007. Hyaluronic acid: A natural biopolymer with a broad range of biomedical and industrial applications. Biotechnol. Lett. 29, 17–25.

99. Kolawole, O.A., Pillay, V., Choonara, Y.E., du Toit, L.C., Ndesendo, V.M.K., 2010. The influence of polyamide 6, 10 synthesis variables on the physiochemical characteristics and drug release kinetics from a monolithic tablet matrix. Pharm. Dev. Technol. 15, 595-612.
100. Kosta, A.K., Solakhia, T.M., Agrawal, S., 2012. Chitosan Nanoparticle- A Drug Delivery System. Int. j. pharm. biol. sci. arch. 3, 737-743.
101. Kowalonek, J., Kaczmarek, H., 2010. Studies of pectin/polyvinylpyrrolidone blends exposed to ultraviolet radiation. European Polymer Journal. 46, 345–353.
102. Krishnaiah, C.H., Reddy, R., Kumar, R., Mukkanti, K., 2010. Stability-indicating UPLC method for determination of Valsartan and their degradation products in active pharmaceutical ingredient and pharmaceutical dosage forms. J. Pharm. Biomed. Anal. 53, 483-489.
103. Kumari, A., Yadav, S.K., Yadav, S.V., 2010. Biodegradable polymeric nanoparticles based delivery systems. Colloids Surf. B Biointerfaces. 75, 1-18.
104. Lachmann, P., 1992. The use of animals in research. B.M.J. 305, 1277–1280.
105. Lapcik, L., De Smedt, S., Demeester, J., Chabrecek, P., 1998. Hyaluronan: preparation, structure, properties, and applications. Chem. Rev. 98, 2663–2684.
106. Laurent, T., 1998. The chemistry, biology and medical applications of hyaluronan and its derivatives. London: Portland Press.
107. Laurent, T.C., Fraser, J.R., 1992. Hyaluronan. FASEB J. 6, 2397–2404.
108. Leach, J.B., Bivens, K.A., Jr, C.W.P., Schmidt, C.E., 2003. Photocrosslinked hyaluronic acid hydrogels: Natural. biodegradable tissue engineering scaffolds. Biotechnol. Bioeng. 82, 578-589.
109. Lee, S.H., Heng, D., Ng, W.K., Chan, H.K., Tan, R.B., 2011. Nano spray drying: A novel method for preparing protein nanoparticles for protein therapy. Int. J. Pharm. 403, 192-200.
110. Lee, K.Y., Kwon, I.C., Kim, Y.H., Jo, W.H., Jeong, S.Y., 1998. Structural investigation of chitosan self-aggregates prepared for gene delivery. Proc. Int. Symp. Control. Rel. Bioact. Mater. 25, 340–341.
111. Lee, J.W., Park, J.H., Robinson, J.R., 2000. Bioadhesive-based dosage forms: the next generation. J. Pharm. Sci. 89, 850–866.
112. Lee, Y., Kwon, I.C., Kim, Y.H., Jo, W.H., Jeong, S.Y., 1998. Preparation of chitosan self-aggregates as a gene delivery system. J. Control. Release. 51, 213– 220.
113. Lehner, R., Wang, X., Marsch, S., 2013. Intelligent nanomaterials for medicine: Carrier platforms and targeting strategies in the context of clinical application. Nanomedicine: Nanotechnology, Biology, and Medicine. 9, 742–757.

114. Lemarchand, C., Gref, R.P., 2004. Couvreur, Polysaccharide-decorated nanoparticles. Eur. J. Pharm. Biopharm. 58, 327–341.
115. Lewis, G.A., Mathieu, D., Phan,-Tan-Luu, R., 1999. Pharmaceutical Experimental Design, Marcel Dekker Inc.: New York: USA.[e-book, Available at: http://books.google.co.za/books?id=jqFZOyBtS98C&printsec=frontcover#v=onepage&q&f=false) Accessed 2014-03-31].
116. Li, F., Bae, B.C., Na, K., 2010. Acetylated Hyaluronic Acid/Photosensitizer Conjugate for the Preparation of Nanogels with Controllable Phototoxicity: Synthesis, Characterization, Autophotoquenching Properties, and in Witro Phototoxicity against HeLa Cells. Bioconjugate Chem. 21, 1312-1320.
117. Li, X., Anton, N., Arpagaus, C., Belleteix, F., Vandamme, T.F., 2010. Nanoparticles by spray drying using innovative new technology: The BUCHI Nano Spray Dryer B-90. J. Control. Release. 147, 304-310.
118. Likenhoker, J.R., Burkholder, TH, Linton, C.G.G., Walden, A., Abusakran-Monday, K.A., Rosero, A.P., Foltz, C.J., 2010. Effective and safe anesthesia for Yorkshire and Yucatan swine with and without cardiovascular injury and intervention. J. Am. Assoc. Lab. Anim. Sci. 49, 344-51.
119. Lin, A., Liu, Y., Huang, Y., Sun, J., Wu, Z., Zhang, X., Ping, Q., 2008. Glycyrrhizin surface-modified chitosan nanoparticles for hepatocyte-targeted delivery. Int. J. Pharm. 359, 247–25.
120. Lin, Y.H., Mi, F.L., Chen, C.T., Chang, W.C., Peng, S.F., Liang, H.F., Sung, H.W., 2007. Preparation and characterization of nanoparticles shelled with chitosan for oral insulin delivery. Biomacromolecule. 8, 146-52.
121. Lipinski, C.A., 2000. Drug-like properties and the causes of poor solubility and poor permeability. J. Pharmacol. Toxicol. Methods. 44, 235–249.
122. Liu, G., Franssen, E., Fitch, M.I., Warner, E., 1997. Patient preferences for oral versus intravenous palliative chemotherapy. J. Clin. Oncol. 15, 110–5.
123. Liu, Z., Jiao, Y., Wang, Y., Zhou, C., Zhan, Z., 2008. Polysaccharides-based nanoparticles as drug delivery systems. Adv. Drug Deliv. Rev. 60, 1650–1662.
124. Lucatan Swine with and without Cardiovascular Injury and Intervention; Journal of American Association for Laboratory Animal Science; 49:344-351.
125. Luessen, H.L., Leeuw, B.J.D., Langemeyer, M.W., Boer, A.G.D., Verhoef, J.C., Junginger,, H.E., 1996. Mucoadhesive polymers in peroral peptide drug delivery VI. Carbomer and chitosan improve the intestinal absorption of the peptide drug buserelin in vivo. Pharm. Res. 13, 1668-1672.

126. Mahouche-Cherguia, S., Guerrouache, M., Carbonnier, B., Chehimi, M.M., 2013. Polymer-immobilized nanoparticles, Colloids and Surfaces A: Physicochem. Eng. Aspects. 439, 43– 68.
127. Makadia, H.K., Siegel, S.J., 2011. Poly lactic-co-glycolic acid (PLGA) as biodegradable controlled drug delivery carrier, Polymers. 3, 1377-1397.
128. Malavasi, L.M., Nyman, G., Augustsson, H., Jacobson, M,. Jensen-Waern, M., 2006. Effects of epidural morphine and transdermal fentanyl analgesia on physiology and behaviour after abdominal surgery in pigs. Lab Anim. 40, 16-27.
129. Mansy, S.S., 2015. Membrane Transport in Primitive Cells. Published by Cold Spring Harbor Laboratory Press. Downloaded from :http://cshperspectives.cshlp.org/ on November 19 2015.
130. Mascher, H., Kikuta, C., Metz, R., Vergin, H., 1992. New, high-sensitivity high-performance liquid chromatographic method for the determination of acyclovir in human plasma, using fluorometric detection. J. Chromatogr. 583, 122-127.
131. Maruyama, A., Ishihara, T., Kim, J., Kim, S.W., Akaike, T., 1997. Nanoparticle DNA Carrier with Poly(L-lysine) Grafted Polysaccharide Copolymer and Poly(D,L-lactic acid. Bioconjugate Chem. 8, 735−742
132. Matyjaszewski, K., Xia, J.H., 2001. Atom transfer radical polymerization, Chem. Rev. 101, 2921–2990.
133. McEwen, B., 2002. The end of stress as we know it, Joseph Henry Press, Washington DC.
134. McMullin, C.M., Kirk, B., Sunderland, J., White, L.O., 1996. Reeves DS, MacGowan AP. A simple high performance liquidchromatography (HPLC) assay for aciclovir and ganciclovirin serum. J. Antimicrob. Chemother. 38, 739–740.
135. Metcalf, A.M., Phillips, S.F., Zinsmeister, A.R., MacCarty R.L., Beart R.W., Wolff B.G., 1987. Simplified assessment of segmental colonic transit. Gastroenterology. 92, 40 47.
136. Miller, E.R., Ullrey, D.E., 1987. The Pig as a Model for Human Nutrition; Annual Review of Nutrition. 7, 361-382.
137. Misra, B.N., Dgra, R., 1980. Grafting onto starch. IV. Grafting copolymerization of methylmethacrylate by use of AIBN as radical initiator. J. Macromol. Sci. Chem. A. 14, 763-770
138. Moad, G., Rizzardo, E., Thang, S.H., 2005. Living radical polymerization by the RAFT process. Aus. J. Chem. 58, 379–410.
139. Moideen, S.M., Kuppuswamy, S., 2014. Significance of nanoparticle drug delivery system than conventional drug delivery system of antihypertensive drugs. 3, 995-1019.

140. Moodley, K., 2013. A polymeric triple-layered tablet for stratified zero-order drug release, M Pharm dissertation, Department of Pharmacy and Pharmacology, University of the Witwatersrand.
141. Mounir, L., 1996. Sterilization of Contaminated Matter with an Atmospheric Pressure Plasma. IEEE Transction on plasma Sceince. 24, 1188-1191.
142. Mukhopadhyay, P., Mishra, R., Rana, D., Kundu, P.P., 2012. Strategies for effective oral insulin delivery with modified chitosan nanoparticles: A review. Prog. Polym. Sci. 37, 1457–1475.
143. Muralidharan, S., Kalaimani, J., Parasuraman, S., Dhanaraj, S.A., 2004. Development and Validation of Acyclovir HPLC External Standard Method in Human Plasma: Application to Pharmacokinetic Studies. pp. 1-5.
144. Murayama, S., Kuroda, S., Osawa, Z., 1993. Hydrophobic and hydrophilic interpenetrating polymer networks composed of polystyrene and poly(2-hydroxyethyl methacrylate): 1. PS-PHEMA sequential IPNs synthesized in the presence of a common solvent. Polymer. 34, 2845-2852.
145. Nakagawa, M., Tanaka, M., Miyata, T., 1997. Evaluation of collagen gel and hyaluronic acid as vitreous substitutes. Ophthalmic. Res. 29, 409–420.
146. Ndesendo, V.M.K, Pillay, V., Choonara, Y.E., du Toit, L.C., Meyer, L.C.R., Buchmann, E., Kumar, P., Khan, R.A., 2011. In vivo evaluation of the release of zidovudine and polystyrene sulfonate from a dual intravaginal bioadhesive polymeric device in the pig model. J. Pharm. Sci. 100, 1416-1435.
147. Nebinger, P., Koel, M., 1993. Determination of acyclovir byultrafiltration and high performance liquid chromatography. J. Chromatogr. B Biomed. Sci. Appl. 619, 342–344.
148. Niwa, T., Takeuchi, H., Hino, T., Kunou, N., Kawashima, Y., 1993. Preparation of biodegradable nano-spheres of water soluble and insoluble drugs with D, L-lactide / glycolide copolymer by a novel spontaneous emulsification solvent diffusion method, and the drug release behaviour. J. Control. Release. 25, 89-98.
149. Niwa, T., Takeuchi, H., Hino, T., Kunou, N., Kawashima, Y., 1994. In vitro drug release behaviour of D, L-lactide / glycolide copolymer (PLGA) nanospheres with nafarelin acetate prepared by novel spontaneous emulsification solvent diffusion method. J. Pharm. Sci. 83, 727-732.
150. Nordstrom, P., 2011. Formation of polymeric nanoparticles encapsulating and releasing a new hydrophobic cancer drug, Goteborg, Sweden. pp.1-50
151. Nov´akov´a, L., Matysov´a, L., Solich, P., 2006. Advantages of application of UPLC in pharmaceutical analysis. Talanta. 68, 908–918.

152. Oberle, R.L., Das, H., Wong, S.L., Chan, K.K., Sawchuk, R.J., 1994. Pharmacokinetics and metabolism of diclofenac sodium in Yucatan miniature pigs. Pharmaceutical Research. 11, 698-703.
153. Ochekpe, N.A., Olorunfemi, Ngwuluka N.C., 2009. Nanotechnology and Drug Delivery Part 2: Nanostructures for Drug Delivery. Trop. J. Pharm. Res. 8, 275.
154. O'Connell, D.W., Birkinshaw, C., O'Dwyer, T.F., 2008. Heavy metal adsorbents prepared from the modification of cellulose: A review. Bioresour .Technol. 99, 6709-6724.
155. Oh, E.J., Park, K., Kim, K.S., Kim, J., Yang, J.A., Kong, J.H., Lee, M.Y., Hoffman, A.S., Hahn, S.K., 2010. Target specific and long-acting delivery of protein, peptide, and nucleotide therapeutics using hyaluronic acid derivatives. J. Control. Release. 141, 2–12
156. Oh, J.K., Lee, D.I., Park, J.M., 2009. Biopolymer-based microgels/nanogels for drug delivery application. Prog. Polym. Sci. 34, 1261-1282.
157. Pandey, M.K., Tyagi, R., Yang, K., Fisher, J.R., Colton, C.K., Kumar, J., Parmar, S.V., Aiazian, E., Watterson, A.C., 2011. Design and synthesis of perfluorinatedamphiphilic copolymers: Smart nanomicelles for theranostic applications. Polymer. 52, 4727-4735.
158. Park, K., Park, H., 1990. Test methods of bioadhesion. In: Lenaerts, V. and Gurny, R. (Eds.), Bioadhesive Drug Delivery Systems, CRC Press, Boca Raton, FL. pp. 43-64
159. Patel, R., 2005. Mechanistic Profiling of Novel Wafer Technology Developed for Rate-Modulated Oramucosal Drug Delivery. MPharm Dissertation, Department of Pharmacy and Pharmacology, University of the Witwatersrand.
160. Pawar, S.N., Edgar, K.J., 2012. Alginate derivatization: a review of chemistry, properties and applications. Biomaterials. 33, 3279–3305.
161. Peh, K.K., Yuen, K.H., 1997. Simple high-performance liquid chromatographic method for the determination of acyclovir in human plasma using fluorescence detection. J .Chromatogr. B Biomed. Sci. 241–244.
162. Pham-Huy, C., Stathoulopoulou, F., Sandouk, P., Scherrmann, J.M., Palombo, S., Girre, C., 1999. Rapid determination of valaciclovir and acyclovir in human biological fluids by highperformance liquid chromatography using isocratic elution. J. Chromatogr. B. 732, 47–53.
163. Polli, J.E., Rekhi, G.S., Augsburger, L.L., Shah, V.P., 1997. Methods to Compare Dissolution Profiles and a Rationale for Wide Dissolution Specifications for Metoprolol tartarate Tablets. J. Pharm. Sci. 86, 690–700.
164. Poirier, J.M., Radembino, N., Jaillon, P., 1999. Determination of acyclovir in plasma by solid-phase extraction and columnliquid chromatography. Therapeutic Drug Monitoring. 21, 129–133.

165. Prestwich, G.D., Marecak, D.M., Marecek, J.F., Vercruysse, K.P., Ziebell, M.R., 1998. Controlled chemical modification of hyaluronic acid: synthesis, applications, and biodegradation of hydrazide derivatives. J. Controll. Release. 53, 93-103.
166. Proano, M., Camilleri, M., Phillips, S.F., Brown M.L., Thomforde G.M., 1990. Transit of solids through the human colon: regional quantification in the unprepared bowel. Am. J. Physiol. 258, 856-862.
167. Pruett, R.C., Schepens, C.L., Swann, D.A., 1979. Hyaluronic acid vitreous substitute; a six-year clinical evaluation. Arch. Ophthalmol. 97, 2325–2330.
168. Qiu, Y., Park, K., 2012. Environment-sensitive hydrogels for drug delivery. Adv. Drug Deliv. Rev. 64, 49–60.
169. Quimby F.W., 2002. Animal Models in Biomedical Research. In: J.G. Fox, L.C. Anderson, F.M. Loew, F.W.Quimby, eds. Laboratory Animal Medicine (Second Edition). New York, Academic Press. Ch 30.
170. Rajaonarivony, M., Vauthier, C., Couarraze, G., Puisieux, F., Couvreur, P., 1993. Development of a new drug carrier made from alginate. J. Pharm. Sci. 82, 912–917.
171. Rao, J.P., Geckeler, K.E., 2011. Polymer nanoparticles: Preparation techniques and size-control parameters. Prog Polym Sci. 36, 887–913.
172. Reddy, N., Yang, Y., 2010. Citric acid cross-linking of starch films. Food Chemistry. 118, 702-711.
173. Rodrigues, J.S., Santos-Magalhaes, N.S., Coelho, L.C.B.B., Couvreur, P., Ponchel, G., Gref, R., 2003. Novel core(polyester)-shell(polysaccharide) nanoparticles: protein loading and surface modification with lectins. J. Control. Release. 92, 103–112.
174. Rowland, M., Tozer, T.N., 1995. Clinical pharmacokinetics concepts and applications, 3rd ed. Lippincott Williams & Wilkins, Philadelphia, Pa.
175. Rubinstein, R., 2000. Natural polysaccharides as targeting tools of drugs to the human colon. Drug Dev. Res. 50, 435–439.
176. Samanidou, V.F., Giannakis, D.E., Papadaki, A., 2009. Development and validation of an HPLC method for the determination of seven penicillin antibiotics in veterinary drugs and bovine blood plasma. J. Sep. Sci. 32, 1302-1311.
177. Sarmento, B., Ribeiro, A., Veiga, F., Sampaio, P., Neufeld, R., Ferreira, D., 2007. Alginate/chitosan nanoparticles are effective for oral insulin delivery. Pharm. Res. 24, 2198–206.
178. Schafroth, N., Arpagaus, C., Jadhav, U.Y., Makne, S., Douroumis, D., 2012. Nano and microparticles engineering of water insoluble drugs using a novel spray-drying process. Colloids. Surf. B Biointerfaces. 90, 8-15.

179. Schanté, C.E., Zuber, G., Herlinb, C., Vandamme, T.F., 2011. Chemical modifications of hyaluronic acid for the synthesis of derivatives for a broad range of biomedical applications. Carbohydr. Polym. 85, 469–489.
180. Schmid, K., Arpagaus, C., Friess, W., 2009. Evaluation of a vibrating mesh spray dryer for preparation of submicron particles, Respiratory Drug Delivery Europe. 323-326.
181. Sell, S.A., Wolfe, P.S., Garg, K., McCool, J.M., Rodriguez, I.A., Bowlin, G.L., 2010. The Use of Natural Polymers in Tissue Engineering: A Focus on Electrospun Extracellular Matrix Analogues. Polymers. 2, 522-553.
182. Sen, G., Singh, R.P., Pal, S., 2010. Microwave-initiated synthesis of polyacrylamide grafted sodium alginate: synthesis and characterization. J. Appl. Polym. Sci. 115, 63–71.
183. Shaikh RP. 2012. Oral Electrospun Multi-Component Membranous Drug Delivery Systems. MPharm Dissertation, Department of Pharmacy and Pharmacology, University of the Witwatersrand.
184. Simone, E.A., Dziubla, T.D., Muzykantov, V.R., 2008. Polymeric carriers: role of geometry in drug delivery, Informa UK Ltd London. UK Drug Deliv. 5, 1283-1300.
185. Singh, B, Kumar, R., Ahuja, N., 2005. Optimizing drug delivery systems using systematic Design of Experiments. Part I: Fundamental aspects. Crit. Rev. Ther. Drug Carrier. Syst. 22, 27-105.
186. Sinha, V.R., Kumria, R., 2001. Polysaccharides in colon-specific drug delivery. Int. J. Pharm. 224, 19–38.
187. Sinha, V.R., Trehan, A., Kumar, M., Singh, S., Bhinge J.R., 2007. Stress Studies on Acyclovir. J. Chromatogr. Sci. 45, 319-24.
188. Sionkowska, A., 2011. Current research on the blends of natural and synthetic polymers as new biomaterials: Review. Prog. Polym. Sci. 36, 1254-1276.
189. Sionkowska, A., 2003. Interaction of collagen and poly(vinyl pyrrolidone) in blends. EurPolym. J. 39, 2135–2140.
190. Sionkowska, A., 2003. Interaction of collagen and poly(vinyl pyrrolidone) in blends. EurPolym. J. 39, 2135–2140.
191. Sonia, T.A., Sharma, T.C., 2011. Chitosan and Its Derivatives for Drug Delivery Perspective. Adv. Polym. Sci. 243, 23–54.
192. Soumya, R.S., Vineetha, V.P., Reshma, P.L., Raghu, K.G., 2013. Preparation and Characterization of Selenium Incorporated Guar Gum Nanoparticle and Its Interaction with H9c2 Cells. PLoS one. 8, 744-11.
193. Stokes, W.S., Marsman, D.S., 2014. Animal Welfare Considerations in Biomedical Research and Testing. In: K.Bayne, P.V. Turner, eds., Laboratory Animal Welfare. New York: Academic Press. Ch 9.’

194. Stuart, B., 2004. Infrared Spectroscopy: Fundamental and Applications. John Wiley & sons, Ltd ISBNs: 0-470-85427-8 (HB); 0-470-85428-6 (PB). pp. 1-221.

195. Susantakumar, P., Gaur, A., Sharma, P., 2011. Comparative Pharmacokinetics, Safety and Tolerability Evaluation of Acyclovir IR 800 Mg Tablet in Healthy Indian Adult Volunteers Under Fasting and Non-fasting Conditions. J. Bioequiv. Availab. 3, 6

196. Svensson, J.O., Barkholt, L., Sawe, J., 1997. Determination of Acyclovir and its metabolite 9-carboxymethoxymethylguanineinserum and urine using solid-phase extraction and highperformance liquid chromatography. J. Chromatogr. B Biomed. Sc.i Appl. 690, 363–366.

197. Swart, K.J., Hundt, H.K.L., Groenewald, A.M., 1994. Automatedhigh-performance liquid chromatographic method forthe determination of acyclovir in plasma. Journal of ChromatographyA. 663, 65–69.

198. Teshima, D., Otsubo, K., Yoshida, T., Itoh, Y., Oishi, R., 2003. A simple and simultaneous determination of acyclovir and ganciclovir in human plasma by high-performance liquid chromatography, Biomed. Chromatogr. 17, 500–503.

199. Thanki, K., Gangwal, R., Sangamwar, A.T., Jain, S., 2013. Oral Delivery of Anticancer Drugs: Challenges and Opportunities. J. Control. Release. 170, 15–40.

200. Tomar, V., Garud, N., Kannojia, P., Garud, A., Jain, N.K., Singh, N., 2010. Enhancement of Solubility of Acyclovir by Solid Dispersion And Inclusion Complexation Methods. Der. Pharmacia. Lettre. 2, 341-352

201. Toole, B.P., 2004. Hyaluronan: from extracellular glue to pericellular cue. Nat. Rev. Cancer. 4, 528–539.

202. Trimaille, T., Mondon, K., Gurny, R., M¨oller, M., 2006. Novel polymeric micelles for hydrophobic drug delivery based onbiodegradable poly(hexyl-substituted lactides). Int. J. Pharm. 319, 147–154.

203. Tzanavaras, P.D., Themelis, D.G., 2007. High-throughput HPLC assay of acyclovir and its major impurity guanine using amonolithic column and a flow gradient approach. J. Pharm. Biomed. Anal. 43, 1526–1530.

204. Ueda, M., Iwara, A., Kreuter, J., 1998. Influence of the preparation methods on the drying release behavior of loperamide-loaded nanoparticles. J. Microencapsulation. 15, 361–372.

205. Vandamme, T.F., Lenourry, A., Charrueau, C.J., 2002. Chaumeil, The use of polysaccharides to target drugs to the colon. Carbohydr. Polym. 48, 219–231.

206. Vandermeulen, G.W.M., Klok, H.A., 2004. Peptide/protein hybrid materials: Enhanced control of improved performance through conjugation of biological and synthetic polymers structure. Macromol. Biosci. 4, 383–398.

207. van Hest, J.C.M., 2007. Biosynthetic-synthetic polymer conjugates, Journal of Macromolecular Science, Part C: Polymer Reviews. 47, 63-92.
208. Vashista, A., Guptab, Y.K., Ahmada, S., 2012. Interpenetrating biopolymer network based hydrogels for an effective drug delivery system. Carbohydr. Polym. 87, 1433–1439.
209. Vilar, G., Tulla-Puche, J., Albericio, F., 2012. Polymers and Drug Delivery Systems. Curr. Drug Deliv. 9, 367-394
210. Volpato, N.M., Santi, P., Laureri, C., Colombo, P., 1997. Assay of acyclovir in human skin layers by high performance liquid chromatography. J. Pharm Biomed. Anal. 16, 515–520.
211. Wagstaff, A.J., Faulds, D., Goa, K.L., 1994. Aciclovir. A reappraisal of its antiviral activity, pharmacokinetic properties and therapeutic efficacy. Drugs. 47, 153- 205.
212. Waman, N., Ajage, R., Kendre, P.N., Kasture, S.B., Kasture, V., 2014. Improved release oral drug delivery of metaxalone. Int J. Pharm. 4, 417-424.
213. Wang, T., Bai, J., Jiang, X., Nienhaus, G.U., 2012. A Study Combining Confocal Microscopy with FTIR Specroelectrochemistry. Cellular Uptake of Nanoparticles by Membrane Penetration. 2, 1251-1259.
214. Werkmeister, J.A., Edwards, G.A., Casagranda, F., White, J.F., Ramshaw, J.A.M., 1998. Evaluation of a collagen-based biosynthetic materials for the repair of abdominal wall defects. J. Biomed. Mater. Res. 39, 429–36.
215. Werle, M., Takeuchi, H., Bernkop-Schnurch, A., 2009. Modified chitosans for oral drug delivery. J. Pharm. Sci. 98, 1643–56
216. Wojtacki, J., Rolka-Stempniewicz, G., Grzegorczyk, G., 2006. Breast cancer patients pref erences for oral versus intravenous second-line anticancer therapy. Eur. J. Can cer (Suppl.). 4, 159–160.
217. Wong, T.W., 2011. Alginate graft copolymers and alginate–co-excipient physical mixture in oral drug delivery. JPP. 63, 1497–1512.
218. Xiao, H., Lin, Q., Liu, G., 2012. Effect of Cross-Linking and Enzymatic Hydrolysis Composite Modification on the Properties of Rice Starches. Molecules. 17, 8136-8146.
219. Xu, W., Ling, P., Zhang, T., 2013. Polymeric Micelles, a Promising Drug Delivery System to Enhance Bioavailability of Poorly Water-Soluble Drugs. 1-15.
220. Xu, X., Jha, A.K., Harrington, D.A., Farach-Carson, M.C., Jia, X., 2012. Hyaluronic Acid-Based Hydrogels: from a Natural Polysaccharide to Complex Networks. Soft. Matter. 8, 3280–3294.
221. Yang, K.W., Li, X.R., Yang, Z.L., Li, P.Z., Wang, F., Liu, Y., 2009. Novel polyion complex micelles for liver-targeted delivery of diammonium glycyrrhizinate: in vitro and in vivo characterization. J. Biomed. Mater. Res. A. 88,140–148.

222. Yerushalmi, N., Margalit, R., 1998. Hyaluronic Acid-Modified Bioadhesive Liposomes as Local Drug Depots: Effects of Cellular and Fluid Dynamics on Liposome Retention at Target Sites. 349, 21-26.
223. Yi, Y.M., Yang, T.Y., Pan, W.M., 1999. Preparation and distribution of 5-fluorouracil 125I sodium alginate-bovine serum albumin nanoparticles. World J. Gastroentero. 5, 57–60.
224. Yih, T.C., Al-Fand, M., 2006. Engineered nanoparticles as precise drug delivery systems. J. Cell. Biochem. 28, 1258-1266.
225. Yuri, S.L., 2002. Polymer blends and interpenetrating polymer networks at the interface with solids. Prog. Polym. Sci. 27, 1721–1801
226. Zeng, L., Nath, C.E., Shaw, P.J.; Earl, J.W., McLachlan, A.J., 2008. HPLC-fluorescence assay for acyclovir in children. Biomed. Chromatogr. 22, 879–887.
227. Zhang, N., Wardwell, P.R., Bader, R.A., 2013. Polysaccharide-Based Micelles for Drug Delivery. Pharmaceutics. 5, 329-352.

APPENDIX A

SEMI-SYNTHETIC BIOPOLYMER COMPLEXES: MODIFIED POLYSACCHARIDES AS ORAL DRUG NANO-CARRIERS FOR ENHANCEMENT OF ORAL BIOAVAILABILITY

Mduduzi N. Sithole[1], Yahya E. Choonara[1], Lisa C. du Toit[1], Pradeep Kumar[1], Pierre P. D. Kondiah[1] and Viness Pillay[1*]

Wits Advanced Drug Delivery Platform Research Unit, Department of Pharmacy and Pharmacology, School of Therapeutic Sciences, Faculty of Health Sciences, University of the Witwatersrand, Johannesburg, 7 York Road, Parktown, 2193, South Africa

*Corresponding Author: viness.pillay@wits.ac.za

Abstract

Semi-Synthetic Biopolymer Complexes have potential as nano-carriers for oral drug delivery due to their exceptional properties obtained by merging the properties of synthetic (e.g. good thermal and mechanical properties) with natural polymers (e.g. biocompatibility); thus, forming a new class of biopolymer materials incorporating the best of both worlds. Despite development in drug delivery systems, oral administration of therapeutic agent is still preferred. Several nano-polymeric systems has been prepared and characterized based on both synthetic polymers and natural polymers, each with its limitations and advantages. Among natural polymers, alginate, chitosan, and hyaluronic acid have been studied broadly for the fabrication of nanoparticles systems. This review discusses a newly investigated class of polymer called Semi-Synthetic Biopolymer Complexes (SSBCs) as oral drug nano-carriers. It also discusses certain significant structural and functional attributes or effects which are essential to be taken into consideration when an oral drug delivery system is developed. The review is aimed at describing complexation of few natural polymers (e.g. polysaccharides) with selected synthetic polymers or synthetic chemicals to indicate some of the factors that influence preparation, solubility, formation and stability of these Semi-Synthetic Biopolymer Complexes.

Keywords: Semi-Synthetic Biopolymers, Drug bioavailability, Oral drug nano-carrier

APPENDIX B

Development of Novel Polymeric Nano-Composite Complex for Low Bioavailability Drugs

Mduduzi N. Sithole[1], Yahya E. Choonara[1], Lisa C. du Toit[1], Pradeep Kumar[1], Pierre P. D. Kondiah[1] and Viness Pillay[1*]

Wits Advanced Drug Delivery Platform Research Unit, Department of Pharmacy and Pharmacology, School of Therapeutic Sciences, Faculty of Health Sciences, University of the Witwatersrand, Johannesburg, 7 York Road, Parktown, 2193, South Africa

*Corresponding Author: viness.pillay@wits.ac.za

Abstract

The major challenge in pharmaceutical research is to improve drug's effectiveness. This research attempts to improve the permeability and solubility of acyclovir (ACV), which has an oral bioavailability of 10-20%. The research also seeks to develop guiding principles in examining and solving key issues of its nano-encapsulation as a means to enhance its oral bioavailability. In this study, a delivery system was designed for ACV, with desirable physicochemical and physicomechenical properties engineered by grafting/modifying natural polymer with synthetic polymer. The resulted hybrid was conjugated with an oral absorption enhancer yielding a specialized Polymeric Nano-Enabled Complex (PNC) to regulate ACV permeability and solubility, producing an "intelligent" nano-enabled drug delivery system. Hence, a PNC was synthesized, and the permeability and solubility of ACV drug from the PNC ascertained, to assess the enhancement of ACV oral bioavailability. The synthetic method of PNC copolymer was based on the covalent coupling of the polymeric chains at their respective reactive functional groups, followed by conjugation with the absorption enhancer. The coupling was accomplished using a variety of chemical means. Nanoparticles were prepared from PNC using emulsion technique. Different characterization methods such as FT-IR, DSC, ^{1}H NMR, and XRD amongst others were used to confirm the successful preparation of TPSNC and also the success of ACV encapsulation. The current investigation provided evidence that the biopolymer PNC copolymer improved the solubility of ACV by 30% and the *ex vivo* permeation by 10% compared to the conventional ACV, consequentially enhanced its bioavailability.

Key Words: solubility, conjugation, semi-synthetic, encapsulation.

APPENDIX C

STRICTLY CONFIDENTIAL

ANIMAL ETHICS SCREENING COMMITTEE (AESC)

CLEARANCE CERTIFICATE NO. 2014/38/C

INVESTIGATORS: Prof V Pillay

CO-INVESTIGATORS (For postgraduate degree purposes): Ms B Choonara
Ms M Siyawamwaya
Mr M Sithole

SCHOOL: Pharmacy & Pharmacology

LOCATION: Faculty of Health Sciences

PROJECT TITLE: *In vivo assessment of innovative polymeric oral drug delivery systems in large White Pigs*

Number and Species

18 Large White Pigs

Approval was given for to the use of animals for the project described above at an AESC meeting held on 24 June 2014 . This approval remains valid until 23 June 2016.

The use of these animals is subject to AESC guidelines for the use and care of animals, is limited to the procedures described in the application form and is subject to any additional conditions listed below:

None.

Signed: _____ (Chairperson, AESC) Date: 1/7/2014

I am satisfied that the persons listed in this application are competent to perform the procedures therein, in terms of Section 23 (1) (c) of the Veterinary and Para-Veterinary Professions Act (19 of 1982)

Signed: _____ (Registered Veterinarian) Date: 27 June 2014

cc: Supervisor: N/A
Director: CAS

Works 2000/lain0015/AESCCert.wps

UNIVERSITY OF THE WITWATERSRAND, JOHANNESBURG
7 York Road, Parktown, 2193 South Africa * E-mail physiology@health.wits.ac.za * Telephone (011)717-2363 * Fax (011) 643-2765

10 April 2014

To: Whom it may concern,

Re: approval for the use of animal tissue samples collected from pigs and rabbits euthanized for other purposes in *in vitro* studies

This letter is to confirm that Prof Viness Pillay does not require full animal ethics clearance to collect pig intestinal tissue. Prof Pillay and his student will be using intestinal tissue from already euthanized animals, hence full animal ethics clearance is not required, as these animals have been euthanized for other purposes. The intestinal tissue from the pigs for *in vitro* studies will be collected with permission from the Central Animal Service Unit at the University of the Witwatersrand. A request for permission to the Animal ethics committee has been initiated.

The following Master of Science in Medicine (Pharmaceutics) student will be involved in these studies as of 2014: Mduduzi Sithole (student number 0309004W). The title of the project is *"The Application of Semi-Synthetic Biopolymer Nano-carrier Complexes for Drugs with low Oral Bioavailability".*

These studies will be performed in the Division of Pharmacology, Department of Pharmacy and Pharmacology.

If you would like any further or more specific information in this regard, do not hesitate to contact me.

Yours sincerely,

Kennedy Erlwanger
(Chairman: Animal Ethics Screening Committee, University of the Witwatersrand)

Assoc Prof Kennedy H. Erlwanger
School of Physiology
Faculty of Health Sciences, University of the Witwatersrand
7 York Road, Parktown, 2193
SOUTH AFRICA

Private bag 3, Wits, 2050, South Africa.
Tel: +27 (0)11 717 2454
Fax: + 27 (0)11 643 2765
Email: Kennedy.Erlwanger@wits.ac.za